Addis Ababa University
School of Graduate Studies
Addis Ababa Institute of Technology
Electrical and Computer Engineering Department

MMSE Rake Receiver MMSE Equalizer for DS CDMA UWB Systems

By
Berhan Oumer

Advisor
Dr. Ing. Getahun Mekuria

A Thesis Submitted to the School of Graduate Studies of Addis Ababa University
in Partial Fulfillment of the Requirements for the Degree of
Masters of Science
In
Electrical Engineering (Communication Engineering)

Addis Ababa, 2012

Addis Ababa University
School of Graduate Studies
Addis Ababa Institute of Technology
Electrical and Computer Engineering
Department

Master of Science Thesis

MMSE Rake Receiver MMSE Equalizer for DS CDMA UWB Systems

By
Berhan Oumer

Approval by Board of Examiners

Chairman, Dept. Graduate Committee	Signature
Advisor	Signature
Internal Examiner	Signature
External Examiner	Signature

Declaration

I, the undersigned, declare that this thesis is my original work, has not been presented for a degree in this or any other university, and all sources of materials used for the thesis have been fully acknowledged.

Berhan Oumer _____

Name Signature

Place:**Addis Ababa**

Date of Submission:**October**

This thesis has been submitted for examination with my approval as a university advisor.

Dr. Ing. Getahun Mekuria _____

Advisor's Name Signature

To ...

Abstract

The increasing demand for portable, high data rate communications has focused much attention on wireless technology. Ultra Wide Band (UWB) waveforms have the ability to deliver megabits of information while maintaining low average power consumption within a short range. Therefore, UWB is regarded as a good PHY layer solution to the PAN applications. In accordance with recent FCC rulings, UWB systems are now allowed to operate in the unlicensed spectrum of 3.1 to 10.6 GHz, motivating renewed interest in the thirty year old concept of impulse radio.

The main subject of this thesis is to develop and check the performance of MMSE Rake Receiver and MMSE Equalizer for DS-CDMA UWB Systems. Since UWB is characterized by longer root-mean square delay spread, this thesis work combines MMSE Rake receiver and a simple linear MMSE equalizer to combat severe ISI which is the result of long delay spread. The MMSE equalizer will be done both in time and frequency domain and comparison will be made.

Using MRC rake receiver the simulation results illustrate that an ideal ARAKE receiver using DS-BPSK-UWB transmitted signal format has the best performance for all type of channel models. The result also shows that at higher SNRs MRC rake receiver exhibit an error floor and, appending an equalizer on MRC rake is better than employing additional rake fingers, especially at higher SNRs and relatively large number of fingers. The proposed Rake-Equalizer outperforms the conventional rake receiver, which maximize the output SNR. The simulation also shows that the cascaded MMSE Rake-Equalizer achieves almost the same BER performance as MRC A-RAKE receiver for CM2 and frequency domain equalizer outperforms time domain MRC rake-equalizer at higher SNRs for CM4. All the above simulations have been conducted using MATLAB software.

Acknowledgment

First and foremost, I thank the gracious Lord for all his numerous blessings bestowed upon me in various ways.

I would like to express my sincere gratitude to my advisor Dr. Ing. Getahun Mekuria for his patient guidance, valuable advice and tremendous technical and moral support.

I would like to acknowledge my former advisor Dr. Ing. Hailu Ayele for giving me the opportunity to do my thesis on UWB communication system, the invaluable guidance he provided and the necessary resources he provided to carry it out.

I am also very grateful to all of my parents and colleagues for their moral and material support during my thesis work.

Contents

List of Figures

List of Tables

List of Symbols and Abbreviations

Abbreviation	Description
UWB	Ultra Wide Band
PHY	Physical
PAN	Personal Area Network
GPS	Global Positioning System
MRC	Maximal Ratio Combining
SNR	Signal-to-Noise Ratio
AWGN	Additive White Gaussian Noise
MMSE	Minimum Mean Square Error
ISI	Inter Symbol Interference
DS	Discrete Sequence
CDMA	Code Division Multiple Access
CM	Channel Model
MAI	Multi Access interference
RAM	Random Access Memory
CPU	Central Processing Unit
RF	Radio Frequency
LNA	Low-Noise Amplifier
DoD	Department of Defense
FCC	Federal Communication Commission
R and O	Report and Order
CW	Continuous Waveform
DC	Direct Current
PSD	Power Spectral Density
ISM	Industrial Scientific and Medical
ITU	International Telecommunications Union
ITU-R	International Telecommunications Union Radio Sector
TG	Task Group
WG	Working Group

Abbreviation	Description
APT	Asia Pacific Telecommunity
APT/ AWF	Asia Pacific Telecommunity Wireless Forum
EU	European Union
US	United States
UMTS	Universal Mobile Telecommunication System
EC	European Commission
CEPT	Conference of European Posts and Telegraphs
ECC	Electronic Communications Committee
DEC	Decision
IEEE	Institute of Electrical and Electronics Engineers
WLAN	Wireless Local Area Network
MII	Ministry of Information and Industry
DAA	Detect and Avoid
EIRP	Effective Isotropic Radiated Power
ACMA	Australian Communications and Media Authority
MIC	Ministry of Internal Affairs and Communications
IDA	Infocomm Development Authority
UFZ	UWB Friendly Zone
LPI/D	Low Probability of Intercept and Detection
LOS	Line of Site
NLOS	Non-Line of Site
BER	Bit Error Rate
CMOS	Complementary Metal-Oxide Semiconductors
ADCs	Analog-to-Digital Converters
PPM	Pulse-Position Modulation
PAM	Pulse Amplitude Modulation
BPSK	Binary Phase-Shift Keying
BPAM	Binary Pulse Amplitude Modulation
OOK	On-Off Keying
MA	Multiple Access
TH	Time Hopping
PSK	Phase-Shift Keying
AGC	Automatic Gain Control
TH-PPM	Time Hopping Pulse Position Modulation
PRF	Pulse Reputation Frequency
DSSS	Direct Sequence Spread Spectrum
IS-95	Interim Standard 95
PN	Pseudo Random
LFSR	Linear Feedback Shift Registers
S-V	Saleh-Valenzuela
MPC	Multi Path Component
TX	Transmitter
RX	Receiver
I-rake	Ideal Rake
A-rake	All Rake

Abbreviation	Description
S-rake	Selective Rake
P-rake	Partial Rake
SC	Selection Combining
SSC	Switch and Stay Combining
EGC	Equal Gain Combining
H-S/MRC	Hybrid Selection/Maximal-Ratio Combining
GSC	General Selection Combining
WPANs	Wireless Personal Area Networks
LANs	Local Area Networks
SINR	Signal-to-Interference-Plus Noise Ratio
WCDMA	Wideband Code Division Multiple Access
LMS	Least Mean Square
MSE	Mean Square Error
NBI	Narrowband Interference
QAM	Quadrature Amplitude Modulation
GA	Genetic Algorithms
CDMA	Code Division Multiple Access
TDE	Time Domain Equalizers
FDE	Frequency Domain Equalizers
FIR	Finite Impulse Response
ZFE	Zero-Forcing Equalizer
MMSE-LE	Minimum Mean-Square Error Linear Equalizer
MC	Multi Carrier
FFT	Fast Fourier Transform
IFFT	Inverse Fast Fourier Transform
OFDM	Orthogonal Frequency Domain Multiplexing
PAPR	Peak-to-Average Power Ratio
SC	Single Carrier
LE	Linear Equalization
CP	Cyclic Prefix

Chapter 1

Introduction

1.1 Motivation for Using Ultra Wide Band

1.1.1 Wireless Trade-Offs

The world continues to increase its dependence on electronic communications. Balancing desired properties for data transmission requires development of new methods for exchanging information. Ideally, large quantities of data are rapidly transmitted by many users, simultaneously, over a significant distance. Unfortunately, these characteristics are in competition with each other and trade-offs must occur to obtain the best solution for a particular application.

Wireless communications have become popular because they address growing demands. Portable wireless devices permit high data rates at low cost and, with improved semiconductor technology, low power consumption. Crowding within existing spectral allocations is driving the need for new ways to efficiently use available frequency bands. The increase in high-speed, wired access to the Internet has increased the demand for high-speed communications within the home. The need for robust forms of transmission that do not interfere with other users, even inside relatively small areas, such as a single room in a building, is a pressing requirement. Ultra wide band (UWB) technology is a form of wireless communications and is becoming a popular choice for addressing these types of issues.

1.1.2 Applications

The field of ultra wide band signaling is just beginning to appear across a vast number of applications where the technology can improve existing systems or provide entirely new capabilities. The following sections present ideas that have been proposed using UWB or, in some cases, ideas that have already been im-

plemented.

One of UWB's application is it's use for advanced radar sensing. Ultra wide band signaling can be implemented with a large bandwidth at relatively low frequencies [79], making it suitable for through-wall imaging and radar sensing applications. Lower frequency components enhance signal propagation through the ground or walls [39] while the larger bandwidth provides higher resolution [27]. In addition, recent studies [26] have indicated that UWB may be more prone to edge diffraction and propagation through large cracks. Such sensing could also be used to locate people within rubble.

The other application is precise locating. The use of GPS provides location data within meters. For outdoor tracking and large scale identification this accuracy is acceptable. GPS satellite signals work well in outdoor applications. However, both signal strength and location resolution are severely degraded indoors [44]. The centimeter level precision and multipath mitigation available with UWB makes it more suitable for the indoor environment. Rescue services could benefit by using UWB technology to locate people inside buildings during emergencies. On a more routine basis, UWB nodes could be installed throughout a building to electronically track people carrying UWB sensors, providing transfers of information throughout a building or adjusting environmental factors to personal preference.

UWB's low power consumption points to another key application called battlefield sensor networks, which are also aided by the fact that UWB is hard to intercept and difficult to jam [48].

One of the key UWB application is location-finding, for inventory control or asset tracking [72]. For tasks like these, the technology promises high precision. Since the bandwidth of the signal is extremely wide , we can resolve to smaller and smaller magnitudes [27].

The same technology, could also be applied in smart homes to control appliances, or on highways to improve safety. Within the home, we can connect all multimedia equipment via a UWB design, eliminating the need for wires throughout the building. Since FCC has established emissions level requirements for vehicular radar systems [22], we can equip vehicle bumpers with UWB sensors so that automobiles do some kind of automatic steering or collision avoidance.

1.2 Problem Statement

The conventional Rake receiver employs the weight vector to perform the MRC which maximizes the output SNR. Maximal ratio combining (MRC) Rake receiver is optimal scheme in the absence of interfering users and inter-symbol interference (ISI) [64][67]. A more effective receiver scheme is the minimum mean square error (MMSE) Rake receiver which achieves a much improved performance for WCDMA system [13] [57]. For a minimum mean square error (MMSE) Rake receiver, the finger selection algorithm is to choose the paths with highest signal-to-interference plus-noise ratios (SINRs). Since only by using MMSE Rake receiver no one can mitigate the severe ISI, which is caused by the longer root-mean square delay spread [54], appending a simple linear equalizer is one way of combating this ISI.

This thesis then combines a Rake receiver and a simple linear equalizer to deal with the large delay spread which is the result of multipath in UWB channel.

1.3 Objective

1.3.1 General Objectives

The main objective of this thesis is to develop and check the performance of MMSE Rake Receiver and MMSE Equalizer for DS-CDMA UWB Systems. The MMSE equalizer will be done both in time and frequency domain and comparison will be made.

1.3.2 Specific Objectives

Therefore, to meet the mentioned general objective, the following specific objectives will be accomplished in this thesis:

- Model and determine rake fingers of MRC Rake receiver.
- Model and determine rake fingers of MMSE Rake receiver.
- Model and determine taps of the MMSE equalizer for both time and frequency domain.
- Compare the performance of different types of MRC rake receiver for different channel models such as CM1, CM2 ,CM3 and CM4.
- Compare the performance of the proposed system, i.e. MMSE Rake-equalizer, with MRC Rake receiver and with MRC Rake-MMSE equalizer for different channel models such as CM1, CM2 ,CM3 and CM4.

- Compare the performance of time domain processing with frequency domain processing.

1.4 Scope

In a CDMA system, many users simultaneously transmit across the entire frequency band and user's data is separated on the basis of their signature waveforms. Even though the codes which are used to differentiate different users are orthogonal to each other at the transmitter, the received signal at the receiver from different users losses orthogonality due to the channel effect i.e. multipath. This loss of orthogonality will lead to Multi access interference (MAI). But in this thesis MAI will not be considered.

1.5 Methodology

This research used *Matlab*® to simulate a complete UWB communication system, including the transmitter, channel, and receiver. Pulse generation, transmission, detection and estimation occur entirely within the software.

1.6 Equipment

Matlab® Version 7.9.0.529 was used for simulation code development, and LED Beta 0.53 LaTeXEditor and MiKTeX 2.9 was used for document preparation. Hardware consisted of a Toshiba Personal Computer running Microsoft Windows 7, Service Pack 1. The computer had 4.0 GB of RAM and used an Intel(R) Core(TM) i3 CPU 2.13 GHz processor. .

1.7 Literature Review

So far many researches have been conducted on different aspects UWB wireless communication systems and on rake receptions. A short literature survey of some selected papers are reviewed here.

Muhammad Gufran Khan, et al. [40] evaluate the performance of RAKE receivers operating in a non line-of-sight (NLOS) scenario in industrial environments, which is characterized by dense multipath with significant energy due to the existence of large number of metallic scatterers in the surroundings. The channels used for the evaluation were measured in a medium-sized industrial environment. In addition, a standard IEEE 802.15.4a channel model was used for comparison with the results of the measured data. The performance of partial RAKE (PRake) and selective RAKE (SRake) was evaluated in terms of uncoded

bit-error-rate (BER) using different number of fingers. The performance of maximal ratio combining (MRC) and equal gain combining (EGC) was compared for the RAKE receiver assuming perfect knowledge of the channel state. Finally, The results show that the SRake receiver always outperforms the PRake using the same number of fingers and the same combining scheme. It also show that the difference in the performance of MRC and EGC combining schemes is not that significant for SRake, while PRake has a considerably better performance using MRC. The comparison of the results also demonstrates that the performance of the RAKE receiver depends to a large extent on the underlying channel and hence the shape of the power delay profiles.

A.G. Klein, et al. [41] propose a modified RAKE receiver that finds an optimal balance between the goal of gathering multipath signal energy, avoiding ISI, and suppressing narrowband interference. For fixed RAKE finger delays, they develop a closed-form expression for the minimum mean squared error (MMSE) combining weights that account for ISI. Then they examine the optimal choice of RAKE finger delays, and show that significant performance gains can be achieved, particularly in an undermodeled situation when there are more channel paths than RAKE fingers. The proposed receiver demonstrates superior performance over conventional MRC when the IS1 dominates the noise.

G. S. Biradar, et al. [12] derive and propose adaptive minimum mean square error (MMSE) Rake receiver for DS-CDMA UWB multipath channels to cancel multi access interference (MAI). Proposed receiver works on chip level equalization and it does not require the spreading code to compute equalizer filter coefficients. Simulation results show that the bit error rate probability performance of the proposed receiver is much better than conventional adaptive MMSE Rake receiver in all the three UWB multipath channel models (CM1-CM3) in the presence of additive white Gaussian noise (AWGN). Further, it offers significant improvement in MAI cancellation in multipath channels. It have shown that the number of users supported by the proposed receiver at BER of 10^{-3} with E_b/N_0 = 20 dB is two times that of the conventional Rake receiver with the same computational complexity.

J. Jeya A Celin, et al. [13] evaluates the performance of Genetic Algorithm based MMSE Rake receiver in WCDMA. It is observed that the BER performance of the Genetic Algorithm based adaptive MMSE Rake receiver is much better than Conventional Rake Receiver for WCDMA environment.

Sato, H. and Ohtsuki, T. [61], evaluates the performance of direct sequence - ultra wideband (DS-UWB) with frequency domain channel estimation (FDCE)

and equalisation (FDE) in the UWB multipath channel and compare it to that of conventional DS-UWB with time domain channel estimation (TDCE) and RAKE receiver. The authors show that when E_b/N_0 is high, DS-UWB with frequency domain process (FDP) has significantly less computational complexity and achieves a better performance than DS-UWB with time domain process (TDP); conversely when Eb/N0 is low, DS-UWB with TDP has significantly more computational complexity and achieves a better performance than DS-UWB with FDP.

Y. Ishiyama and T. Ohtsuki [35] evaluate the bit error rate (BER) of UWB-IR and DS-UWB with MMSE-FDE and compare it to that of UWB-IR and DS-UWB with maximal ratio combining (MRC)-RAKE. It is shown that UWB-IR with MMSE-FDE can achieve better BER than UWB-IR with MRC-RAKE. And it is also shown that DS-UWB with MMSE-FDE has a better BER than DS-UWB with MRC-RAKE particularly when SNR is large.

It is reported in [10] that the single carrier (SC) with frequency domain equalizer (FDE) has few problems of peak to average power ratio (PAPR) and also obtains an excellent performance as well as orthogonal frequency division multiplexing (OFDM) even in the strong frequency selective channel where multipath is spread over dozens of symbols.

1.8 Thesis Organization

This document is organized into six (6) chapters. This first chapter provides an introduction of the thesis. Such as the motivation, objectives, literature survey of some selected papers and outlines the thesis document. Chapter 2 provides introduction to ultra wide band (UWB) communications and UWB background information based on relevant literature and previously published results. Topics like the definition of UWB, the features and related legal issues, the UWB signal representation, modulation and multiple access schemes and the multipath channel are addressed. Chapter 3 and 4 describes the UWB receiver structure, specifically chapter 3 discusses rake reception and chapter 4 is about equalization. Simulation results are presented in Chapter 5. Chapter 6 provides conclusions and suggested future work related to this thesis. Two appendices are included that contain additional simulation results and provide the$Matlab^{®}$ code used in the simulations.

Chapter 2

UWB Communication Technology

2.1 Introduction

As the consumer demand for higher capacity, faster service, and more secure wireless connections increases, new enhanced technologies have to find their place in the overcrowded and scarce radio frequency (RF) spectrum. This is because every radio technology allocates a specific part of the spectrum. As a result, the constraints on the availability of the RF spectrum become more and more strict with the introduction of new radio services. Ultra-Wide Band (UWB) technology offers a promising solution to the RF spectrum drought by allowing new services to coexist with current radio systems with minimal or no interference. This coexistence brings the advantage of avoiding the expensive spectrum licensing fees that providers of all other radio services must pay.

2.2 History of UWB

Ultra-Wide Band communications is fundamentally different from all other communication techniques because it employs extremely narrow RF pulses to communicate between transmitters and receivers. Utilizing short-duration pulses as the building blocks for communications directly generates a very wide bandwidth and offers several advantages.

Ultra-Wide Band (UWB) is a 30-year-old military wireless communications technology. It is not a new technology; in fact, it was first employed by Guglielmo Marconi in 1901 to transmit Morse code sequences across the Atlantic Ocean

using spark gap radio transmitters. However, the benefit of a large bandwidth and the capability of implementing multiuser systems provided by electromagnetic pulses were never considered at that time. Approximately fifty years after Marconi, modern pulse-based transmission gained momentum in military applications in the form of impulse radars, this technology was restricted to military and Department of Defense (DoD) applications under classified programs such as highly secure communications. However, the recent advancement in microprocessing and fast switching in semiconductor technology has made UWB ready for commercial applications. Therefore, it is more appropriate to consider UWB as a new name for a long-existing technology. As interest in the commercialization of UWB has increased over the past several years, developers of UWB systems began pressuring the FCC to approve UWB for commercial use. In February 2002, the FCC approved the First Report and Order (R and O) for commercial use of UWB technology under strict power emission limits for various devices [22].

2.3 What is UWB

Traditional narrow Band communications systems modulate continuous waveform (CW) RF signals with a specific carrier frequency to transmit and receive information. A continuous waveform has a well-defined signal energy in a narrow frequency band that makes it very vulnerable to detection and interception [48]. UWB systems use carrier less, short-duration (picoseconds to nanosecond) pulses with a very low duty cycle (less than 0.5 percent) for transmission and reception of the information [79]. Low duty cycle offers a very low average transmission power in UWB communications systems. The average transmission power of a UWB system is on the order of microwatts, which is a thousand times less than the transmission power of a cell phone!

However, the peak or instantaneous power of individual UWB pulses can be relatively large, but because they are transmitted for only a very short time (T_{on} less than 1 nanosecond), the average power becomes considerably lower. Consequently, UWB devices require low transmit power due to this control over the duty cycle, which directly translates to longer battery life for handheld equipment. Since frequency is inversely related to time, the short-duration UWB pulses spread their energy across a wide range of frequencies-from near DC to several gigahertzes (GHz) with very low power spectral density (PSD).

2.4 UWB Regulations

In order to not to cause interference UWB is subject to regulations. Because UWB uses a large bandwidth it also uses a large part of the frequency spectrum. This spectrum is already very crowded which makes it hard to find an unused spot for UWB. To transmit in part of the spectrum a license is required in order to ensure proper operation of the licensed radio. There are some parts of the spectrum that can be used without a license; examples being the Industrial Scientific and Medical (ISM) bands at 2.4-2.483 GHz and at 5.725-5.875 GHz. However, these bands are already overcrowded. For instance Bluetooth and 802.11a/g operate at these frequencies.

2.4.1 International and Regional Regulatory Frameworks

2.4.1.1 International Telecommunications Union (ITU)

At the global level, the (ITU-R) plays the major role in providing recommendations. In July 2002, ITU-R Study Group 1 established (TG 1/8) to study the compatibility between UWB devices and radio communication services, comprising four Working Groups:

- WG1 - UWB characteristics,
- WG2 - UWB compatibility with other radio services,
- WG3 - UWB spectrum management framework, and
- WG4 - UWB measurement techniques [5].

While the ITU, through its Recommendation SM.1756, identifies a general user licensing regime as best suited for regulating short range UWB communications, it does not recommend a particular spectral mask. The ITU recognizes the sovereign rights of administrations for regulating UWB communication devices within their territorial boundaries and recommends the adoption of rigorous product certification provisions. ITU recommendations are available at [6].

2.4.1.2 Asia Pacific Telecommunity (APT)

The (APT/ AWF) released a report (APT/AWF/REP-17) in August 2007, which provides details of UWB regulatory developments in the Asia Pacific region and abroad. The document states the positions of Japan and Korea on UWB, where unlicensed use has been allowed but with different spectrum masks to those adopted in Europe and the USA. These spectrum masks are “notched”to allow protection in particular bands between 3.1 and 10.6 GHz. The report also

describes the regulatory developments in other relevant administrations around the world such as the USA and Europe. The APT report recommends the adoption of harmonized regulatory provisions to protect existing radio communication services under the following guidelines:

- To allow deployment of UWB devices in parts of the bands below 10.6 GHz while ensuring protection of existing and planned radio communication services,
- To adopt license-exempt or class licensing approach for operating UWB devices,
- To cap the maximum power spectral density at -41.3 dBm/MHz for license exempt or class license devices - whilst incorporating notching requirements to ensure protection of existing and planned stations in the allocated bands; and
- To consider implementing other mitigation techniques to protect the existing radio communication services.

APT/ AWF report can be found in [1].

2.4.1.3 Europe

After years of discussion between UWB supporters and opponents, the EU has finally issued regulations concerning UWB. A final agreement was struck between those who wanted UWB to be introduced with US-like characteristics and those who felt that other radio users needed greater protection. Finally, the similarity to US characteristics is needed because otherwise the equipment is likely to be imported and used anyway [46].

Among the opponents are telecom operators who have paid a large amount of money for their UMTS licenses and do not want to share their spectrum with other users. Other opponents are astronomers, who measure at very low power spectral density and fear large scale use of UWB will interfere with their measurements.

In March 2004 (and later again in 2005), the (EC) mandated the Conference of European Posts and Telegraphs (CEPT) to develop technical implementation measures for the harmonized use of radio spectrum for UWB within the EU. The outcome of the studies undertaken by CEPT resulted in the EC adopting a license exempt regime for UWB, on a non-interference, non- protected basis. The EC defined spectral and power limits for UWB technology below 10.6 GHz

and excluded the deployment of UWB communication devices in fixed outdoor locations, automotive vehicles, railway vehicles and aircraft. This decision came into force in July 2007.

The EC approach is somewhat different to the US regulatory approach, since it mandates more stringent power limits in the spectral mask (as shown in fig. 2.1. These limits reflect the findings of the CEPT studies in Report 64 delivered to ECC in 2005 [3], which identified that the majority of the radio services below 10.6 GHz required more protection than that afforded by the FCC mask. The EC decision also places special consideration on coexistence issues for the protection of specific bands: for example the 3.4-3.8 GHz band. Section 18 of the European Commission decision 2007/131 specifies that "UWB technology without appropriate mitigation techniques should be time limited and be replaced by more restrictive conditions beyond the date 31 December 2010, because there is an expectation that equipment of this type should operate exclusively above 6 GHz in the longer term".

The final decision on UWB regulation in Europe was published in February

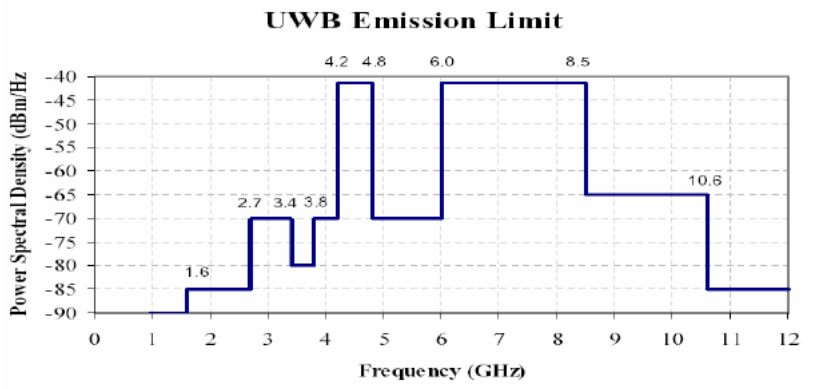

Figure 2.1: Emission limits in Europe (source: APT/AWF (Amended ECC/DEC/(06)04))

2007. This decision specifies the final emission limits for UWB communications, makes provisions for the utilization of mitigation techniques including low duty cycle considerations and other operational conditions.

2.4.2 Country Specific Regulatory Frameworks

2.4.2.1 United States of America

In the USA the limit for unintentional radiation is set by the so-called part 15 rules at -41.3 dBm/MHz [22]. Industries have argued that intentional radiation at this power level should also be permitted, because interference introduced to

other systems at this power level is minimal. In view of this argument and after investigation and measurements by government agencies, industries and the department of defense, the US Federal Communications Commission (FCC) issued the First Report and Order (R and O), which permitted UWB for unlicensed operation and commercial deployment in 2002 [22].

There are three classes of devices defined in the R and O document:

- Imaging systems (e.g., ground penetrating radar systems, wall imaging systems, through-wall imaging systems, surveillance systems, and medical systems),
- Vehicular radar systems and
- Communications and measurement systems.

The FCC allocated a block of unlicensed radio spectrum from 3.1 - 10.6 GHz for the above applications where each category was allocated a specific spectral mask. Note that the FCC only specified a spectral mask, and the bandwidth limitations of a UWB device, but not the type of signal and modulation scheme [22]. The relevant specifications are shown in fig. 2.2.

According to FCC rules, a signal is defined as UWB if its absolute bandwidth,

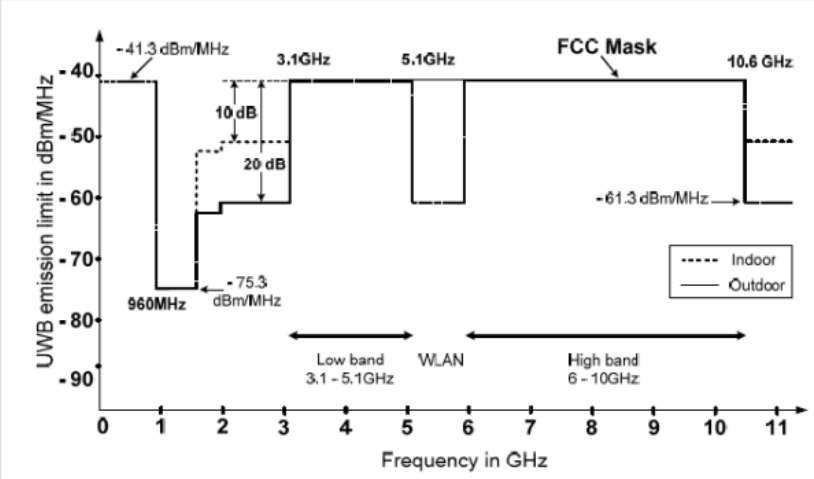

Figure 2.2: FCC Emission Limits for Indoor and Outdoor Communication systems (source: FCC)

is at least 500 MHz or the fractional bandwidth, B_f is greater than 20% [22]. For wireless communications, the FCC regulated power levels are very low (i.e., -41.3 dBm/MHz), which allows UWB technology to overlay with available services such as the GPS and the IEEE 802.11 WLAN. Additionally, the FCC prohibits UWB communications in toys, aircraft or satellites [22].

2.4.2.2 China

MII combined into Ministry of Industry and Information Technology of the People's Republic of China has issued a public call for comments on the draft UWB regulation from May, 28th, 2008 – Sep., 30th, 2008. The MII specification for UWB is shown in fig. 2.3.

Some of the key points of the MII draft were:

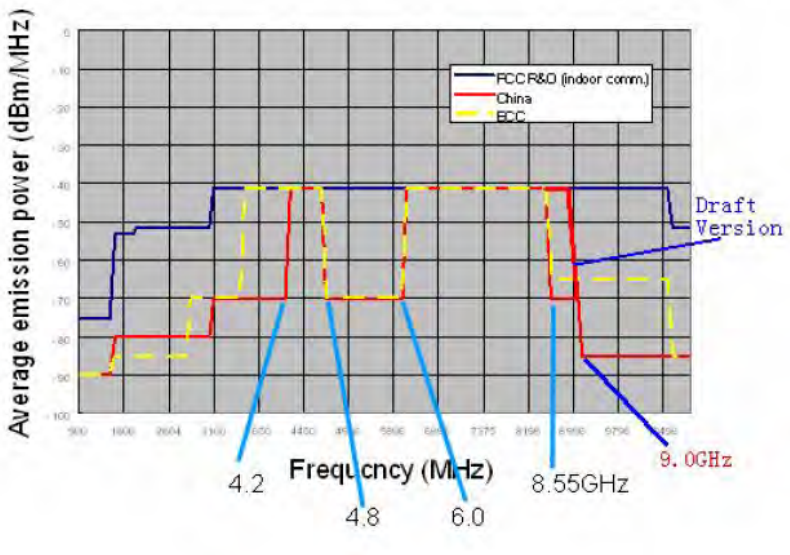

Figure 2.3: Chinese spectrum mask compared to FCC and ECC regulation

- The UWB in band transmission is restricted to the frequency range of 4.2-4.8GHz and 6.0-9.0GHz;
- Device using UWB technology which has UWB transmission in 4.2-4.8GHz is restricted to be used in door.
- Device using UWB technology which has UWB transmission in 6.0-9.0GHz can be used both in door and out door.
- Any UWB radiation from the device using UWB technology (including in band transmission and out of band emission) should meet the requirement.

In 4.2-4.8GHz, the max EIRP can be restricted to -41.3dBm/MHz by the date of 31th Dec, 2010. After that, the UWB devices shall adopt the Interference Relief Technology, such as DAA.

2.4.2.3 Australia

Australia has, so far, adopted a cautious approach. Since publishing a "Background Brief"on UWB in May 2003 [2], the (ACMA), the spectrum regulator

of Australia, has issued a few interim apparatus licenses (authorized under a temporary "scientific assigned"license). The view of the ACMA at this stage is that only applications with low potential to cause interference will be authorized under these interim licensing arrangements.

2.4.2.4 Japan

In Japan, the Ministry of Public Management, Home Affairs, Post and Telecommunications, the Japanese spectrum regulator, proposed a preliminary spectral mask for UWB in September 2005 [8]. This mask includes particular requirements for products operating in the bands 3.4-4.8 GHz. It specifies the implementation of Detection and Avoidance (DAA) technique to ensure coexistence with existing services. The limit of -41.3dBm/MHz has been imposed for unlicensed UWB communications devices operating between 3.4-4.8 GHz and between 7.25-10.25 GHz for indoor applications (see fig. 2.4). On 27 March 2006, Japan's Ministry of Internal Affairs and Communications (MIC) issued a preliminary approval for UWB emissions policy in Japan [7].

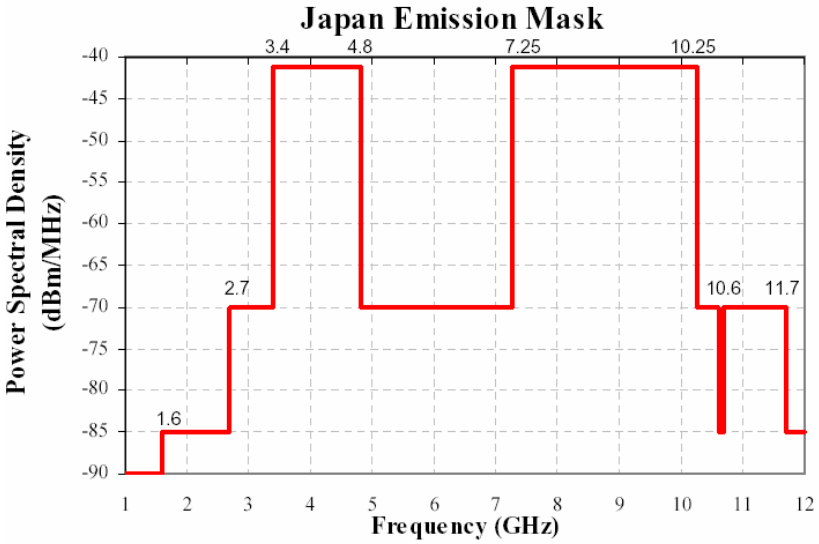

Figure 2.4: Emission limits in Japan (source APT/ AWF)

2.4.2.5 Korea

Similarly to Japan, Korea has adopted a modified FCC mask. MIC of Republic of Korea) released a UWB regulation in July, 2006 [1].

Korea requires use of DAA technology for the UWB devices operating in the 3.1 to 4.2 GHz band from April 2007, and for those operating in the 4.2 to 4.8

MHz band from July 2010. Without DAA in 3.1 4.8GHz band , the emission power is limited to -70dBm/MHz or less. DAA Mechanism is studied to mitigate the emission power to less than -70dBm/MHz within two seconds when a signal stronger than - 80dBm/MHz is detected. The specification for UWB is shown in fig. 2.5.

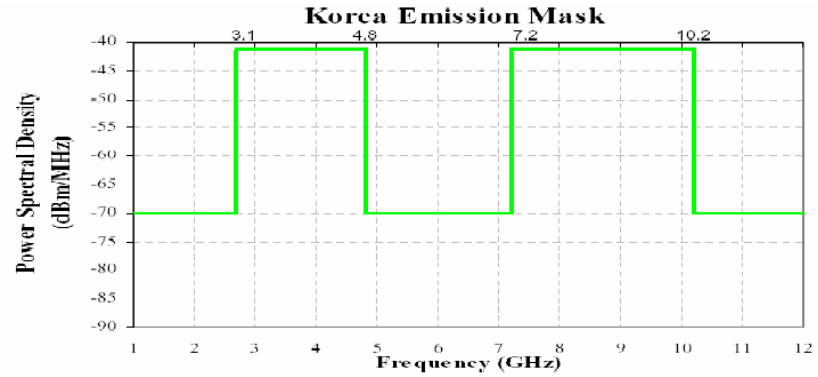

Figure 2.5: Emission limits in Korea (source: APT/AWF)

2.4.2.6 Singapore

IDA, the spectrum regulator of Singapore, launched its UWB program in February 2003. Trials were set up by the IDA to permit controlled UWB emissions within a specific area in Singapore (named as the UFZ) as part of the effort to introduce UWB. In 2007, IDA released an emission mask and technical specifications for UWB devices [4] (see fig 2.6. This resolution specifies rules similar to those established by Europe.

2.5 Advantages and Challenges of UWB

The nature of the short-duration pulses used in UWB technology offers several advantages over narrow band communications systems. In this section, we discuss some of the key benefits that UWB brings to wireless communications.

One of UWB's advantage is it's ability to Share the Frequency Spectrum. The FCC's power requirement of -41.3 dBm/MHz, equal to 75 nano watts/ MHz for UWB systems [22], puts them in the category of unintentional radiators, such as TVs and computer monitors. Such power restriction allows UWB systems to reside below the noise floor of a typical narrow band receiver and enables UWB signals to coexist with current radio services with minimal or no interference. However, this all depends on the type of modulation and multiple access schemes

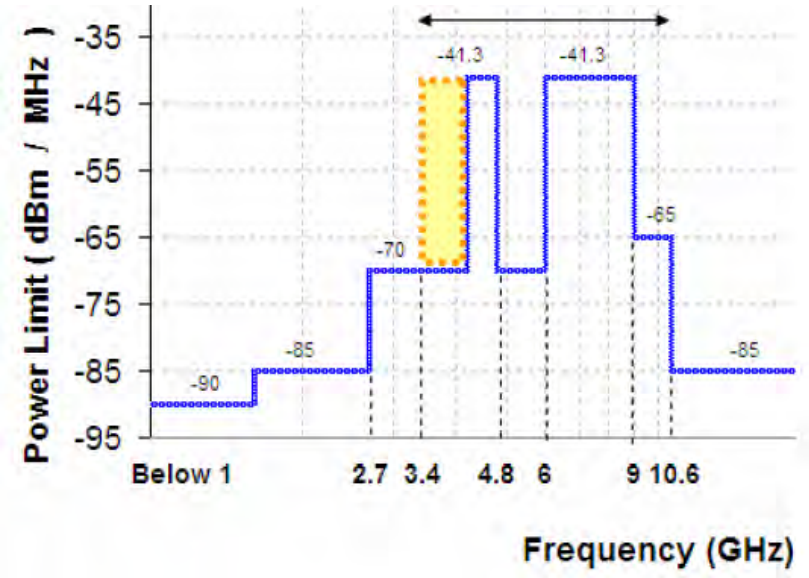

Figure 2.6: Emission limits in Singapore (source: IDA)

used for data transfer in a UWB system [53]. Some modulation schemes generate undesirable discrete spectral lines in their PSD, which can increase the chance of interference to other systems [53]. Fig. 2.7 illustrates the general idea of UWB's coexistence with narrow band and wide band technologies.

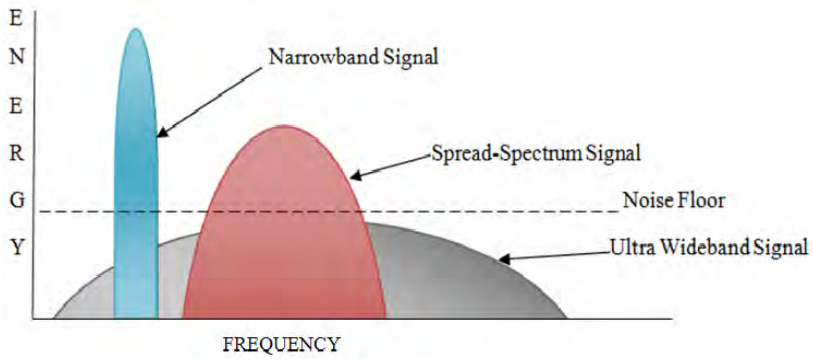

Figure 2.7: Coexistence of UWB signals with narrowband and wideband signals in the RF spectrum

The other benefit from using UWB is acquiring large channel capacity. Since Hartley- Shannon's capacity formula tells us channel capacity is directly proportional to bandwidth , and UWB has very large bandwidth [22], large channel capacity can be achieved from UWB communications systems

The other advantage is it's ability to work with low Signal-to-Noise Ratios. The Hartley-Shannon formula for maximum capacity also indicates that the channel capacity is only logarithmically dependent on SNR. Therefore, UWB communications systems are capable of working in harsh communication channels with low SNRs and still offer a large channel capacity as a result of their large bandwidth.

Because of their low average transmission power[22], UWB communications systems have an inherent immunity to detection and intercept [48]. In addition, UWB pulses are time modulated with codes unique to each transmitter/receiver pair [77]. The time modulation of extremely narrow pulses adds more security to UWB transmission, because detecting picosecond pulses without knowing when they will arrive is next to impossible. Therefore, UWB systems hold significant promise of achieving highly secure, low probability of intercept and detection (LPI/D) communications that is a critical need for military operations.

The other merit of UWB communication system is it's resistance to Jamming [48]. Since UWB spectrum covers a vast range of frequencies from near DC to several gigahertz and offers high processing gain for UWB signals[77]. The frequency diversity caused by high processing gain makes UWB signals relatively resistant to intentional and unintentional jamming, because no jammer can jam every frequency in the UWB spectrum at once. Therefore, if some of the frequencies are jammed, there is still a large range of frequencies that remains untouched.

The other advantage is it gives better performance in multipath channels [58]. Because the transmission duration of a UWB pulse is shorter than a nanosecond in most cases [77][75], the reflected pulse has an extremely short window of opportunity to collide with the LOS pulse and cause signal degradation. In fact, by using Rake Reception techniques we can resolve individual multipath components to have better BER performance.

UWB has superior penetration properties. The low frequencies included in the broad range of the UWB frequency spectrum have long wavelengths, which allows UWB signals to pass a variety of materials, including walls [39]. This property makes UWB technology viable for through-the-wall communications and ground-penetrating radars.

UWB communication system has simple transceiver architecture [11]. As mentioned earlier, UWB transmission is carrier less [77], meaning that data is not modulated on a continuous waveform with a specific carrier frequency, as in narrow band and wide band technologies. Carrier less transmission requires fewer RF components than carrier based transmission. For this reason UWB transceiver

architecture is significantly simpler and thus cheaper to build. The transmission of low-powered pulses eliminates the need for a power amplifier in UWB transmitters. Also, because UWB transmission is carrier less, there is no need for mixers and local oscillators to translate the carrier frequency to the required frequency band; consequently there is no need for a carrier recovery stage at the receiver end.

UWB technology for communications is not all about advantages. In fact, there are many challenges involved in using nanosecond-duration pulses for communications. Some of the main difficulties of UWB communications will be discussed next.

Realizing efficient wideband front end devices for receiving UWB signals is a challenge. Losses coming from the difficulty in having power efficient antennas (especially electrically small ones), pulse shape distortions and ringing due to filter characteristics of the antenna are major challenges in implementing UWB front-end in portable devices [29][49]. Difficulty to match Wideband LNA and the fact that Wideband LNAs are power consuming [11] are also major challenges in implementing UWB front-end in portable devices.

The other main challenge of UWB technology is pulse-shape distortion. The weak and low-powered UWB pulses can be distorted significantly by the transmission link. Since Friis transmission formula says that the received signal power decreases quadratically with the increase in frequency, the wide range of frequencies that is covered by the UWB spectrum affect the received power drastically and thus distorts the pulse shape. This will limit the performance of UWB receivers that correlate the received pulses with a predefined template such as classical matched filters.

The other challenge is the need for fast sampling. In order to sample nanosecond pulses, very fast (on the order of gigahertz) ADCs are needed. Moreover, the strict power limitations and short pulse duration make the performance of UWB systems highly sensitive to timing errors such as jitter and drift [33]. This can become a major issue in the success of pulse-position modulation (PPM) receivers, which rely on detecting the exact position of the received signal.

2.6 UWB Signals

As defined by the FCC's First Report and Order, UWB signals must have bandwidths of greater than 500 MHz or a fractional bandwidth larger than 20 percent at all times of transmission [22]. A UWB signal can be any one of a variety of wideband signals, such as Gaussian [75], chirp, wavelet, or Hermite-based short-

duration pulses [15].

Since Gaussian pulses have wider bandwidth, no DC component and no side lobes in their spectrum compared to other pulses [75], most of the time UWB systems use these pulses. This thesis work will also use those pulses.
The Gaussian monocycle is Given by:

$$W(t) = \frac{A}{\sqrt{2\pi}\sigma} \exp(-\frac{t^2}{2\sigma^2}) \tag{2.1}$$

Where σ is the variance or time constant and is defined as:

$$\sigma = \frac{0.5887}{B_{-3db}} \tag{2.2}$$

Here B is the -3dB bandwidth of the Gaussian mono cycle. The Fourier transform is:

$$W(f) = A \exp\{-\frac{(2\pi f\sigma)^2}{2}\} \tag{2.3}$$

In the frequency domain the pulse shape and the pulse width of the transmitted pulse select the spectral allocation of the UWB signal. The PSD of the first derivative Gaussian pulse does not meet the FCC requirement no matter what value of the pulse width is used [66][62]. Therefore, a new pulse shape must be found that satisfies the FCC emission requirements. One possibility is to shift the center frequency and adjust the bandwidth so that the requirements are met. This could be done by modulating the mono cycle with a sinusoid to shift the center frequency. UWB, however, is a carrier less system [77]; modulation will increase the cost and complexity. Therefore, alternative approaches are required for obtaining a pulse shape which satisfies the FCC mask.

The theoretical analysis shows that, the higher the derivative order of the Gaussian pulses the better the roll-off and increase in number of zero crossings (fig. 2.10), which shifts the transmitted spectra to the higher frequencies (fig. 2.82.9), so the pulse can satisfy the FCC spectral mask without requiring additional pulse-shaping filters [66].

The k^{th} order derivative of the Gaussian mono cycle is recursively given by [81]:

$$W^{(k)}(t) = -\frac{n-1}{\sigma^2} W^{(k-2)}(t) - \frac{t}{\sigma^2} W^{(k-1)}(t) \tag{2.4}$$

With Fourier transform [81]:

$$W_k(f) = A(j2\pi f)^k \exp\{-\frac{(2\pi f\sigma)^2}{2}\} \tag{2.5}$$

Analysis in [66], shows that one needs to take at least the 7^{th} derivative to the Gaussian pulse in order to fit the pulse power spectral density (PSD) inside the

FCC mask for the outdoor applications (see fig. 2.9). It is shown in [66][65], that the PSD of the 5^{th} derivative Gaussian pulse meet the FCC mask for the indoor applications (see fig. 2.8).

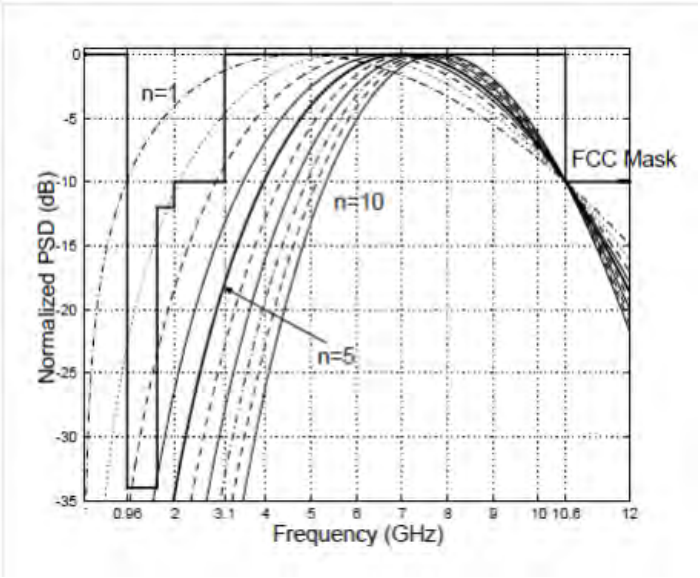

Figure 2.8: PSD of the higher-order derivatives of the Gaussian pulse for UWB indoor systems

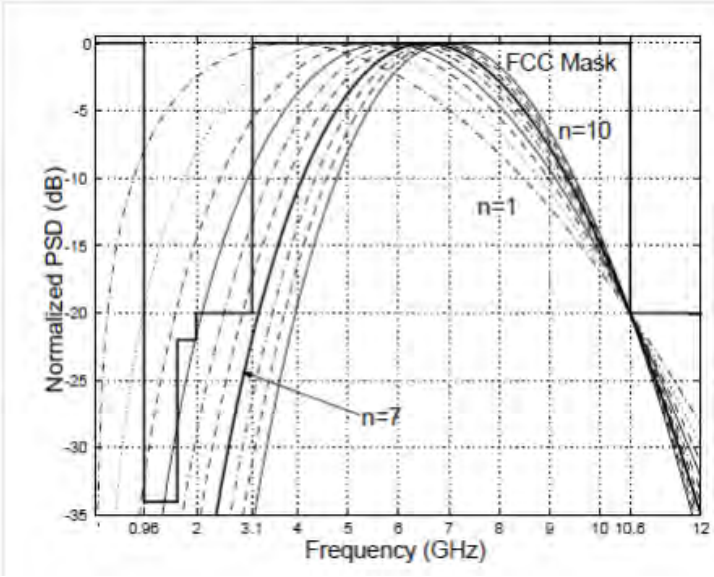

Figure 2.9: PSD of the higher-order derivatives of the Gaussian pulse for UWB outdoor systems

As it can be seen from fig. 2.10, monocycle waveform has the maximum positive

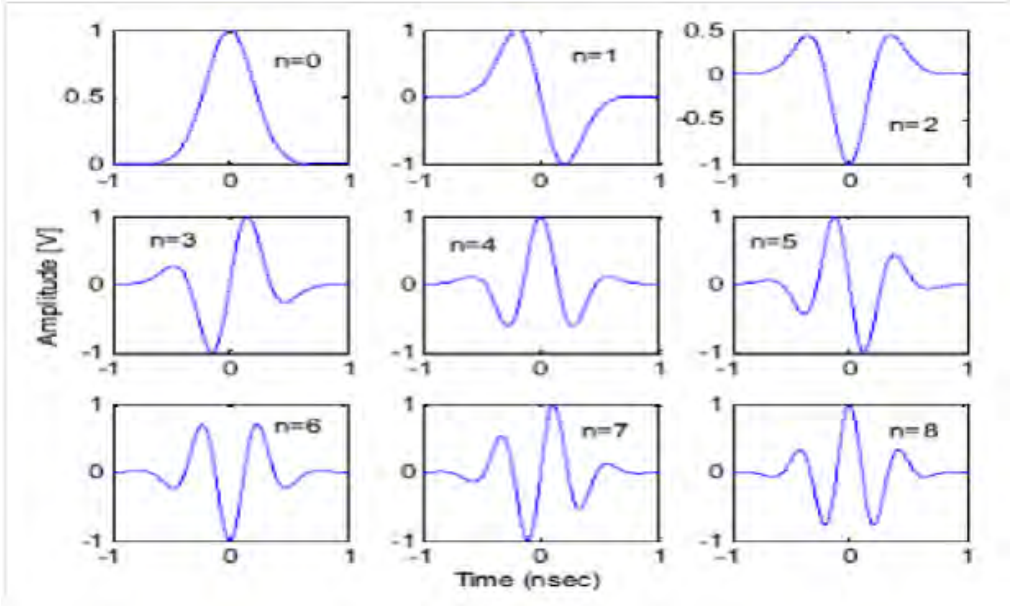

Figure 2.10: Time domain representation of the first 8 derivatives of the Gaussian monocycle

amplitude at t=0 for even order Gaussian pulses and positive slope at t=0 for odd order pulses. And as it can be seen from fig. 2.8 and 2.9, as the order increases the usable bandwidth decreases. Therefore, optimum pulse shape is selecting lower even order Gaussian pulse with a reasonable pulse width so that the spectrum becomes compliant with FCCs requirement. Hence, in the remainder of this thesis work a 2^{nd} derivative Gaussian monocycle with duration of 0.5 ns (T_p =0.5 ns), which results in a center frequency of 3.9GHz will be used. Since $T_p \approx 7\sigma$;σ=71.4 ps. The 2^{nd} derivative of a Gaussian monocycle is then given by:

$$w(t) = A\left(\frac{t^2}{\sqrt{2\pi}\sigma^5} - \frac{1}{\sqrt{2\pi}\sigma^3}\right)\exp\left(-\frac{t^2}{2\sigma^2}\right) \tag{2.6}$$

UWB Antenna in the transmitter and receiver has an effect of high pass filter, or equivalently saying time-derivative [21][49]. Considering this, at the transmitter side, if an even order, 2^{nd} Gaussian pulse is generated, an odd order 3^{rd} derivative pulse will be sent in the air; at the receiver side, the signal output by the receiver antenna will be an even order 4^{th} derivative pulse. On the other side, given the ultra wide bandwidth of the UWB signal, and the fact that it is very difficult for the transmitting and receiving antenna to have a flat spectrum response over so wide a bandwidth and in all direction (omni direction), the antenna will bring distortion to the UWB pulses, both in time domain and in spectrum [63]. Therefore, UWB antennas need to be optimized for a wide range of frequencies, and pulse waveform distortion by the antennas is no longer negligible, as is reasonably assumed for carrier-based systems [63]. But, In this thesis work we will not dis-

cuss the design and properties of UWB antenna. Hence, for simplicity we assume that the antenna brings no time-derivative or distortion to the pulses.

2.7 UWB Signal Modulation Schemes

Information can be encoded in a UWB signal in various methods. Due to UWB regulations, UWB transmit power will likely be limited by the power spectral density (PSD) of the transmitted signal, affecting the choice of modulation in two ways. First, the modulation technique needs to be power efficient. In other words, the modulation needs to provide the best error performance for a given energy per bit. Second, the choice of a modulation scheme affects the structure of the PSD and thus has the potential to impose additional constraints on the total transmitted power. As we compare different modulation schemes, therefore, we examine both the power efficiency and the effect of the modulation on the PSD.

In the sections that follow, we examine several modulation schemes that have been proposed for UWB including pulse-position modulation (PPM) and several forms of pulse amplitude modulation (PAM) including binary phase-shift keying (BPSK) and on-off keying (OOK).

2.7.1 Bi phase Modulation

In generic pulse modulation terms, PAM transmits data by varying the amplitude of each pulse based on binary data. The most common form of PAM in UWB communications is 2-PAM, or bi phase modulation, where the polarity of a pulse is modulated. In this situation, a positive pulse is transmitted for a "1"and a negative pulse is transmitted for a "0". The signaling waveform for the bi phase modulation technique is shown in fig. 2.11b and mathematically described as [34] :

$$s(t) = \sum_{j=-\infty}^{\infty} b_j w(t - jT_f) \tag{2.7}$$

where:

s(t) is the transmitted UWB signal
$b_j \, \epsilon \, \{-1, 1\}$ data bits
w(t) is the pulse shape
T_f is the frame period in seconds

One advantage of bi phase modulation is its improvement over OOK in BER performance, as the Eb/No is 3 dB less than OOK for the same probability of bit error, as shown in fig. 2.13. The probability of bit error for bi phase modulation

assuming matched filter reception is [34] :

$$P_e = Q(\sqrt{\frac{2E_b}{N_0}}) \tag{2.8}$$

where:

Q is the Q function
E_b is the average energy per bit in Joules
N_0 is the noise power at the detector in Joules

The Q-function is defined by [16] :

$$Q(x) = \frac{1}{\sqrt{2\pi}} \int_x^\infty e^{\frac{-\lambda^2}{2}} d\lambda \tag{2.9}$$

The PSD for BPSK is given by[74]:

$$\Phi_{ss,BPSK}(f) = \frac{1}{T_f}|W(f)|^2 \tag{2.10}$$

where:

W(f) is the Fourier transform of w(t)

Another benefit of biphase modulation is its ability to eliminate spectral lines due to the change in pulse polarity as it is shown in eq. 2.10. This aspect minimizes the amount of interference with conventional radio systems. A decrease in the overall transmitted power could also be attained, making biphase modulation a popular technique in UWB systems when energy efficiency is a priority.

2.7.2 OOK

OOK, or otherwise known as unipolar signaling in the analog baseband world, is a simple pulse modulation technique where a pulse is transmitted to represent a binary "1", while no pulse is transmitted for a binary "0". The baseband representation, which is illustrated in fig. 2.11a, of the transmitted signal is [34]:

$$s(t) = \sum_{j=-\infty}^{\infty} b_j w(t - jT_f) \tag{2.11}$$

where:

$b_j \, \epsilon \, \{0, 1\}$ data bits

One obvious advantage to using OOK is the simplicity of the physical implementation, as one pulse generator is necessary, as opposed to two, as is the case with biphase modulation. A single RF switch can control the transmitted pulses by switching on for a "1"data bit and off for a "0"data bit. This effortless

transmitter configuration makes OOK popular for less complex UWB systems. Although OOK has a very straightforward implementation, there are numerous

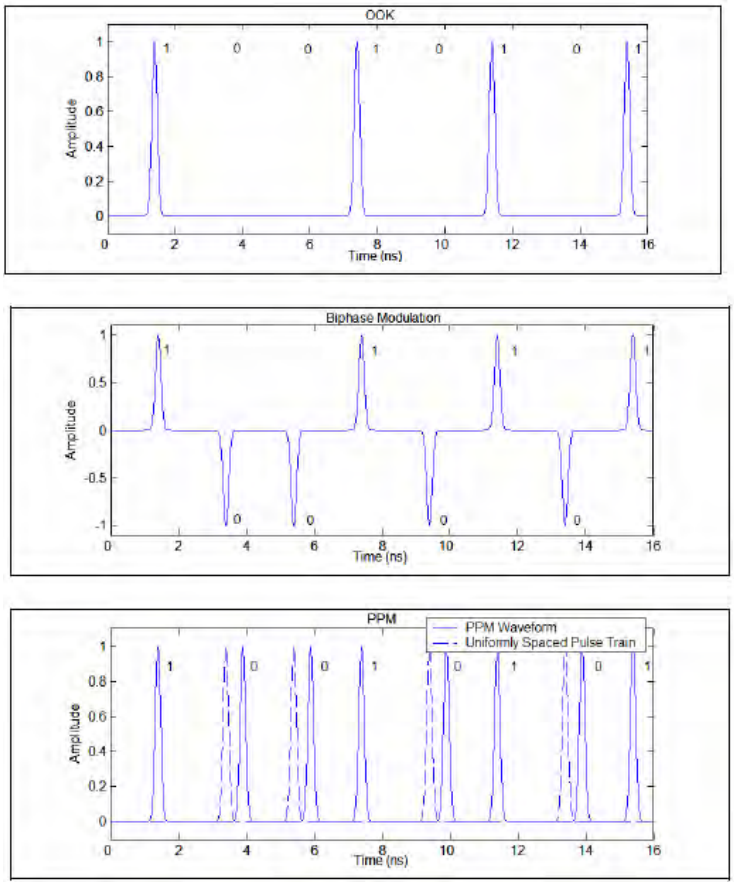

Figure 2.11: Common UWB Modulation Techniques (a) On-Off Keying, (b) Biphase Modulation, (c) Pulse Position Modulation with Binary "0" Offset from the Regularly Spaced Pulse Train (Binary PPM)

system drawbacks. In either a hardware or software based receiver design, synchronization can be easily lost if the data contains a steady stream of "0's". Also, the BER performance of OOK is worse than biphase modulation due to the smaller symbol separation for equal symbol energy. As shown in fig. 2.12, the difference in pulse amplitude is A, whereas in biphase modulation the difference is twice the pulse amplitude, or 2A. Bit errors occur less often when the amplitude difference is greater because more distortion is necessary in the channel to affect a bit decision. This effect is demonstrated in the probability of bit error for baseband OOK using a matched filter receiver, which is compared in fig. 2.13 with biphase modulation and binary PPM [16]:

$$P_e = Q(\sqrt{\frac{E_b}{N_0}}) \tag{2.12}$$

The PSD for OOK is given by[74]:

$$\Phi_{ss,OOK}(f) = \frac{1}{T_f}|W(f)|^2 + \frac{1}{{T_f}^2}\sum_{k=-\infty}^{\infty}|W(\frac{k}{T_f})|^2\delta(f-\frac{k}{T_f}) \tag{2.13}$$

where:

$\delta(f)$ is a unit impulse

As we see from eq. 2.13 OOK results in discrete spectral lines in the PSD of the UWB signal. In a system where transmit power must be constrained to meet limits on power spectral density, the presence of spectral lines may lead to reduction in total transmit power unless the lines can be reduced in some other way.

2.7.3 Binary PPM

The last popular UWB modulation scheme to be discussed is PPM, which is a technique where the timing of each pulse is altered to transmit data instead of varying the amplitude. The simplest form of PPM is binary PPM, where a pulse in a uniformly spaced pulse train represents a "0"and a pulse offset in time from the pulse train represents a "1". Conceptually, the binary PPM technique is shown in fig. 2.11c and stated in equation form as [34]:

$$s(t) = \sum_{j=-\infty}^{\infty} w(t - jT_f - \delta b_j) \tag{2.14}$$

where:

$b_j \epsilon \{0, 1\}$ data bits

δ is the modulation index

One of the disadvantages of PPM is its BER performance. As shown in fig. 2.12, the distance between symbols is the same as in OOK. This lack of signal energy causes binary PPM to have the same probability of bit error as OOK, or 3 dB worse than biphase modulation. This similarity between binary PPM and OOK is displayed in fig. 2.13 and the probability of bit error equation for binary PPM can be described by eq. 2.12 [34].

After considering the advantages and disadvantages of each of the mentioned modulation schemes, this thesis work used BPSK or BPAM modulation throughout the work.

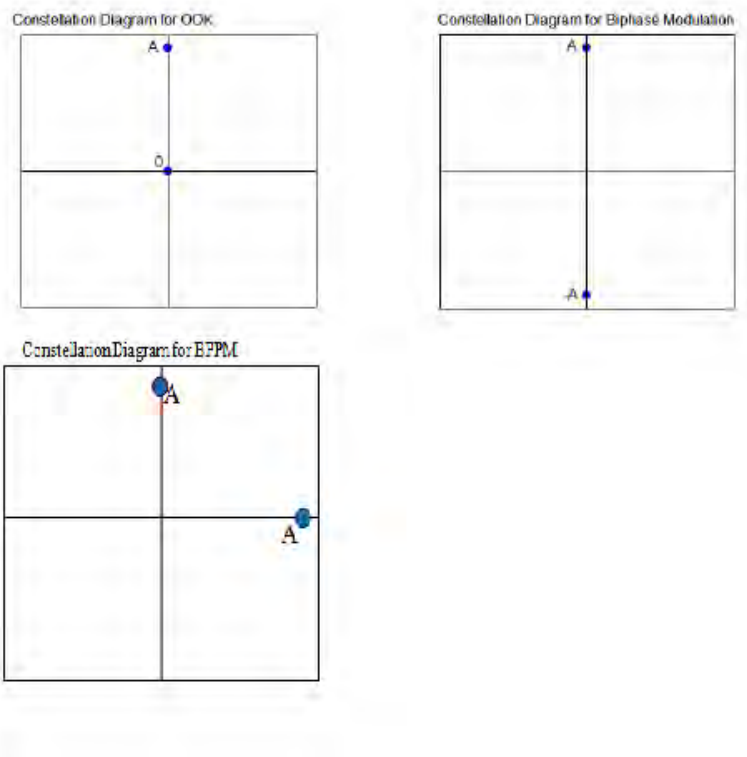

Figure 2.12: Constellation Diagram of OOK, Bi phase Modulation, and Binary PPM

2.8 Spectrum Spreading

UWB systems can use spread spectrum techniques, along with modulation, to enable multiple access (MA) capability; Time Hopping (TH) and Direct Sequence (DS) are two commonly used methods.

In Time Hopping Pulse Position Modulation (TH-PPM), the information in a train of Gaussian pulses is contained in the pulse position relative to the repetition time interval T_f. To allow asynchronous communications and multiple access, a time hopping factor delay is added to offset the position of each signal of user k. A data modulation factor delay is included to shift pulses in a binary PPM scheme.

At the reception, one can achieve processing gain due to the pulse repetition (repetition coding) which is given by:

$$G_N = 10 \log 10(N) \quad [dB] \tag{2.15}$$

where: N is the number of pulses per a single information bit.

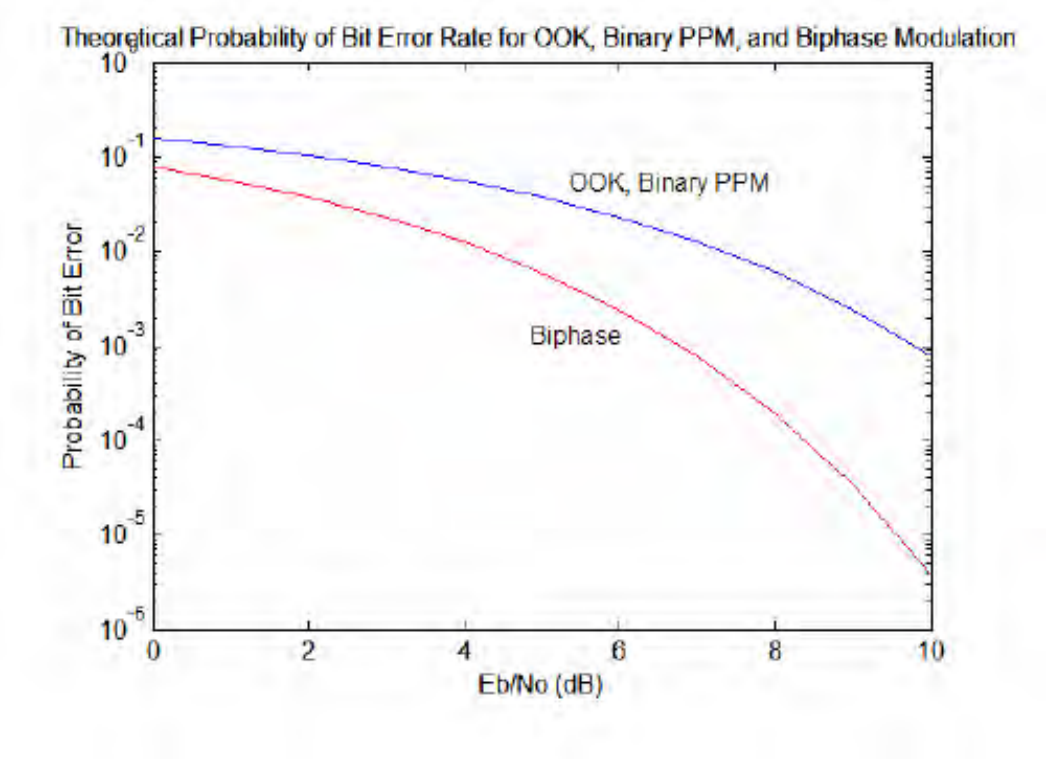

Figure 2.13: Theoretical Probability of Bit Error Rates for OOK, Binary PPM, and Bi phase Modulation

And since in TH-UWB the pulse does not necessarily occupy the entire chip period, the duty cycle can be extremely low. Therefore, Additional processing gain in TH-UWB is brought in by the low duty cycle called pulse processing gain [36]. Duty cycle is the ratio of the pulse width T_p and the pulse repetition interval T_f. Processing gain due to the low duty cycle is given by:

$$G_d = 10 \log 10(\frac{T_f}{T_p}) \quad [dB] \tag{2.16}$$

Total processing gain in the TH-UWB concept is therefore:

$$G_t = G_N + G_d \quad [dB] \tag{2.17}$$

The second form of multiple access modulation is Direct Sequence Binary Phase Shift Keying (DS-BPSK) [23]. Rather than modulate the signal by a time delay, DS-UWB uses 180^o phase shifts for binary signaling. TH-PPM spreads the signal in time to obtain multiple access. DS-BPSK spreads the signal by multiplying each pulse by a user specific code of amplitude ± 1. To distinguish users, a distinct spread spectrum code is assigned.

The processing gain in DS-UWB comes only from the pulse repetition, i.e, G_N. Since $T_f = T_p$ duty cycle for DS-UWB becomes 100% , therefore G_d becomes zero. Hence, total processing gain in the DS-UWB concept is equals to processing gain due to the pulse repetition (repetition coding).

Though TH-PPM and DS-BPSK appear to be the most common forms of signal modulation in UWB communications, other modulation techniques can be employed. Literature is available on virtually every type of UWB modulation scheme, including: Pulse Position Modulation (PPM), Binary Phase Shift Keying (BPSK)or antipodal signaling, On-Off Keying (OOK), and Pulse Amplitude Modulation(PAM).

Several papers have evaluated the strengths and weaknesses of TH-PPM, TH-BPSK, and DS-BPSK [23][68]. These first findings indicate that DS may reduce the impact of multiuser interference but time-hopping is more efficient at reducing multipath and narrow band interference effects. For a simple matched filter receiver, it is claimed that bipolar modulation performs better than TH-PPM. In [68], it is stated that DS-BPSK is more suitable for high data rate systems since it can accommodate higher PRF values than time-hopping codes. But, the TH spreading would force the PRF to be smaller, and thus limit the system to lower data rates. This is because in order to have a TH spreading code with good correlation properties, the range of values of the spreading code must be reasonably large. This forces the T_f to be larger, i.e., the PRF to be smaller.

Since the original objective of this thesis is proposing better receiver for UWB systems with high data rate, DS spreading sequence is chosen.

2.8.1 Time Hopping and Pulse Position Modulation

Historically, Time Hopping PPM (TH-PPM) has become synonymous with time-modulated UWB. In a TH-PPM pulse train of Gaussian monocycles, signal information is contained in the pulse position relative to repetition time interval T_f. For instance, a pulse arriving at T_f is considered a binary value 0 while a pulse arriving just after the reference time is deemed a 1. A mathematical TH-PPM representation is[62]:

$$s(t) = \sqrt{N_c P} * \sum_{i} \sum_{j=0}^{N_s-1} w(t - iT_s - jT_f - c_{iN_s+j}T_c - d_i\delta) \tag{2.18}$$

where:

P = Average power (one code period)
N_c = Spreading code length

t = Transmitter's clock time
T_s = Symbol period
T_c = Spreading code chip period
w = Transmitted monocycle waveform
T_f = Pulse repetition time or frame time
c_j = Unique time-hopping code
d_i = Data sequence of the transmitter
δ = Modulation index

2.8.2 Direct Sequence and Binary Phase Shift Keying

Similar to conventional DSSS, DS-UWB has a high duty cycle, phase coded sequence of wide band pulses transmitted at near gigahertz rates. The receiver uses a similar code to convert (de-spread) the signal back to its original data rate. In this way, multiple pulses are encoded to represent one data bit.

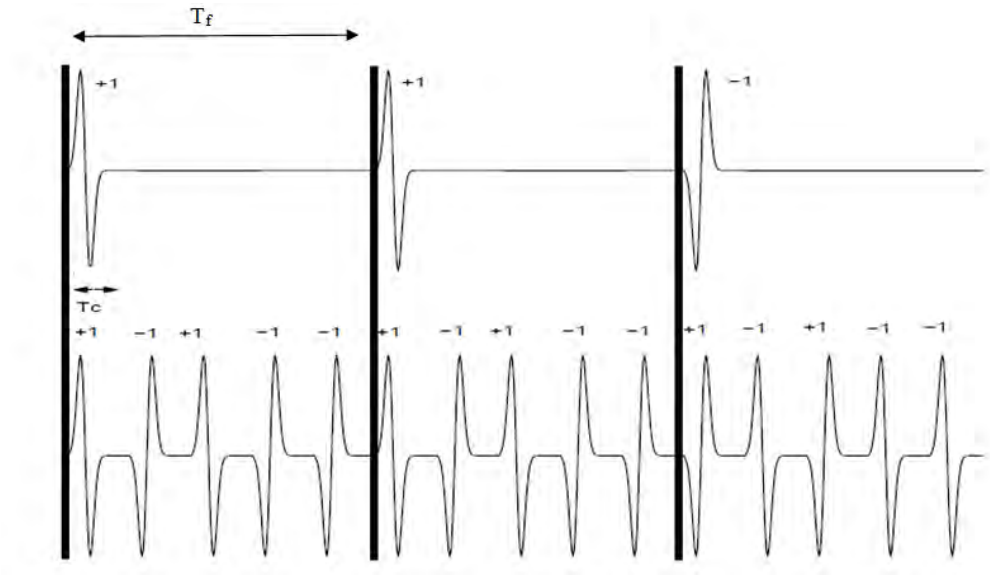

Figure 2.14: Direct Sequence Binary Phase Shift Keying for UWB Illustration

The use of DS-BPSK modulation for UWB communications, as described in [23], is illustrated in fig. 2.14. The DS-UWB technique uses 180^o phase shifts to enable binary signaling as [80]:

$$s(t) = \sqrt{P} * \sum_{j=-\infty}^{\infty} \sum_{n=0}^{N-1} b_j c_n * w(t - jT_s - nT_c) \tag{2.19}$$

where:

N = Spread spectrum processing gain

b_j = Modulated data symbol value (± 1)
T_s = symbol period
c_n = Spreading chip value (± 1)

The DS-BPSK modulation technique spreads the signal across each PRI by multiplying each pulse by a user specific code of amplitude ± 1 and duration T_c. To distinguish users, the PRI T_f is an integer multiple of T_c so that multiple pulses are used to represent the multiple chips of the spread spectrum code.

The need for DS CDMA arises in cellular communication systems like IS-95, CDMA2000 and UMTS or in satellite navigation system where all users use the same bandwidth at the same time but with different spreading codes called Pseudo random codes (PN codes). PN code may be broadly divided into two groups namely, Orthogonal codes like Walsh Hadamard codes and Non-orthogonal codes like Maximal-length codes(m- sequence), Gold codes, Kasami codes.

2.8.2.1 Orthogonal Codes

Orthogonal codes are those, which provide a zero cross correlation when there is no offset between the codes. They make use of Orthogonality property, which refers to dot product between the two spreading codes, is equal to zero. Hadamard transform is one of the best known code expansion techniques to generate orthogonal codes.

Walsh and Hadamard Sequences are generated by mapping codeword rows of a Hadamard transform. In practice, Walsh sequences provide zero cross correlation when there is zero offset between the sequences, but in order to provide a zero offset all users have to be synchronized in time. This problem can be solved by using a pilot sequence for synchronization.

2.8.2.2 Non Orthogonal Codes

Maximal Length Sequences are the longest codes that can be generated using a linear feedback shift registers [LFSR]. It is not completely random but it is generated by a well defined logic. The same logic is used at the transmitter and receiver. The pseudo noise sequences can be generated by a feedback shift register and the combinational logic.The data of one shift register is shifted to the next one whenever a clock pulse is applied. The output of these shift registers is given to the logic circuit depending upon the outputs of the shift registers the output of the logic circuit is decided. This logic circuit output is given as the input to the first shift register. The pseudo random sequence is generated at the output of the last shift register. At each pulse of the clock, the state of the shift register is shifted to the next shift register and logic circuit output is shifted in

the first shift register.

One of m-sequence drawback is it's inability to be immune to cross-correlation problems, and they may have large cross-correlation values which are not good in case of multiple access interfaces, it causes difficulty in differentiating users [18]. The cross correlation between two different sequences has a value equal to $\frac{1}{2m-1}$ where m is the number of shift registers.

Gold Sequences are obtained by linearly combining two m-sequences. If the m-sequences that are modulo-2 added to produce a gold codes are chosen randomly, then the cross correlation of the code may be quite poor. Thus, Gold sequences are generated by the modulo-2 addition of preferred pairs of m-sequences. Finding preferred pairs of m-sequences is necessary in defining sets of Gold codes.

Gold codes provide a very large number of codes and has small cross correlation value. Therefore, by using Gold codes we can attain less interference between the users. Due to their rapid synchronization and good correlation features these codes are widely used in GPS systems.In this work also these codes will be used as spreading sequence.

Kasami Sequences Have properties that are similar to preferred sequences used to generate Gold codes, and they are also derived from m-sequences. There are two sets of kasami sequences namely, small set and large set. A similar procedure to that used for generating Gold sequence will generate the small set of Kasami sequences.

As Kasami codes have better cross-correlation and auto correlation properties than Gold codes, they are widely used in 3G applications.

2.9 UWB Channels and their Models

As it has been said earlier UWB systems spread the data over larger bandwidth (according to FCC bandwidth should be $\geq$ 500 MHZ). The large bandwidth of UWB channels may raise new effects in the receiver compared to narrow band wireless channels.

Since a unique characterization of the channel guarantees a fair comparison of the different proposals, IEEE 802.15.3a formed a subgroup for the development of channel model. In order to develop a common channel model, the IEEE 802.15.3a standards body considered three (3) possibilities. These are:

- The tap-delay line Rayleigh fading model [24],

- The Saleh-Valenzuela (S-V) model [59] and
- The Δ-K model [30]

as well as several novel modifications to these approaches that better matched the measurement characteristics [51]. Each channel model was parameterized in order to best fit the important channel characteristics. Although many good models were contributed to the group, the model finally adopted was based on a modified S-V model [59] that seemed to best fit the channel.

2.9.1 UWB Propagation

We find for narrowband propagation that each interaction of a transmitted (narrowband) wave with another object leads only to an attenuation, phase shift, and change in direction (and thus delay) [38]. But, in UWB the transmitted signal contains many frequency components, each multipath components "sees" a different propagation environment. For example, the diffraction coefficient of a corner changes as the frequency changes from 100 MHz to 1GHz [52]. The channel description is then given by:

$$h(\tau) = \sum_{i=1}^{N} \alpha_i \chi_i(\tau) x \delta(\tau - \tau_i) \tag{2.20}$$

where:

$\chi_i(\tau)$ denotes the distortion of the i-th echo by the frequency selectivity of the interactions with the environment.
α_i is the gain of the i^{th} MPC,
τ_i is the delay of the i^{th} MPC

Another important difference to narrow band models arises from the fine delay resolution of UWB receivers (proportional to the inverse bandwidth). The number of echoes (multipath components) falling into each resolvable delay bin cannot be assumed to be very large [27], due to the existence of large bandwidth, therefore central limit theorem is not applicable. Hence, the small-scale statistics of the amplitude fading are not Rayleigh (or Rice) [59] anymore. Appropriate statistical distributions for the description of this effect will be mentioned in next section (Section 2.9.2).

Finally, we notice that in most narrowband channels, the impulse response is "dense" in the sense that each resolvable delay bin contains significant energy. This is not necessarily the case for UWB systems. Not every resolvable delay bin contains MPCs [51], so that delay bins containing MPCs are interspersed

with empty delay bins. The resulting PDP is becomes sparse. Therefore, it is necessary to characterize the likelihood that this happens, and that an empty bin is followed by a full one.

2.9.2 IEEE 802.15.3a Channel Model

The model was developed by the IEEE 802.15.3a standardization group for UWB communications systems in office and residential indoor environments with a range of less than 10 m [51]. It distinguishes between four radio environments:

- LOS with a distance between TX and RX of 0 - 4m (CM1),
- NLOS for a distance 0 - 4m (CM2),
- NLOS for a distance 4 - 10m (CM3) and
- An extreme NLOS multipath channel for a distance of 4-10m (CM4).

The model is a modified Saleh-Valenzuela model [59]. The IEEE 802.15.3a task group chooses the S-V model for the following reasons.

- UWB channel measurement shows that the multipath components are arriving in a cluster form unlike narrowband signal.
- The arrival time and the inter-arrival time of multipath components of a UWB signal is Poisson and exponentially distributed respectively.
- The S-V model requires four different parameters to describe an environment: the cluster arrival time, the ray arrival time within a cluster, the cluster decay factor, and the ray decay factor. These four parameters provide great flexibility to model different environments
- Unlike Δ-K model the S-V model used two independent Poisson distribution to model the cluster and ray arrival time. The $\Delta - K$ model have used single Poisson distribution to model the cluster and ray arrival time by changing the average. Hence, S-V model provide more flexibility in determining the cluster and ray arrival times when compared to the Δ-K model and provide a more accurate model of the paths arrival times.

The arrival of MPCs is modeled by using a statistically random process; it is based on Poisson distribution. In other words, the inter arrival time between multipath components is based on exponential distribution. The multipath arrival of UWB signals are grouped into two categories: cluster arrival and ray arrival within a cluster. This model requires four parameters to describe indoor channel environments. They are cluster decay factor (Γ), ray decay factor (γ),

Table 2.1: Parameter for the IEEE UWB Channel Model

Model Parameters	CM1 or case A	CM2 or case B	CM3 case C	CM4 or case D
Λ ($\frac{1}{nsec}$)	0.0233	0.4	0.0667	0.0667
λ ($\frac{1}{nsec}$)	2.5	0.5	2.1	2.1
Γ	7.1	5.5	14	24
γ	4.3	6.7	7.9	12
σ (db)	3	3	3	3

cluster arrival rate (Λ) and ray arrival rate (λ). Ray arrival rate is the arrival rate of path within each cluster. The cluster arrival rate which is always smaller than the ray arrival rate. The rays within each cluster are also based on Poisson process.

The reason to modifiy the original S-V model is because UWB has different amplitude distribution. The amplitude statistics in S-V model were based on Rayleigh distribution, the power of which is controlled by the cluster and ray decay factor. However recent measurements in UWB channel [51] show that amplitudes do not follow Rayleigh distribution rather it follows lognormal distribution.

The multipath model adopted by the IEEE 802.15.3a committee for the evaluation of UWB physical layer proposals consists of the following discrete time impulse response:

$$h(t) = \chi \sum_{l=0}^{L-1} \sum_{k=0}^{K-1} \alpha_{k,l} \delta(t - T_l - \tau_{k,l}) \tag{2.21}$$

where:

L = the total number of clusters,
K = the total number of ray paths relative to the l^{th} cluster,
T_l = delay or arrival time of first path of l^{th} cluster,
$\tau_{k,l}$ = delay of k^{th} path within the l^{th} cluster relative to T_l,
$\alpha_{k,l}$ = multipath gain coefficient of k^{th} ray related to l^{th} cluster and
χ = lognormal shadowing effect.

The ray arrival and cluster arrival time distribution are given by:

$$p(T_l/T_{l-1}) = \Lambda \exp[-\Lambda(T_l - T_{l-1})], l > 0 \tag{2.22}$$

$$p(\tau_{k,l}/\tau_{(k-1),l}) = \lambda \exp[-\lambda(\tau_{k,l} - \tau_{(k-1),l})], k > 0 \tag{2.23}$$

where:

Λ = cluster arrival rate and
λ = ray arrival rate

Chapter 3

Rake Receptions

3.1 Introduction

Indoor wireless communications channels typically experience significant multipath propagation[30]. A conventional narrowband system lacks the temporal resolution required to separate the closely arriving paths and detects the combined envelope as a single faded signal. Multipath resolution, however, increases as the bandwidth increases. An ultrawideband (UWB) system is therefore capable of resolving individual multipath arrivals with path length differences on the order of centimeters[9].

The signal bandwidth for the UWB system is set at $\geq$ 500 MHz [22]. This high bandwidth allows the received signal to be split into distinct multipaths with high resolution. Therefore, the multipath components have useful information. This feature motivates the use of RAKE multipath combining techniques to provide diversity and capture as much energy as possible at the UWB receiver. A rake receiver collects different multipath propagated signal components and coherently combines these in order to form a complete replica of a transmitted signal. Rake receiver attempts to collect the time shifted versions of the original signal by providing a separate correlation receiver for each of the multipath signals (as shown in fig. 3.1). This can be characterized as a type of time diversity. The combination of different signal components will increase the signal-to-noise ratio (SNR), which will improve link performance.

3.2 Rake Receiver Types

There exist different complexity rake receivers. Ideal rake receiver structure captures all of the received signal power by having a number of fingers equal to the

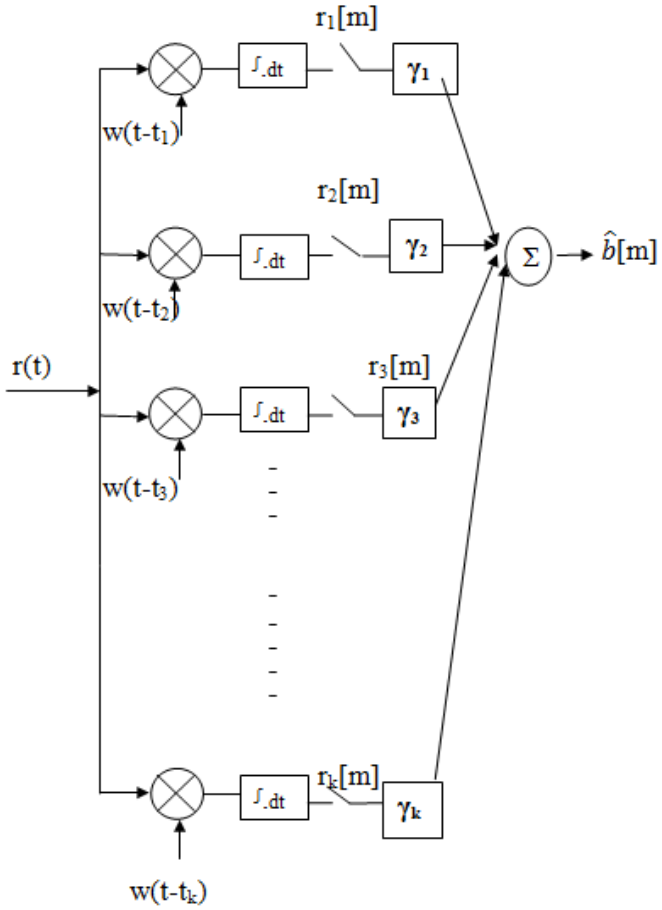

Figure 3.1: A rake receiver with K fingers and finger weight vector $\gamma = (\gamma_1, \gamma_2, ..., \gamma_k)$.

number of multipath components. Combining all resolvable paths provides the optimal performance [14]. However, the number of MPCs that can be utilized in a typical Rake combiner is limited by power consumption constraints, complexity considerations, and the availability of channel estimates [76]. In typical UWB scenarios, the available number of MPCs at the receiver is often more than 100 [76]; hence the ARake UWB receiver serves only as a benchmark and provides a bound on the performance that is achievable by other suboptimal combining schemes. Consequently, implementation of the A-rake is not possible [76].

The complexity can be reduced, at the price of a performance penalty, by employing a practical rake receiver implementation called Selective rake, S-rake. The reason for the reduction of complexity in S-rake is due to the selection of those multipath components that are instantaneously strongest [14]. Selective-rake is more realistic implementation than a-rake since it provides reduction in

the number of correlators and thus reduces power consumption. However, the selection procedure still requires full channel estimation [17], which may not be easily available. Therefore, both A-rake and S-rake receivers require computationally expensive channel estimation.

A third rake type is a partial-rake (p-rake) where the n first arriving signal components are processed at the receiver. The principle behind this approach is that the first multipath components will typically be the strongest and contain the most of the received signal power [14][17]. The disadvantage is that the multipath components that the P-rake receiver combines are not necessarily the strongest multipath components, so optimum performance will not be achieved [17]. This is the simplest rake receiver since estimation of all the multipath components are not required. Being less complex and less power consuming than A-rake or S-rake, partial-rake can still be almost as good in performance. Since in a line-of-sight channel the majority of the signal energy is in the couple of tens of first arriving multipath components, the n first taps only can be enough for a reliable decision [17]
.
Under ideal conditions, the A-rake outperforms the S-rake, which typically outperforms the P-rake. However, if the strongest propagation paths are at the beginning of the channel impulse response, the S-rake and P-rake will give the same performance.

3.3 Combining Techniques

A rake receiver consists of multiple branches, or fingers, that track individual multipath components (MPCs). The MPCs generally have unequal average SNRs. The finger outputs are combined using linear or decision-oriented diversity combining schemes. Three popular examples of linear diversity combining are Equal Gain Combining, Selection Combining (SC) and Maximal-Ratio Combining (MRC)[70]. The objective of these methods is to determine a set of weights $\gamma = [\gamma_1, \gamma_2, ..., \gamma_k]$ to combine the received signals (see fig. 3.1).

Equal gain diversity combining is a suboptimal version of diversity combining where signals from all diversity branches are added up without weighing. In other word, the receiver set all:

$$\gamma_m = 1 \tag{3.1}$$

Although suboptimal, EGC with coherent detection is often an attractive solution since it does not require estimation of the fading amplitudes and hence results in reduced complexity relative to the optimum MRC scheme. However, EGC is often limited in practice to coherent modulations with equal-energy symbols

(M-ary PSK signals). Indeed, for signals with unequal energy symbols such as M-QAM, estimation of the path amplitudes is needed anyway for automatic gain control (AGC) purposes, and thus for these modulations, MRC should be used to achieve better performance [70].

MRC can be applied to maximize the output SNR. A receiver with MRC will coherently combine the diversity branches by weighting them by the complex conjugate of their respective fading gains and adding them. In the absence of interference, MRC is the optimal combining scheme [64][67] but, comes at the expense of complexity since MRC requires knowledge of channel fading parameters. The instantaneous SNR for MRC is the sum of the instantaneous SNR's of the rake branches[43]. For MRC, not only the combined instantaneous SNR is the sum of the individual instantaneous SNR's, but also the combined average SNR is the sum of the individual average SNR's[43].

The two former combining techniques (MRC and EGC) require a separate receiver chain for each diversity branch, which adds to the overall receiver complexity. On the other hand, SC-type systems process only one of the diversity branches. Specifically, in its conventional form, the SC combiner chooses the branch with the highest SNR.

SC in its conventional form may still be impractical since it requires simultaneous and continuous monitoring of all the diversity branches [70]. Hence SC is often implemented in the form of switched or scanning diversity, in which rather than continually picking the best branch, the receiver selects a particular branch until its SNR drops below a predetermined threshold. When this happens the receiver switches to another branch. SSC diversity is obviously the least complex diversity scheme to implement.

The optimal MRC rake, that combines all resolved paths, offers the highest SNR gain. A full-band UWB system spanning a 7.5 GHz bandwidth and operating in a rich scattering environment can often resolve over a hundred incident paths [50]. An MRC rake with such a large number of fingers is, however, impracticable with the current device technology [76]. On the other hand, SC uses only one path out of the L available multipaths and hence doesn't fully exploit the amount of diversity offered by the channel. To bridge the gap between these two extremes (MRC and SC) researches have been conducted and propose GSC [19], which adaptively combines (following the rules of MRC) the L_c strongest (highest SNR) paths among the L available ones. Suboptimal rake reception with hybrid selection/maximal-ratio combining (H-S/MRC), sometimes also referred to as general selection combining (GSC) or selective rake (SRake), offers a flex-

ible alternative as it allows a tradeoff between complexity and performance by combining only a subset of the resolved paths [42].

The conventional Rake receiver employs the weight vector to perform the MRC which maximizes the output SNR. Maximal ratio combining Rake receiver is optimum only when the disturbance to the desired signal is sourced by additive white Gaussian noise (AWGN) but, in the presence of interfering users and intersymbol interference it is not optimal [64][67].

UWB technology has been proposed for use in WPANs. Under the conditions where such transceivers are expected to operate, the multipath channel spread over dozens of symbols in the case of ultra high-speed communications of several hundreds Mbps, which results in a strong frequency selective channel [25]. Consequently, the conventional MRC Rake receiver needs a large number of fingers and the computational complexity of the Rake receiver becomes high [78] this makes it infeasible to practically implement it. And WPANs including those with a UWB physical layer, will be typically required to operate in proximity to other wireless networks, for example, the proliferating local area networks (LANs). But, in the presence of severe ISI and narrowband interference emitted by LANs, a UWB receiver with a conventional MRC Rake combiner, with minimum affordable rake fingers, achieves poor BER performance [64]. Therefore improvements to conventional RAKE reception is necessary.

Due to the above mentioned problem with MRC rake receiver, a more effective receiver scheme is the minimum mean square error (MMSE) Rake receiver [57] which achieves a much improved performance for WCDMA system [13].

3.4 MMSE Rake Receiver

The proposed adaptive MMSE Rake receiver in fig. 3.2 has K fingers to collect signal energy and mitigate severe ISI. Those K best components are determined by a finger selection algorithm. The paths with highest signal-to-noise ratios (SNRs) are selected and then each finger weighting factor (i.e.γ) is decided by using LMS algorithm.

The filter coefficients are updated using the error signal. The receiver minimizes the cost function $\xi = \mathrm{E}\{|\mathrm{e[m]}|^2\}$ to acquire information on how to improve the final estimate $\hat{b}[m]$. The weight coefficients of the K taps for the MMSE filter are chosen as to minimize the MSE between the desired bit and the rake output of the combined finger.

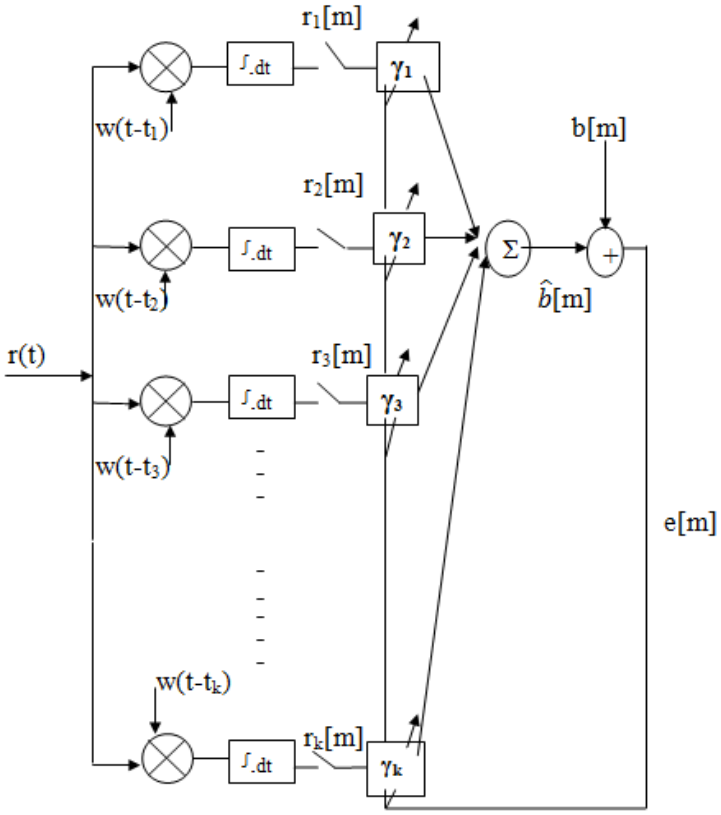

Figure 3.2: mmse rake receiver with K fingers and finger weight vector $\gamma = [\gamma_1, \gamma_2, ..., \gamma_k\ ]$.

The cost function is given by :

$$\xi = E\{|e[m]|^2\} = E\{e[m]e[m]\} \tag{3.2}$$

Where:

$$e[m] = b[m] - \hat{b}[m] \tag{3.3}$$

Where:

$$\hat{b}[m] = r^{(m)}\gamma^{(m)T} \tag{3.4}$$

Where:

$$r^{(m)} = [r_1[m], r_2[m], ..., r_k[m]] \tag{3.5}$$

Where:

$$\gamma^{(m)} = [\gamma_1, \gamma_2, ..., \gamma_k] \tag{3.6}$$

A necessary condition for the filter coefficients $\gamma^{(m)}$ to minimize the squared error is that the derivative of ξ with respect to the coefficients $\gamma^{(m)}$ vanishes [32], i.e.

$$\frac{dE\{\xi\}}{d\gamma^{(m)}} = 0 \tag{3.7}$$

substituting eq. 3.2 and eq. 3.3 into eq. 3.7 yields:

$$E\left\{\frac{d\{\{b[m]-\hat{b}[m]\}e[m]\}}{d\gamma^{(m)}}\right\}=0 \tag{3.8}$$

Substituting the value of the estimate:

$$E\left\{\frac{d\{b[m]e[m]-r^{(m)}\gamma^{(m)T}e[m]\}}{d\gamma^{(m)}}\right\}=0 \tag{3.9}$$

This yields the Orthogonality Principle which is:

$$E\{r^{(m)}e[m]\}=0 \tag{3.10}$$

The filter coefficients which minimize the MSE should be choosen in order to make the estimation error orthogonal to the observation that make up the estimate.

From eq. 3.10 we can get:

$$E\{r^{(m)}\{b[m]-r^{(m)}\gamma^{(m)T}\}\}=0 \tag{3.11}$$

This yields:

$$R_{rb}=R_{rr}\gamma^{(m)T} \tag{3.12}$$

Where:

R_{rb} is the cross correlation between the observation and the desired signal.
R_{rr} is the auto correlation of the observation signal.

From eq. 3.12 to get filter coefficients, which minimizes the MSE, we need to perform matrix inversion which might be computationally difficult or, we can use the Levinson-Durbin recursive algorithm to obtain the optimum coefficients [32].

Alternatively, an iterative procedure that avoids the direct matrix inversion may be used to compute the rake weighting coefficients. Probably the simplest iterative procedure is the method of steepest descent, in which one begins by arbitrarily choosing the vector γ. This yields the basic LMS algorithm for recursively adjusting the tap weight coefficients of the equalizer first proposed by Widrow and Hoff (1960). Therefore weight updates are performed using:

$$\gamma^{(m+1)}=\gamma^{(m)}+\mu e[m]r^{(m)} \tag{3.13}$$

Where:

μ is a scale factor that controls the rate of adjustment.

Here it has been assumed that the receiver has knowledge of the transmitted

information sequence in forming the error signal between the desired symbol and its estimate. Such knowledge can be made available during a short training period in which a signal with a known information sequence is transmitted to the receiver for initially adjusting the tap weights.

So far, we have selected paths which maximize output SNRs and modify the weighing vector so as to minimize MMSE. But, selection of optimal subset of multipath components is important for the performance of RAKE receiver. Since UWB is characterized by longer delay spread, the effect of ISI dominates the effect of noise [54]. Therefore, designing rake which minimize effect of ISI will outperform rake that maximizes output SNR. This means, rather than selecting paths that have larger multipath gain, which maximizes the output SNR, choosing paths which considers ISI will give better performance. And A.G. Klein, et al. [41] shows that choosing of RAKE finger delays in such a way that avoids ISI and combat narrowband interference achieves significant performance gains than MRC rake, particularly when there are more channel paths than RAKE fingers, which is typical UWB receiver designing aspect.

Therefore, selecting paths by considering ISI will give better performance. For a minimum mean square error Rake receiver, the "conventional"finger selection algorithm is to choose the paths with highest SINRs. The proposed system uses a Genetic Algorithm based finger selection.

3.4.1 Finger Selection Using Genetic Algorithm

Our case doesn't deal with multiuser UWB communication but we study channels with high delay dispersion, so we model the ISI as the only interference to be minimized.

3.4.1.1 Genetic Algorithm

Genetic Algorithms are a family of computational models inspired by Darwin's theory about evolution which is "survival of the fittest ". These algorithms encode a potential solution to a specific problem on a simple chromosome like data structure and apply recombination operators to these structures so as to preserve critical information. Genetic algorithms are often viewed as function optimizers [31].

Genetic Algorithms (GAs) are adaptive heuristic search algorithm based on the evolutionary ideas of natural selection and genetics for searching for the global optimum of an objective function [31]. An objective function is the target function which is going to be optimized, in our case SINR of the received signal.

An implementation of a genetic algorithm begins with a population of (typically random) chromosomes, where each chromosome is represented by a binary string. One then evaluates these structures and allocates reproductive opportunities in such a way that those chromosomes which represent a better solution to the target problem are given more chances to "reproduce"than those chromosomes which are poorer solutions. The "goodness"of a solution is typically defined with respect to the current population.

Let N_{ipop} denote the number of chromosomes in this population. Then, the fittest N_{pop} of these chromosomes are selected, according to a objective function. After that, the fittest N_{good} chromosomes, which are also called the "parents", are selected and paired among themselves (pairing step). From each chromosome pair, two new chromosomes are generated, which is called the mating step. In other words, the new population consists of N_{good} parent chromosomes and N_{good} children generated from the parents by mating. After the mating step, the mutation stage follows, where some chromosomes (the fittest one in the population can be excluded) are chosen randomly and are slightly modified; that is, some bits in the selected binary string are flipped. After that, the pairing, mating and mutation steps are repeated until a threshold criterion is met. The main characteristics of the GA algorithm is that it can get close to the optimal solution, if the steps of the algorithm are designed appropriately, and they tend to be computationally expensive. Flow chart for GA is given in 3.3.

3.4.1.2 Assignment Vector

The problem is to choose the optimal set of multipath components $\varphi = \{r_1, r_2, ..., r_k\}$, that maximizes the overall SINR of the system. In other words, we need to choose the best samples, in the context of maximum SINR ratio, from the L received samples $r_l, l = 1, 2, ..., L$.

In order to reformulate this combinatorial problem, we first define an "assignment vector"s, the i^{th} element of which is equal to 1 if the i^{th} MPC is selected, and 0 otherwise. Since K MPCs are selected by the Rake receiver, s satisfies $\sum_{i=1}^{L}[s]_i = K$, where $[s]_i$ denotes the i^{th} element of s. Also let p_s denote an M X 1 vector, the elements of which are the indices of the non-zero elements of s. For example, if the third and the fourth MPCs are selected for a system with L = 5 and K = 2, then s = [0 0 1 1 0] and p_s = [3 4].

From the assignment vector s, we define a K X L "selection matrix"S as follows:

$$S = [e_{[p_s]_1}, e_{[p_s]_2}, ..., e_{[p_s]_K}]^T \tag{3.14}$$

where e_i is an L X 1 unit vector having a 1 at its ith position and zero elements for all other entries, and $[p_s]_i$ represents the i^{th} element of p_s.

3.4.1.3 Objective Function

The objective function is the SINR of received signal, which is the target function which is going to be optimized. Since our case doesn't deal with multiuser UWB communication but we study channels with high delay dispersion, we model the ISI as the only interference to be minimized.

We consider single user, binary phase shift keyed DS CDMA UWB system, in which the transmitted signal from the user is represented by:

$$s(t) = \sqrt{P} * \sum_{j=-\infty}^{\infty} \sum_{n=0}^{N-1} b_j c_n * w_{tx}(t - jT_s - nT_c) \tag{3.15}$$

where:

N = Spread spectrum processing gain
b_j = Modulated data symbol value for the user (± 1)
c_n = Spreading chip value for the user (± 1)
P = Average power (one code period)
$w_{tx}(t)$ = Transmitted UWB pulse
t = transmitter's clock time
T_s = symbol period
T_c = Spreading code chip period

A common and convenient model for characterization of the multiptah channel is the discrete-time impulse response model. If time difference of consecutive multipath contributions is smaller than the pulse duration, the signal contributions overlap and are not independent. Measurements [30] have shown that the typical average multipath arrival rate is in the range of 0.5-2ns. For DS UWB system, which is common UWB system, the typical pulse width is less than 0.5ns [28]. In this situation, there couldn't be severe overlapping between adjacent received pulses. Therefore, we can assume that received adjacent paths are separated in time by at least one pulse width or chip period. So, let's consider the discrete representation of the channel, $\beta = [\beta_1, \beta_2, ..., \beta_L]^T$ for the user, where L is assumed to be the number of MPCs, and T_c is the multipath resolution. The channel is of the form:

$$h(t) = \sum_{l=1}^{L} \beta_l \delta(t - \tau_l) \tag{3.16}$$

where:

τ_l = Delay of l^{th} path

β_l = channel coefficeint of l^{th} path

Then, the received signal can be expressed as

$$r(t) = \sqrt{P} * \sum_{j=-\infty}^{\infty} \sum_{n=0}^{N-1} \sum_{l=1}^{L} \beta_l b_j c_n * w_{rx}(t - jT_s - nT_c - (l-1)T_c) + n(t) \quad (3.17)$$

where:

$w_{rx}(t)$ = received unit-energy UWB pulse

n(t) = zero mean white Gaussian noise with unit spectral density.

The received pulse is usually modeled as the 2^{nd} derivative of $w_{tx}(t)$ due to the effects of the transmit and receive antennas (see section 2.6). But, in this work we won't consider antenna effect. Therefore, both the transmitted and received pulses have same shape which is the 2^{nd} order gaussian pulse.

The received signal (see eq. 3.17) has severe ISI. If the cumulative ISI energy dominates the current transmitted pulse energy, wrong decision will be made by the detector. Domination of either ISI or the transmitted pulse depends on SINR of a particular received pulse, where the interference is only ISI. These interference occurs when m^{th} path of pulse k collides with l^{th} path pulse i. Since each pulse has same energy the only thing that affects pulse detection is channel gain of a particular path. If channel gain of m^{th} path is greater than channel gain of l^{th} path, pulse k will be decided. If channel gain of m^{th} path is smaller than channel gain of l^{th} path, pulse i will be decided. Therefore, let's model the received signal in terms of channel coefficients. Let's define a matrix which has dimension of length of multipath by number of transmitted pulses (i.e. L X number of transmitted pulses).

$$\psi = \begin{Bmatrix} \psi_{11} & \psi_{12} & \psi_{13} & \cdots & \psi_{1np} \\ \psi_{21} & \psi_{22} & \psi_{23} & \cdots & \psi_{2np} \\ \psi_{31} & \psi_{32} & \psi_{33} & \cdots & \psi_{3np} \\ \vdots & \vdots & \vdots & \ddots & \vdots \\ \psi_{L1} & \psi_{L2} & \psi_{L3} & \cdots & \psi_{Lnp} \end{Bmatrix}$$

where:

L = number of multipath components

np = number of transmitted pulses

Each column of ψ describes received signal of a chip at each rake fingers, considering all rake (i.e. ψ_{ij} describes sum of multipath signals at i^{th} rake position for j^{th} chip to be detected.). For example, $\psi_{11} = \beta_1^1$, i.e. received signal at the

first rake for the first chip to be detected, $\psi_{21} = \beta_2^1 + \beta_1^2$, received signal at the second rake for the first chip to be detected, $\psi_{13} = \beta_1^3 + \beta_2^2 + \beta_3^1$, received signal at the first rake for the third chip to be detected, and so on, where β_j^i is channel gain of j^{th} path when pulse "i"is sent. Therefore, ψ becomes:

$$\psi = \begin{pmatrix} \beta_1^1 & \beta_1^2+\beta_2^1 & \cdots & \beta_1^{np-2}+\beta_2^{np-3}+..+\beta_L^{np-L-1} & \beta_1^{np-1}+\beta_2^{np-2}+..+\beta_L^{np-L} & \beta_1^{np}+\beta_2^{np-1}+..+\beta_L^{np-L+1} \\ \beta_2^1+\beta_1^2 & \beta_2^2+\beta_1^3+\beta_3^1 & \cdots & \beta_1^{np-1}+\beta_2^{np-2}+..+\beta_L^{np-L} & \beta_1^{np}+\beta_2^{np-1}+..+\beta_L^{np-L+1} & \beta_2^{np}+\beta_3^{np-1}+..+\beta_L^{np-L+2} \\ \vdots & \vdots & \ddots & \vdots & \vdots & \vdots \\ \beta_1^{L-2}+\beta_2^{L-3}+..+\beta_{L-2}^1 & \beta_1^{L-1}+\beta_2^{L-2}+..+\beta_{L-1}^1 & \cdots & \beta_{L-4}^{np}+\beta_{L-3}^{np-1}+..+\beta_L^{np-4} & \beta_{L-3}^{np}+\beta_{L-2}^{np-1}+..+\beta_L^{np-3} & \beta_{L-2}^{np}+\beta_{L-1}^{np-1}+\beta_L^{np-2} \\ \beta_1^{L-1}+\beta_2^{L-2}+..+\beta_{L-1}^1 & \beta_1^{L}+\beta_2^{L-1}+..+\beta_L^1 & \cdots & \beta_{L-3}^{np}+\beta_{L-2}^{np-1}+..+\beta_L^{np-3} & \beta_{L-2}^{np}+\beta_{L-1}^{np-1}+\beta_L^{np-2} & \beta_{L-1}^{np}+\beta_L^{np-1} \\ \beta_1^{L}+\beta_2^{L-1}+..+\beta_L^1 & \beta_1^{L+1}+\beta_2^{L}+..+\beta_L^2 & \cdots & \beta_{L-2}^{np}+\beta_{L-1}^{np-1}+\beta_L^{np-2} & \beta_{L-1}^{np}+\beta_L^{np-1} & \beta_L^{np} \end{pmatrix}$$

Let's split the above matrix into two different matrix which is a matrix which has the needed signal at each finger ψ_s and the other matrix is the ISI at each finger ψ_{ISI}. $\psi = \psi_s + \psi_{ISI}$.

$$\psi_\jmath = \begin{pmatrix} \beta_1^1 & \beta_1^2 & \beta_1^3 & \cdots & \beta_1^{np-2} & \beta_1^{np-1} & \beta_1^{np} \\ \beta_2^1 & \beta_2^2 & \beta_2^3 & \cdots & \beta_2^{np-2} & \beta_2^{np-1} & \beta_2^{np} \\ \beta_3^1 & \beta_3^2 & \beta_3^3 & \cdots & \beta_3^{np-2} & \beta_3^{np-1} & \beta_3^{np} \\ \vdots & \vdots & \vdots & \ddots & \vdots & \vdots & \vdots \\ \beta_{L-2}^1 & \beta_{L-2}^2 & \beta_{L-2}^3 & \cdots & \beta_{L-2}^{np-2} & \beta_{L-2}^{np-1} & \beta_{L-2}^{np} \\ \beta_{L-1}^1 & \beta_{L-1}^2 & \beta_{L-1}^3 & \cdots & \beta_{L-1}^{np-2} & \beta_{L-1}^{np-1} & \beta_{L-1}^{np} \\ \beta_L^1 & \beta_L^2 & \beta_L^3 & \cdots & \beta_L^{np-2} & \beta_L^{np-1} & \beta_L^{np} \end{pmatrix}$$

And:

$$\psi_{\mathcal{ISI}} = \begin{pmatrix} 0 & \beta_2^1 & \cdots & \beta_2^{np-3}+..+\beta_L^{np-L-1} & \beta_2^{np-2}+..+\beta_L^{np-L} & \beta_2^{np-1}+..+\beta_L^{np-L+1} \\ \beta_1^2 & \beta_1^3+\beta_3^1 & \cdots & \beta_1^{np-1}+..+\beta_L^{np-L} & \beta_1^{np}+..+\beta_L^{np-L+1} & \beta_3^{np-1}+..+\beta_L^{np-L+2} \\ \vdots & \vdots & \ddots & \vdots & \vdots & \vdots \\ \beta_1^{L-2}+\beta_2^{L-3}+..+\beta_{L-3}^1 & \beta_1^{L-1}+\beta_2^{L-2}+..+\beta_{L-3}^3+\beta_{L-1}^1 & \cdots & \beta_{L-4}^{np}+\beta_{L-3}^{np-1}+\beta_{L-1}^{np-3}+\beta_L^{np-4} & \beta_{L-3}^{np}+\beta_{L-1}^{np-2}+\beta_L^{np-3} & \beta_{L-1}^{np-1}+\beta_L^{np-2} \\ \beta_1^{L-1}+\beta_2^{L-2}+..+\beta_{L-2}^2 & \beta_1^{L}+\beta_2^{L-1}+..+\beta_L^1 & \cdots & \beta_{L-3}^{np}+\beta_{L-2}^{np-1}+\beta_L^{np-3} & \beta_{L-2}^{np}+\beta_L^{np-2} & +\beta_L^{np-1} \\ \beta_1^{L}+\beta_2^{L-1}+..+\beta_{L-1}^2 & \beta_1^{L+1}+\beta_2^{L}+..+\beta_{L-1}^3 & \cdots & \beta_{L-2}^{np}+\beta_{L-1}^{np-1} & \beta_{L-1}^{np} & 0 \end{pmatrix}$$

Now we have differentiated the ISI from the required signal in the received signal. Let's consider a linear receiver structure that combines the elements of "r" linearly, i.e.

$$\hat{b}[m] = r\gamma^H \tag{3.18}$$

where:

γ is selected fingers weighting vector.

For the linear receiver structure defined above, the SINR of the output $\hat{b}[m]$ defined in eq. 3.18 can be calculated as:

$$SINR = \frac{E|\gamma^H S\beta|^2}{\gamma^H \hat{R}\gamma} \tag{3.19}$$

where:

S is the selection matrix,

E is energy of the transmitted pulse and

$$\hat{R} = SE\{\hat{n}\hat{n}^T\}S^T \tag{3.20}$$

Where:

$$\hat{n} = \psi_{ISI}AB + n \tag{3.21}$$

where:

ψ_{ISI} is the ISI matrix,

A is a n_pxn_p diag$\{\sqrt{E}, \sqrt{E}, \ldots, \sqrt{E}\}$,

n is the vector of background noise components n = $[n_1, n_2, \ldots, n_L]^T$ and

B is vector of transmitted pulses, B = $[b_1, b_2, b_3, \ldots, b_{np}]^T$

For an MMSE-Rake receiver, the received signal samples selected by the finger selection algorithm are combined in such a way to minimize the MSE between the information bit b_i and the decision variable in eq. 3.18. Therefore, for MMSE rake receiver the weighting vector γ in eq. 3.18 is given by: [73]

$$\gamma = \hat{R}^{-1}S\beta \tag{3.22}$$

Therefore, for equiprobable binary symbols, $\hat{R}$ can be expressed as:

$$\hat{R} = S\psi_{ISI}A^2\psi_{ISI}^T S^T + \sigma_n^2 I \tag{3.23}$$

where:

I is a KxK identity matrix, K is number of selected fingers of the rake.

Hence, the SINR of the system can be obtained by substituting eq. 3.22, eq. 3.18 and eq. 3.23 into eq. 3.19 as:

$$SINR(S) = \frac{E}{\sigma_n^2}\beta^T S^T (I + \frac{1}{\sigma_n^2} S\psi_{ISI} A^2 \psi_{ISI}^T S^T)^{-1} S\beta \tag{3.24}$$

Hence, the optimal finger selection problem can be formulated as finding S that solves the following problem:

$$(SINR(S))_{max} \tag{3.25}$$

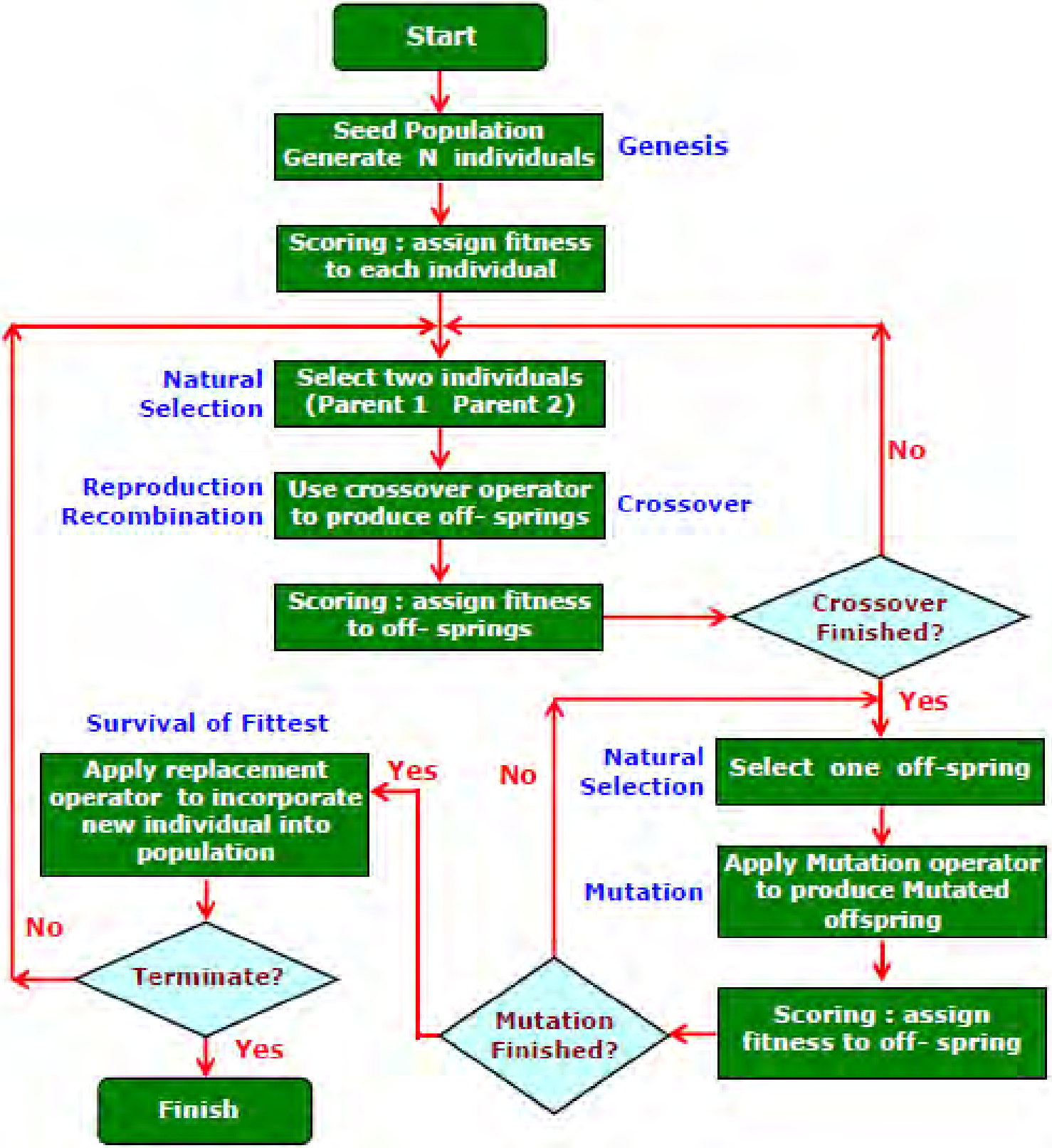

Figure 3.3: Flow chart for GA

Chapter 4

Time and Frequency Domain Equalization

4.1 Introduction

In wireless communications systems, efficient use of the available spectrum is one of most critical design issues. Therefore, modern communication systems must evolve to work as close as possible to channel capacity to achieve the demanded rates. We need to design digital communication systems that implement novel approaches for both channel equalization and coding and, moreover, we should be able to link them together to optimally detect the transmitted information.

Equalizer has recently attracted much attention [10] as a means to overcome the resulting inter-symbol interference and a long delay spread in the characterization of the UWB channel. It is reported that equalizer can obtain an excellent performance even in strong frequency selective channels [20].

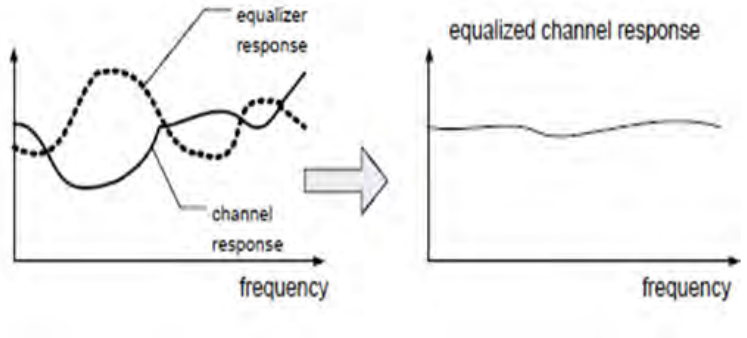

Figure 4.1: Equalized channel response

We can categorize equalizers into two groups based on the way how previous decisions incorporated into current decision. These categories are determined from how the output of an equalizer is used for subsequent control (feedback) of the equalizer. The analog signal $\hat{d}(t)$ (i.e. the estimate of d(t), where d(t) is the transmitted signal) is processed by the decision maker in the receiver. This device determines the value of the digital data being received and applies threshold operation in order to determine the value of the d(t). If d(t) is not used in the feedback path to adapt the equalizer, the equalization is linear. On the other hand, if d(t) is fed back to change the subsequent outputs of the equalizer, the equalization is nonlinear. Many filter structures are used to implement linear and nonlinear equalizers. Further, for each structure, there are numerous algorithms used to adapt the equalizer. We can categorize equalizers also into time domain equalizers (TDE) and frequency domain equalizers (FDE).

4.2 Linear time domain equalization

4.2.1 Introduction

Every channel can be characterized by an equivalent discrete-time transfer function. This equivalent channel response, expressed in the time domain, also can be described mathematically by its frequency response H(z). The zero-ISI condition exists when the transfer function, replicated in the frequency domain at every multiple of the sampling frequency, sums to a flat spectrum. When that is not the case, ISI will occur [56].

There are two basic approaches to linear equalization, aimed at different optimizing criteria. The simplest linear equalizer can be implemented as an FIR filter. In such an equalizer, the current and past values of the received signal are linearly weighted by the filter coefficient and summed to produce the output, as shown in fig. 4.2. The output of this filter before decision making is:

$$\hat{b}_k = \sum_{n=-N_1}^{N_2} (c_n^*) y_{k-n} \tag{4.1}$$

where c_n^* represents the complex filter coefficients or tap weights, $\hat{d}_k$ is the output at time index k, y_i is the input received signal at time $t_0 + iT$, t_0 is the equalizer starting time, and $N = N_1 + N_2 + 1$ is the number of taps. The values N_1 and N_2 denote the number of taps used in the forward and reverse portions of the equalizer, respectively.

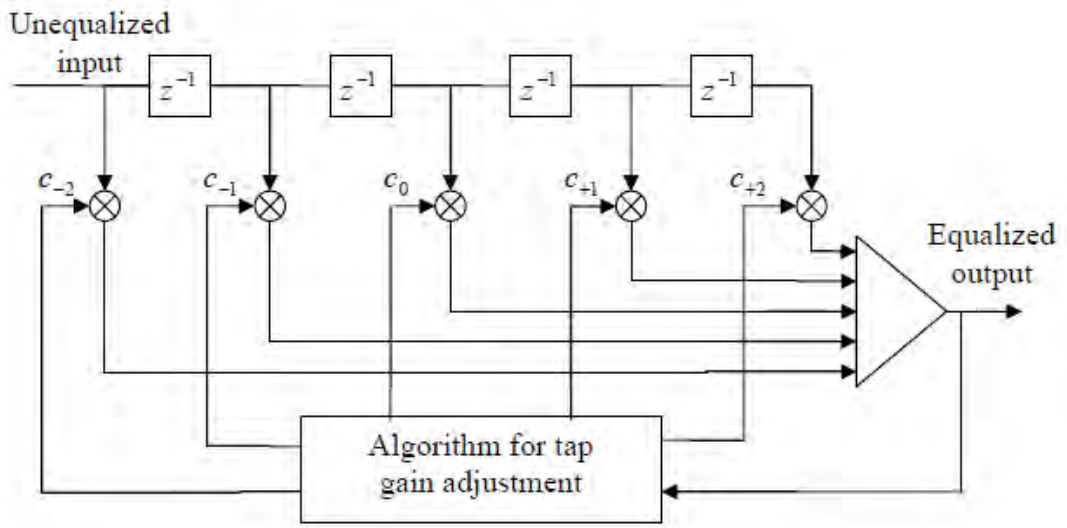

Figure 4.2: Linear transversal filter equalization structure with 5 taps

4.2.2 Algorithms for linear equalization

4.2.2.1 Zero Forcing Equalizer (ZFE)

This section examines the ZFE, which is the easiest type of equalizer to analyze and understand, but has inferior performance to some other equalizer to be introduced in later section (Section 4.2.2.2).

In zero-forcing equalization, the equalizer attempts to completely inverse the channel by forcing. The equalizer tries to restore the Nyquist Pulse character to the channel. In so doing, the ZFE ignores the noise and shapes the signal so that it is free of ISI.

It is shown in [55] that, the equivalent transfer function for an equalizer (i.e. ZFE) based on the peak distorition criterion is given by:

$$C(z) = \frac{1}{F(z)} \tag{4.2}$$

Where C(z) denotes the transfer function of the equalizer and F(z) is the channel transfer function. This equation indicates that complete elimination of the ISI requires the use of an inverse filter to F(z).

If we have a noise-whitening filter, the cascade of the noise-whitening filter having the transfer function $\frac{1}{F^*(z^{-1})}$ and the zero-forcing equalizer having the transfer

function $\frac{1}{F(z)}$ results in an equivalent zero-forcing equalizer having the transfer function:

$$C(z) = \frac{1}{F(z)F^*(z^{-1})} \tag{4.3}$$

There is a problem with the ZF approach when spectral nulls exist, since the gain of C(z) in those regions becomes very high. That results in excessive noise enhancement, since the channel noise will also be passing through the equalizer.

The ZF criterion aims to eliminate ISI completely. But because of the problems cited, it may be more desirable from an error-probability standpoint to allow some ISI if the upshot would be less noise enhancement and a smaller overall mean square error (MSE) at the equalizer output from the exact transmitted symbol. Such an approach is called the MSE criterion, resulting in LE-MSE. Next we will discuss MMSE.

4.2.2.2 Minimum Mean-Square Error (MMSE)-equalizer

The Minimum Mean-Square Error (MMSE) equalizer balances a reduction in ISI with noise enhancement. The MMSE-LE always performs as well as, or better than, the ZFE and is of the same complexity of implementation [55]. Nevertheless, it is slightly more complicated to describe and analyze than is the ZFE. The MMSE-LE uses a linear time-invariant filter c_k , but the choice of filter impulse response c_k is different than the ZFE.

The MSE criteria for filter design does not ignore noise enhancement because the optimization of this filter compromises between eliminating ISI and increasing noise power. Instead, the filter output is as close as possible, in the Minimum MSE sense, to the data symbol b_k.

While the ideal criterion would be minimum detection-error probability, that is not a straightforward figure to determine. A reasonable design goal is to minimize the combined error of additive white Gaussian noise (AWGN) and ISI. In the MSE criterion, the tap weight coefficients C_j of the equalizer are adjusted to minimize the mean square value of the error.

$$e_k = b_k - \hat{b}_k \tag{4.4}$$

Where b_k is the information symbol transmitted in the K^{th} signaling interval and $\hat{b_k}$ is the estimate of that symbol at the output of the equalizer, i.e.

$$\hat{b}_k = \sum_{j=-K}^{K} c_j y_{k-j} \tag{4.5}$$

where c_j represents the filter coefficients or tap weights, $\hat{b}_k$ is the equalizer output at time index k, y_i is the input received signal at time $t_0 + iT$, t_0 is the equalizer starting time, and $N = 2K + 1$ is the number of taps.

It is shown in [55] that, the equivalent transfer function for an equalizer based on the MSE criterion is given by:

$$C(z) = \frac{F^*(z^{-1})}{F(z)F^*(z^{-1}) + N_0} \tag{4.6}$$

Where C(z) denotes the transfer function of the equalizer, F(z) is the channel transfer function and N_0 is the noise spectral density.

When the noise-whitening filter is incorporated into C(z), we obtain an equivalent equalizer having the transfer function:

$$C(z) = \frac{1}{F(z)F^*(z^{-1}) + N_0} \tag{4.7}$$

In the limit as $N_0 \longrightarrow 0$, the two criterion yield the same solution for the tap weights. Consequently, when N_0=0, the minimization of the MSE results in complete elimination of the ISI. When $N_0 \neq 0$, there is both residual ISI and additive noise at the output of the equalizer. And when spectral nulls exist the gain of C(z) in those regions becomes low because of the existence of N_0 in the denominator of eq. 4.7.

Let us consider a finite time duration transversal equalizer. The output of the equalizer in the K^{th} signaling interval is given by eq. 4.5:

The MSE for the equalizer having 2K+1 taps, denoted by J(K), is

$$J(K) = E|b_k - \hat{b}_k|^2 = E|b_k - \sum_{j=-K}^{K} c_j y_{k-j}|^2 \tag{4.8}$$

Minimization of J(K) with respect to the tap weights C_j or, equivalently, forcing the error $e_k = b_k - \hat{b_k}$ to be orthogonal to the signal samples $y^*_{j-l}, |l| \leq K$, yields the following set of simultaneous equations:

$$\sum_{j=-K}^{K} c_j E(y_{k-j} y^*_{k-l}) = E(b_k y^*_{k-l}), \qquad l = -K, ..., -1, 0, 1, ..., K \tag{4.9}$$

If we express the set of linear equations in matrix form,

$$\Gamma C = \xi \tag{4.10}$$

where C denotes the column vector of $2K+1$ tap weight coefficients, Γ denotes the $(2k+1)X(2k+1)$ Hermitian covariance matrix of the observation signal or the received signal (i.e. y_k) and ξ is a $(2K+1)$ dimensional column vector which is the cross correlation between the observation signal (y_k) and the original data signal (b_k). Therefore, the solution for eq. 4.10 becomes:

$$C_{opt} = \Gamma^{-1}\xi \tag{4.11}$$

The solution of C_{opt} can be efficiently performed by use of the Levinson-Durbin algorithm.

Alternatively, an iterative procedure that avoids the direct matrix inversion may be used to compute C_{opt}. Probably the simplest iterative procedure is the method of steepest descent, in which one begins by arbitrarily choosing the vector C. This yields the basic LMS algorithm for recursively adjusting the tap weight coefficients of the equalizer first proposed by Widrow and Hoff (1960).

$$\hat{C}_{k+1} = \hat{C}_k + \Delta e_k y_k^* \tag{4.12}$$

Here it has been assumed that the receiver has knowledge of the transmitted information sequence in forming the error signal between the desired symbol and its estimate. Such knowledge can be made available during a short training period in which a signal with a known information sequence is transmitted to the receiver for initially adjusting the tap weights.

4.3 Frequency Domain Equalization

4.3.1 Introduction

As we have seen in the previous section (Section 4.2) time domain equalization can be used as ISI mitigation technique in SC digital communication systems. Even though TDEs were developed for narrowband wire line channels for dial-up modems, by Robert Lucky at Bell Laboratories in 1965, they are also being used in broadband wireless communication systems. But, the number of operations in TDEs per signaling interval grows linearly with the delay spread (ISI) span [69].

An alternative approach to mitigate ISI is using MC transmission. Using OFDM is one of the low complexity optimal solutions for ISI mitigation [47]. It is being used by major manufacturers and by standardization bodies for a wide range of applications physical layer. But, OFDM has drawbacks such as need for accurate frequency synchronization [60] and large peak-to-average power ratio (PAPR) [45].

Another approach to mitigate ISI is using SC modulation with frequency domain equalization. Single carrier modulation, with receiver Linear Equalization (LE) in frequency domain has approximately equal complexity to OFDM, without the power back-off penalty [37]. Even in some scenarios results show that single carrier with frequency domain equalization gets better performance than OFDM systems [10].

4.3.2 Frequency Domain Equalizer System Model

Let us consider a block of signals b(k), ($0 \leq k \leq N-1$), which is transmitted with length N in a single frame. Since the purpose of frequency domain equalization (FDE) is to eliminate inter symbol interference (ISI) within individual transmission blocks (i.e. intra block interference), we have to have a means to avoid inter block or inter frame interference. To mitigate this inter block interference a cyclic prefix is added at the front of each block. A block diagram representation of SC-FDE system is shown in fig. 4.3.

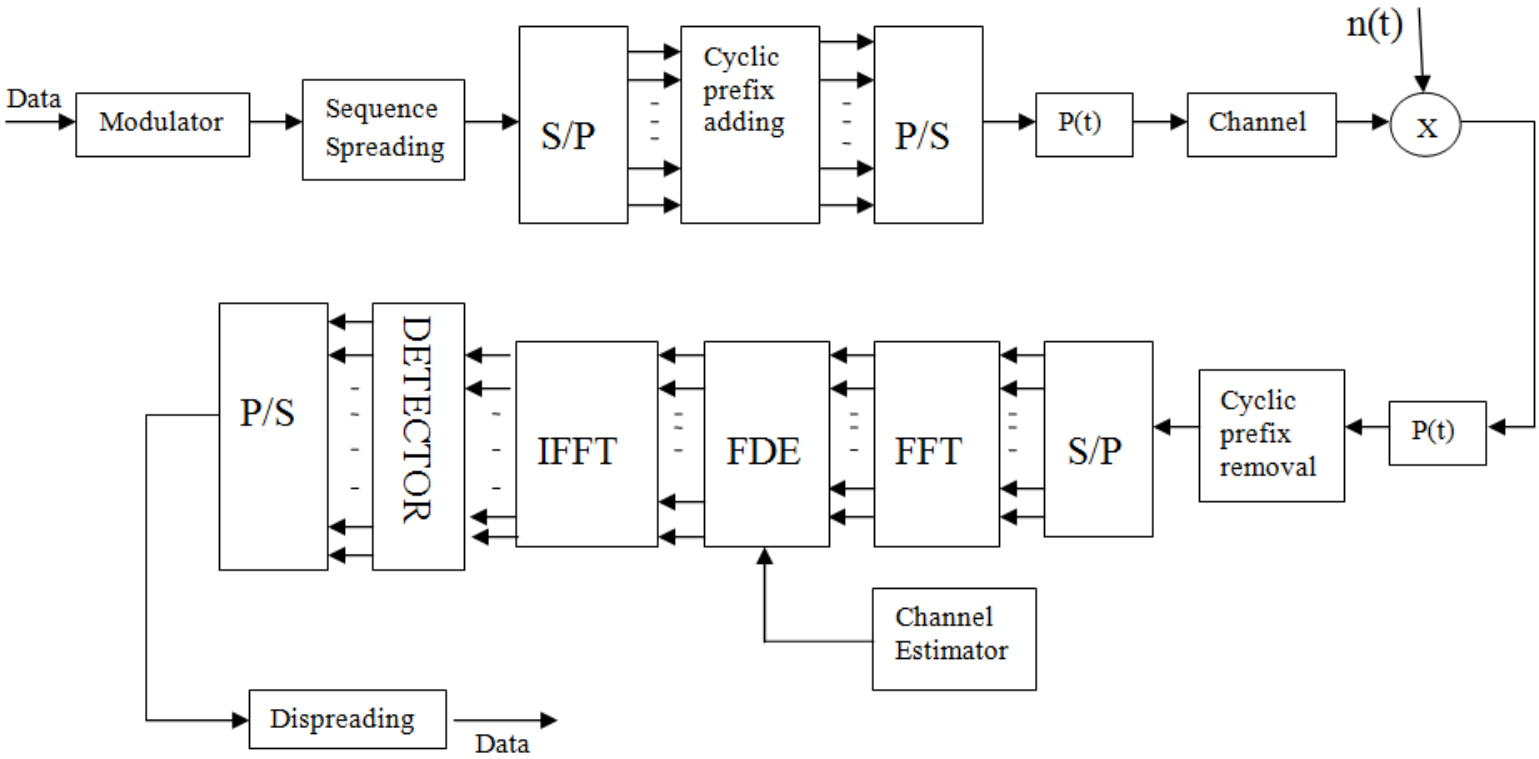

Figure 4.3: Block diagram of SC-FDE system

Assuming perfect time synchronization and supposing that the equivalent chip level spaced channel impulse response is of order L with taps $\beta = [\beta_1, \beta_2, ..., \beta_L]$,

the frequency domain equalizer taps are given by:

$$C_k = \frac{B_k^*}{|B_k|^2 + \sigma_n^2/\sigma_b^2} \tag{4.13}$$

Where:

σ_n^2 is the variance of noise

σ_b^2 is the $E[|b(n)|^2]$

and

$$B_k = \sum_{l=0}^{L} \beta(l) exp^{-j\frac{2\pi}{N}kl} \tag{4.14}$$

As we see in eq. 4.14 to perform frequency-domain channel equalization, the estimation of channel coefficients (i.e. β's) is required. After removing the cyclic prefix and changing the block data into frequency domain, equalization can be performed in frequency domain then pulse detection can be performed in time domain after IFFT.

4.4 Proposed Cascaded MMSE Rake-Equalizer

Since UWB channel is characterized by severe inter-symbol interference (ISI) and a long delay spread due to sub-nano seconds narrow pulse and the large transmission bandwidth, appending an equalizer will give better performance than using only rake[71]. Therefore, let's see a cascade of spatial diversity combining and equalizer scheme for a strong frequency selective fading UWB channel. The general block diagram is shown in fig. 4.4.

The rake output can be determined using eq. 3.4:

$$X[n] = r^{(n)}\gamma^{(n)H} \tag{4.15}$$

And the combined Rake-Equalizer output can be expressed by using eq. 4.5:

$$\hat{b}_k = \sum_{j=-K}^{K} c_j X_{k-j} \tag{4.16}$$

The GA based finger selection algorithm selects paths which have relatively larger SINR. Then using LMS algorithm both weighing values of MMSE rake fingers and taps of the MMSE equalizer determined. The equalizer perform symbol level equalization.

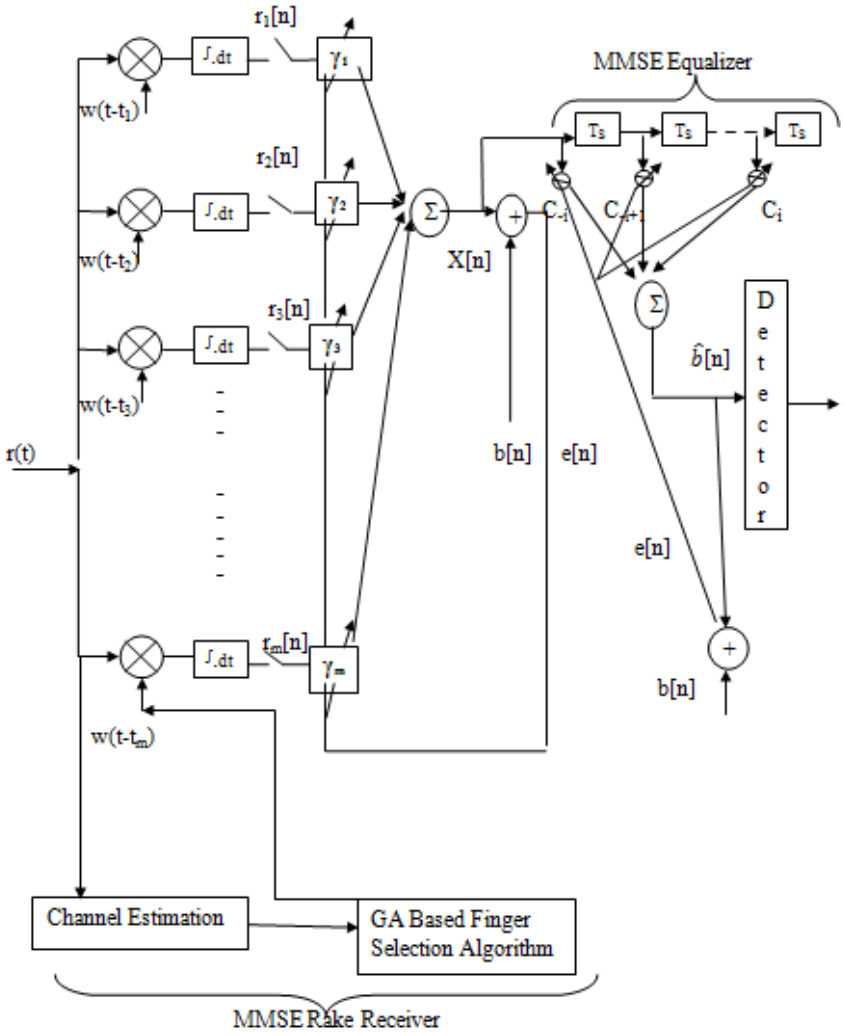

Figure 4.4: The structure of the cascaded MMSE Rake-equalizer receiver model

Chapter 5

Simulation Results and Discussions

5.1 Simulation Setup

In this chapter, simulation set-up and simulation results for MRC and MMSE RAKE, and adaptive MMSE Equalizer (both in TD and FD) have been shown. A personal computer equipped with MATLAB was used as a platform for simulation. The block diagram of the simulation is shown in fig. 5.1 below and table 5.1 provides system parameters that are used in the simulation and their corresponding values. The values for the different simulation parameters are selected in such a way that the whole system meets some standard regulations and have practical applicability.

5.1.1 Simulation Flowchart

The block diagram that have been used for the simulation for both RAKE and adaptive MMSE equalizer is shown in fig. 5.1 below.

5.1.2 Simulation Assumptions and Parameters

Assumptions used in this thesis work include:

- The receiver has perfect channel knowledge or perfect channel estimation is assumed,
- Perfect time synchronization between the transmitter and receiver is assumed,
- No both transmitter and receiver antenna distortion,

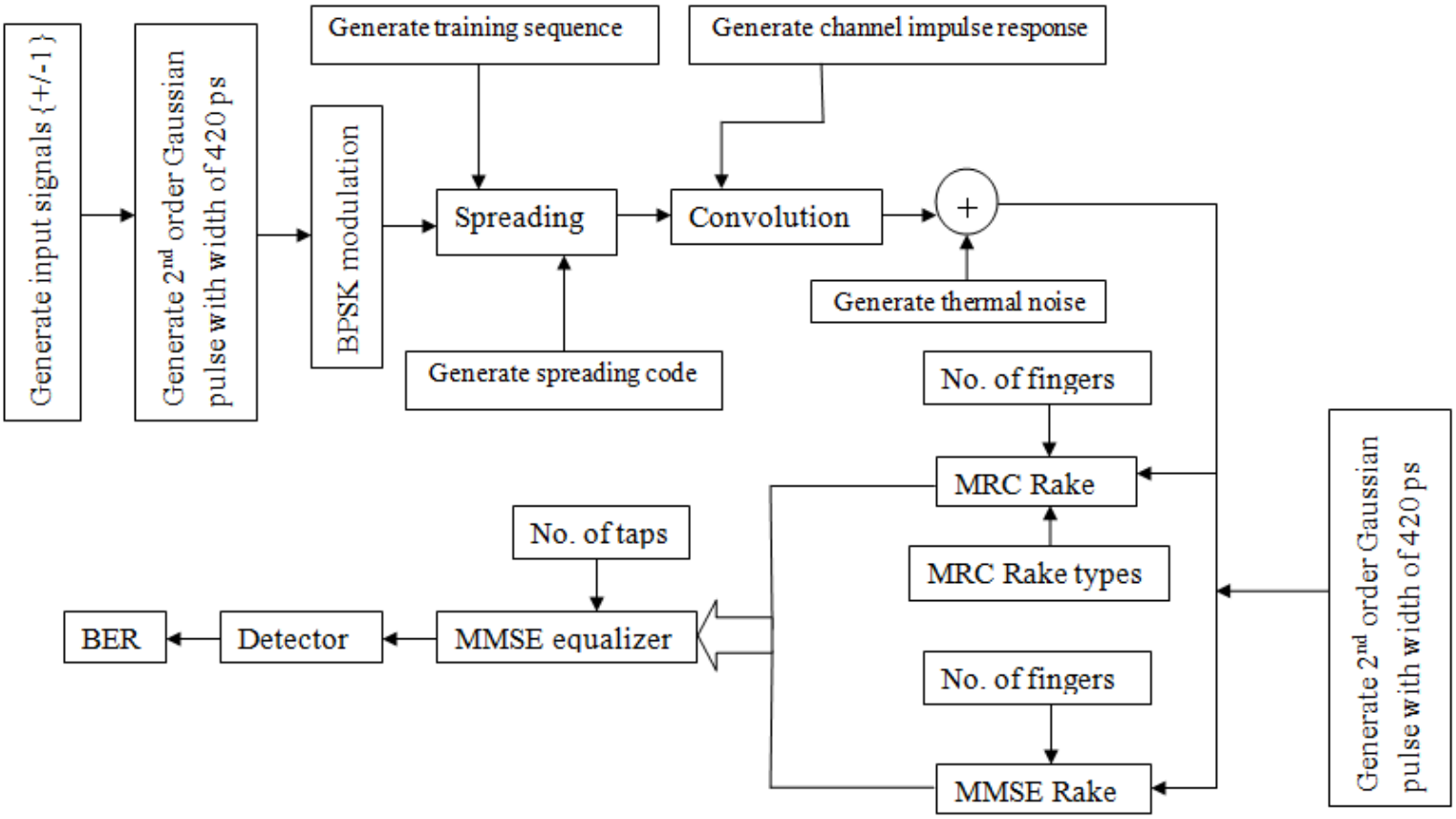

Figure 5.1: Block diagram of simulation

- No MAI and Narrowband Interference

Simulation parameters and their values that were used are described in Table 5.1 below.

5.2 Performance Evaluation of MRC RAKE Receiver

In this section, the BER performance analysis and comparison of MRC RAKE receiver is provided. The performance analysis and comparison includes different RAKE receiver types, number of RAKE fingers and channel types.

5.2.1 Performance for different rake types with different number of rake fingers for case A

Fig. 5.2 shows the BER performance of ARAKE, SRAKE and PRAKE receivers for CM1 (0-4m LOS Channel). SRAKE and PRAKE receivers with 5 and 10 fin-

Table 5.1: Simulation parameters and their values.

Parameters	Assumed value
Pulse Type	Gaussian 2nd order pulse
Pulse width	0.5 nsec
Average Transmitted Power	-30 dBm
Sampling Frequency	100 GHZ
Bandwidth	4.2 Ghz
Center frequency	2.8 Ghz
Data rate	64.5 Mbps
Data Modulation Type	Bpsk
Spreading code	31 Gold Code sequence
Chip Duration	0.5 nsec
Equalizer training sequence duration	3.1 μsec = 200 symbols
Rake receiver training sequence duration	0.4 μsec = 800 chips
Cyclic prefix duration	0.4 μsec
Frame duration	1.2 μsec
Number of Transmitted Symbols	2000
Number of Channel Realization	100
Channel Model	modified the Saleh-Valenzuela (S-V) model
User Distance for CM1 and CM2	2 m
Reference Attenuation for CM1	47 dB
Reference Attenuation for CM2, CM3 and CM4	51 dB
Attenuation Exponent for CM1	1.7
Attenuation Exponent for CM2, CM3 and CM4	3.5
User Distance for CM3 and CM4	8 m
User Speed	5 km/hr
Coherence time	6.9 msec
Channel delay bins	0.5 nsec
Population Size	280
Mutation rate	0.15
Fraction of population kept	0.5
Lms parameter of convergence	0.001

gers are used for BER performance comparison with the ideal ARAKE receiver.

It is clearly seen that performance improves with increasing number of Rake fingers since more energy is effectively used in the receiver as the number of Rake fingers increases. And we can observe that SRAKE with 5 fingers has almost 0.3 db gain over PRAKE with 5 fingers at BER of 10^{-1}. Since the channel is LOS, which is the majority of the signal energy is in the couple of tens of first arriving multipath components, the graph shows SRAKE and PRAKE with 10 fingers has almost same BER performance. As anticipated, the ARAKE receiver has the best performance gaining almost 2dB SNR over both SRAKE and PRAKE receivers with 10 fingers at BER of 10^{-2}. At BER of 0.02, PRAKE receiver with 5 fingers has a SNR loss of about 3dB and PRAKE receiver with 10 fingers has only 1dB SNR loss compared to ARAKE receiver. SRAKE receiver with 10 fingers has nearly the same performance as that of ARAKE receiver. In addition, PRAKE receiver with 10 fingers and SRAKE receiver with 5 fingers have almost the same performance.

5.2.2 Performance for different rake types with different number of rake fingers for case B

Fig. 5.3 shows the BER performance of ARAKE, SRAKE and PRAKE receivers for CM2 (0-4m NLOS Channel). SRAKE and PRAKE receivers with 5 and 10 fingers are used for BER performance comparison with the ideal ARAKE receiver.

It is clearly seen that performance improves with increasing number of Rake fingers since more energy is effectively used in the receiver as the number of Rake fingers increases. And we can observe that SRAKE with 5 fingers has almost 1 db gain over PRAKE with 5 fingers at BER of 0.08. Unlike fig. 5.2 there is a considerable performance improvement between PRAKE and SRAKE. The performance improvement is due to the fact that the channel is NLOS. SRAKE with 10 fingers has almost 0.4 db gain over PRAKE with 10 fingers at BER of 0.009. And as anticipated, the ARAKE receiver has the best performance gaining almost 1.4 dB and 1.75 over SRAKE and PRAKE receivers with 10 fingers at BER of 10^{-2} respectively.

5.2.3 Performance for different rake types with different number of rake fingers for case C

Fig. 5.4 shows the BER performance of ARAKE, SRAKE and PRAKE receivers for CM3 (4-10m NLOS Channel). SRAKE and PRAKE receivers with 5 and 10 fingers are used for BER performance comparison with the ideal ARAKE receiver.

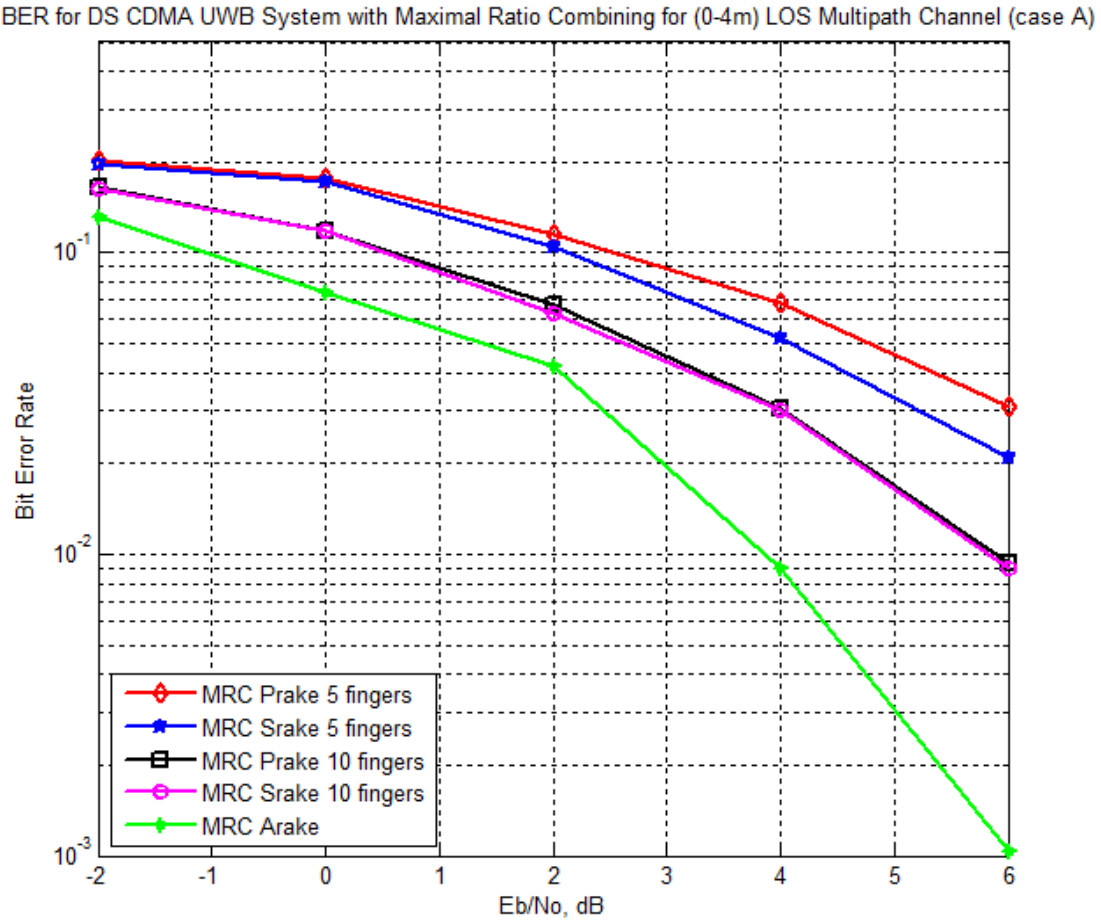

Figure 5.2: BER for DS CDMA UWB System with Maximal Ratio Combining for (0-4m) LOS Channel (Case A)

Like both CM1 and CM2 the performance improves with increasing number of Rake fingers since more energy is effectively used in the receiver as the number of Rake fingers increases. SRAKE with 5 fingers has almost 1.4 db gain over PRAKE with 5 fingers at BER of 0.12. Since the channel is NLOS, there is a considerable BER performance change between SRAKE and PRAKE. SRAKE with 10 fingers has almost 1.35 db gain over PRAKE with 10 fingers at BER of 0.1. Like both CM1 and CM2 the ARAKE receiver has the best performance gaining almost 3.65 db and 4.75 db over SRAKE and PRAKE receivers with 10 fingers at BER of 0.07 respectively.

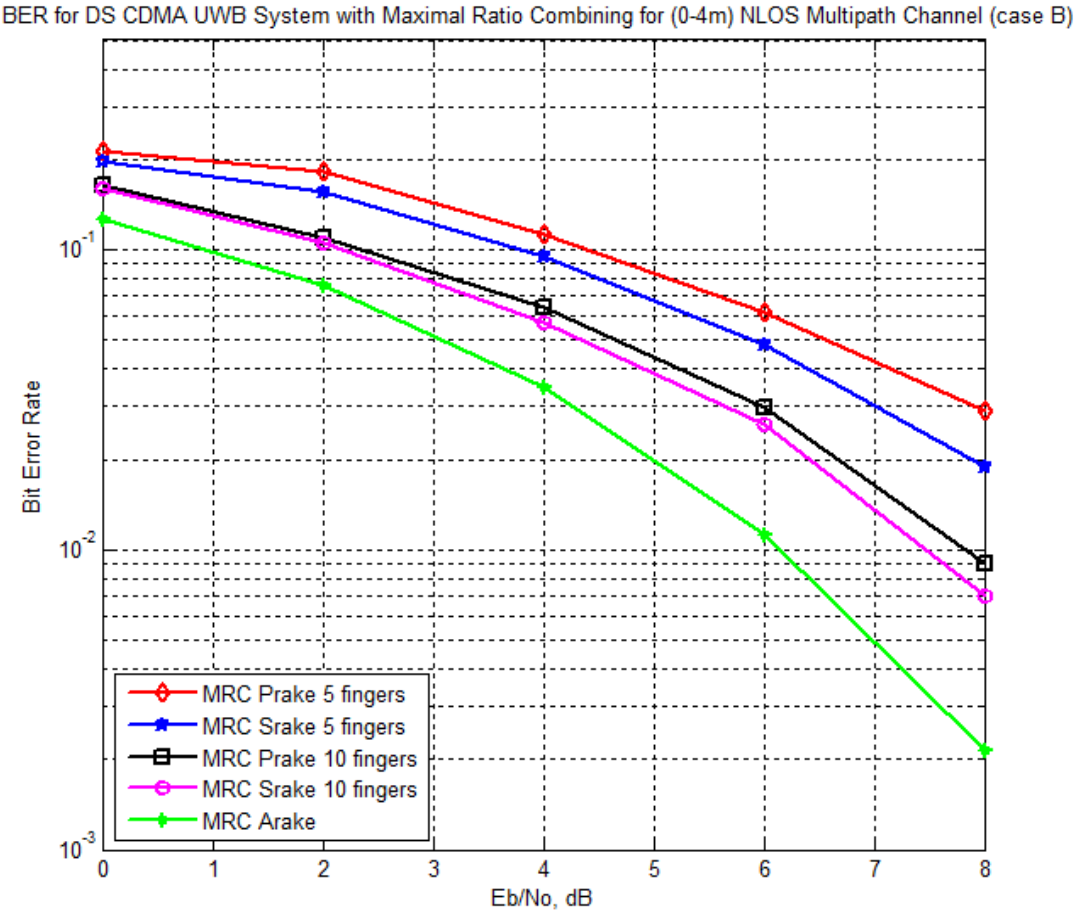

Figure 5.3: BER for DS CDMA UWB System with Maximal Ratio Combining for (0-4m) NLOS Channel (Case B)

5.2.4 Performance for different rake types with different number of rake fingers for case D

Fig. 5.5 shows the BER performance of ARAKE, SRAKE and PRAKE receivers for CM4 (Extremely NLOS Channel). SRAKE and PRAKE receivers with 5 and 10 fingers are used for BER performance comparison with the ideal ARAKE receiver.

Like previous results the performance improves with increasing number of Rake fingers since more energy is effectively used in the receiver as the number of Rake fingers increases. And we can observe that SRAKE with 5 fingers has almost 2.5 db gain over PRAKE with 5 fingers at BER of 0.2. Unlike fig. 5.2 there is a considerable performance improvement between PRAKE and SRAKE. The performance improvement is due to the existence of NLOS channel. SRAKE with

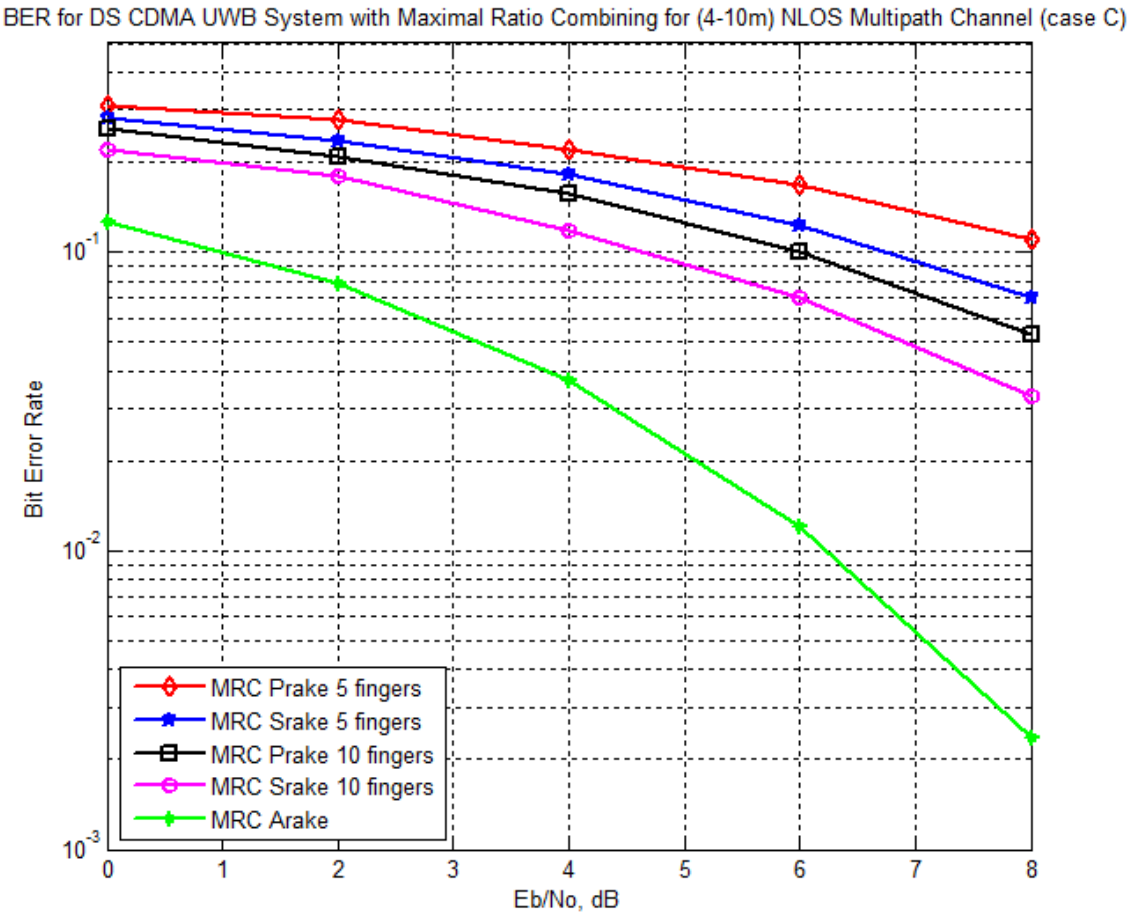

Figure 5.4: BER for DS CDMA UWB System with Maximal Ratio Combining for (4-10m) NLOS Channel (Case C)

10 fingers has almost 1.75 db gain over PRAKE with 10 fingers at BER of 0.1. And as it was expected, the ARAKE receiver has the best performance gaining almost 5.25 dB and 7 db over SRAKE and PRAKE receivers with 10 fingers at BER of 10^{-1} respectively.

5.3 Performance evaluation of adaptive MMSE equalizer

In this section, the BER performance analysis and comparison of MMSE equalizer is provided. The performance analysis and comparison includes different number of equalizer taps and channel types.

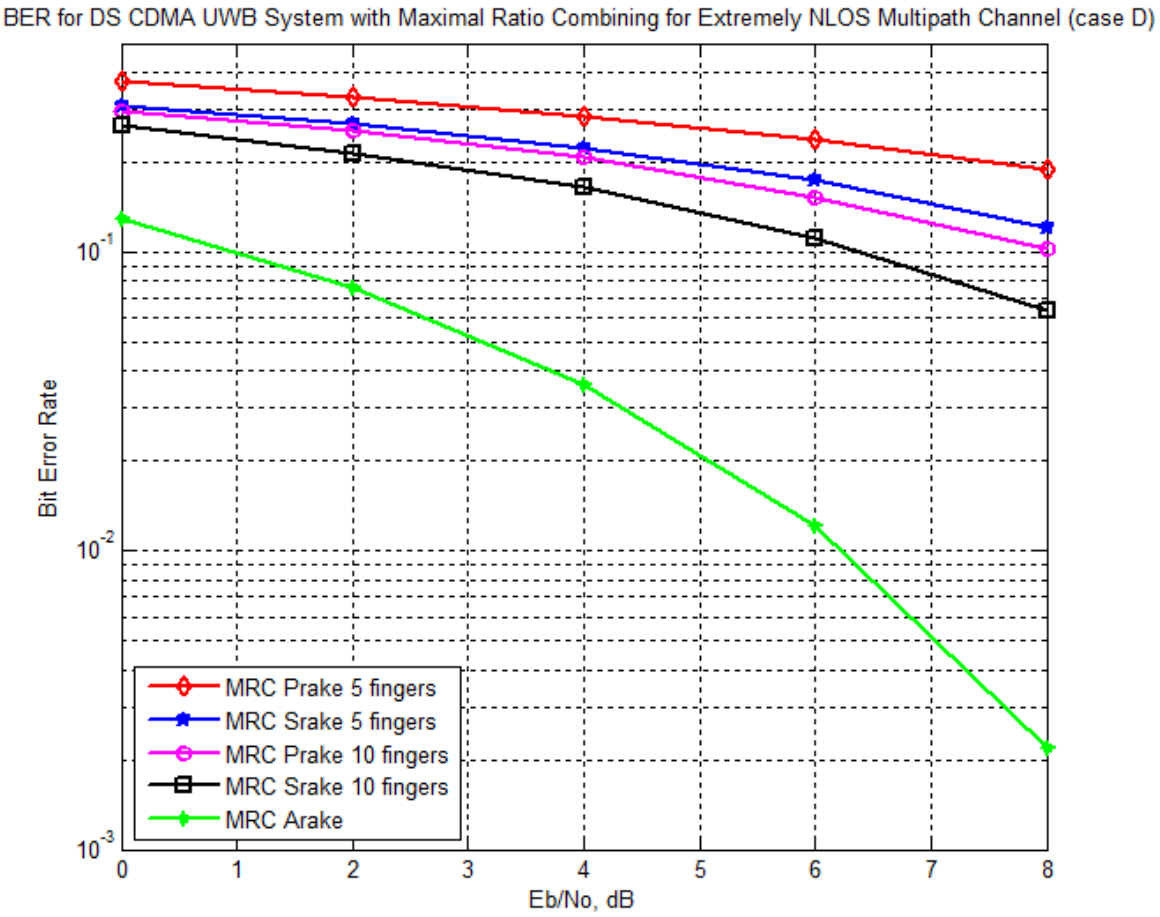

Figure 5.5: Performance for Different RAKE Types with Different Number of RAKE Fingers for Extremely NLOS Channel (Case D)

5.3.1 Performance evaluation of adaptive MMSE equalizer for (0-4m) LOS channel (case A)

Fig. 5.6 present the BER performance of the combined 12 fingers MRC rake, and 3 and 5 taps MMSE equalizer with 5, 10, 12 and 20 fingers MRC rake receiver with perfect channel estimation for the case of CM1 channel.

The result shows the performance improves with increasing number of both rake fingers and equalizer taps. Appending an equalizer on 12 fingers MRC SRAKE yields better BER performance than increasing fingers of MRC SRAKE receiver. But, less performance improvement achieved by appending 5 taps equalizer on 5 fingers SRAKE MRC receiver. 12 fingers SRAKE MRC receiver with 3 taps equalizer has almost 0.3 db and 1.3 db gain over MRC SRAKE with 20 fingers and 12 fingers respectively at BER of 0.01. And 12 fingers SRAKE MRC re-

ceiver with 5 taps equalizer has almost 0.7 and 1.7 db gain over 20 fingers MRC SRAKE and 12 fingers MRC SRAKE respectively at BER of 0.01. But, 5 fingers MRC SRAKE receiver with 5 taps has SNR loss of about 0.3 db compared to 10 fingers MRC SRAKE receiver at a BER of 0.02. This analysis shows that appending an adaptive MMSE equalizer on MRC SRAKE receivers, which have relatively large number of fingers, is better than employing additional rake fingers over CM1 channel, especially at higher SNRs we can achieve a significant performance improvement by appending an equalizer rather than adding additional fingers.

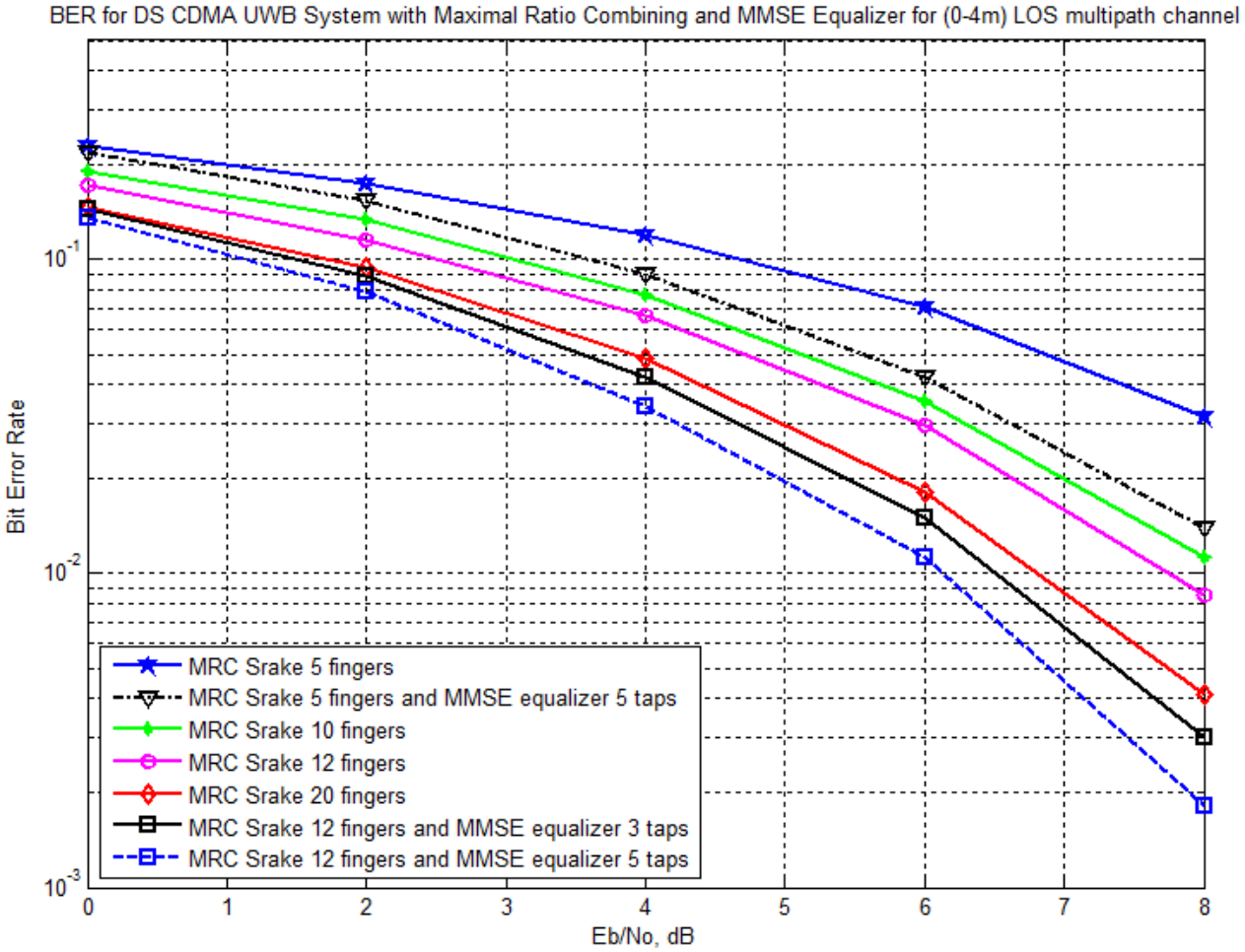

Figure 5.6: BER for DS CDMA UWB System with Maximal Ratio Combining and MMSE Equalizer for (0-4m) LOS Channel (Case A)

5.3.2 Performance evaluation of adaptive MMSE equalizer for (0-4m) NLOS channel (case B)

Fig. 5.7 present the BER performance of the combined 12 fingers MRC rake and 3 and 5 taps MMSE equalizer with 5, 10, 12 and 20 fingers MRC rake receiver with perfect channel estimation for the case of CM2 channel.

Like fig. 5.6, the result shows the performance improves with increasing number of both rake fingers and equalizer taps. Appending an equalizer on 12 fingers MRC SRAKE yields better BER performance than increasing fingers of MRC SRAKE receiver. But, less performance improvement achieved by appending 5 taps equalizer on 5 fingers SRAKE MRC receiver. 12 fingers SRAKE MRC receiver with 3 taps equalizer has almost 0.3 db and 0.7 db gain over MRC SRAKE with 20 fingers and 12 fingers respectively at BER of 0.01. And 12 fingers SRAKE MRC receiver with 5 taps equalizer has almost 0.6 and 1.1 db gain over 20 fingers MRC SRAKE and 12 fingers MRC SRAKE respectively at BER of 0.01. But, 5 fingers MRC SRAKE receiver with 5 taps has SNR loss of about 0.2 db compared to 10 fingers MRC SRAKE receiver at a BER of 0.02. We can conclude that appending an adaptive MMSE equalizer on MRC SRAKE receivers, which have relatively large number of fingers, is better than employing additional rake fingers over CM2 channel, especially at higher SNRs we can achieve a significant performance improvement by appending an equalizer rather than adding additional fingers.

5.3.3 Performance evaluation of adaptive MMSE equalizer for Extremely NLOS channel (Case D)

Fig. 5.8 present the BER performance of the combined 12 fingers MRC rake and 3 and 5 taps MMSE equalizer with 5, 10, 12 and 20 fingers MRC rake receiver with perfect channel estimation for the case of CM4 channel.

Like fig. 5.6 and fig. 5.7 this result also show performance improvement with increasing number of both rake fingers and equalizer taps. 12 fingers SRAKE MRC receiver with 3 taps equalizer has almost 0.1 db and 1.2 db gain over MRC SRAKE with 20 fingers and 12 fingers respectively at BER of 0.1. And 12 fingers SRAKE MRC receiver with 5 taps equalizer has almost 0.6 and 1.7 db gain over 20 fingers MRC SRAKE and 12 fingers MRC SRAKE respectively at BER of 0.1. But, 5 fingers MRC SRAKE receiver with 5 taps has SNR loss of about 0.25 db compared to 10 fingers MRC SRAKE receiver at a BER of 0.1. Like both CM1 and CM2 this analysis also shows that appending an adaptive MMSE equalizer on MRC SRAKE receivers, which have relatively large number of fingers, is better than employing additional rake fingers over CM4 channel, especially at higher

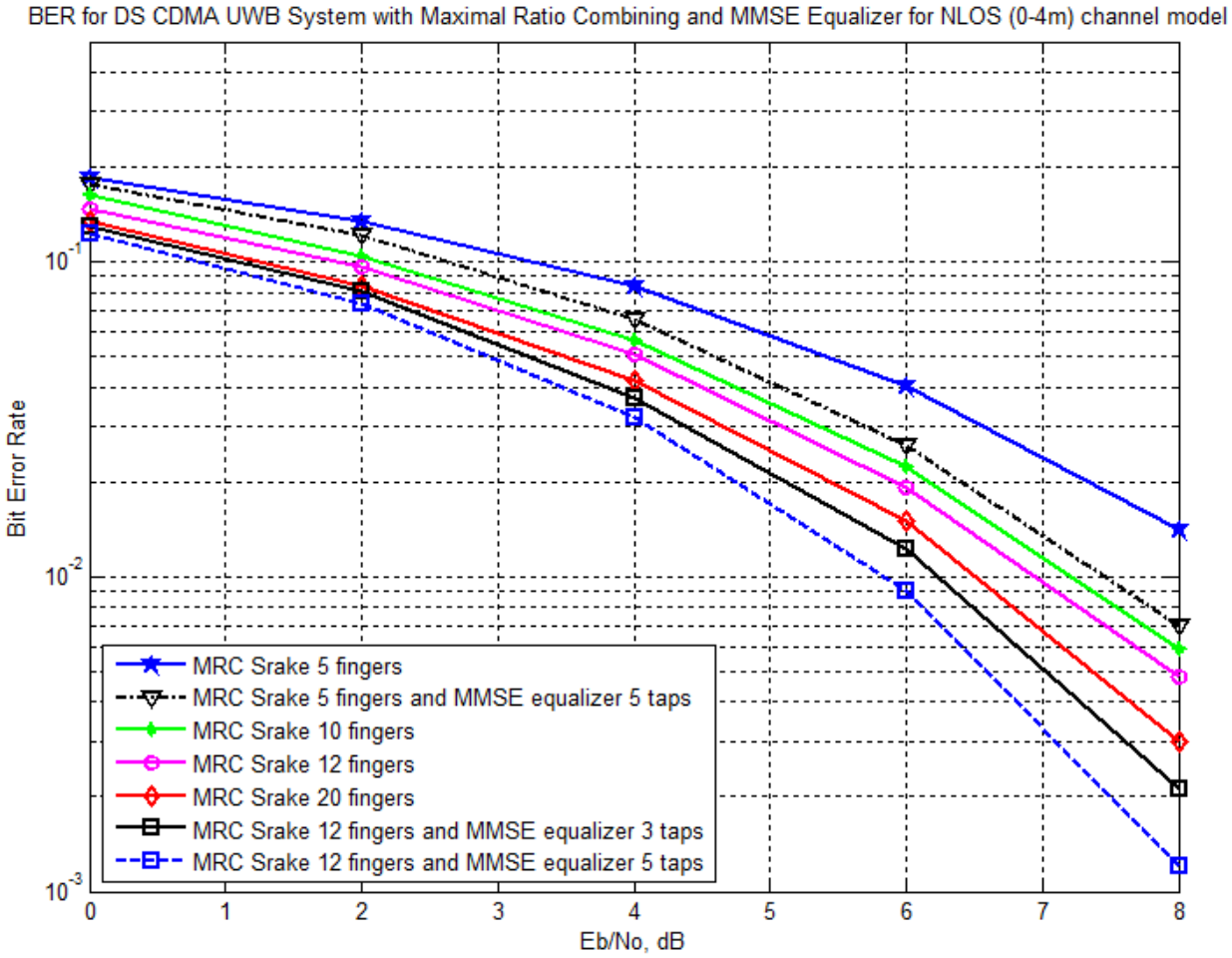

Figure 5.7: BER for DS CDMA UWB System with Maximal Ratio Combining and MMSE Equalizer for (0-4m) LOS Channel (Case A)

SNRs we can see a significant improvement change by appending an equalizer rather than adding additional fingers.

5.4 Performance evaluation of adaptive MMSE rake receiver with MMSE equalizer

In this section, the BER performance analysis and comparison of the cascaded MMSE Rake-Equalizer is provided. The performance analysis and comparison includes different number of fingers and equalizer taps and channel types.

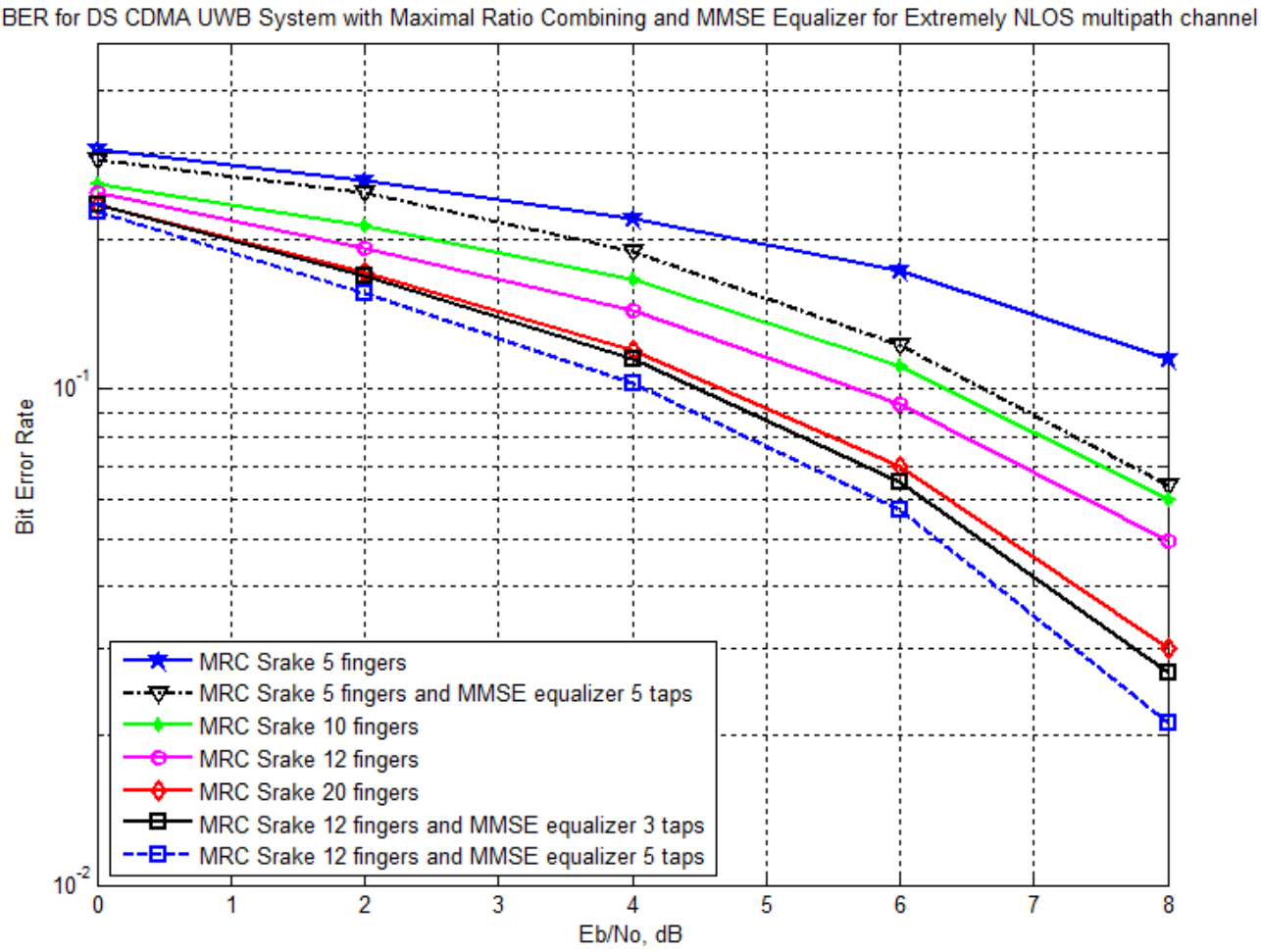

Figure 5.8: BER for DS CDMA UWB System with Maximal Ratio Combining and MMSE Equalizer for Extremely NLOS Channel (Case D)

5.4.1 Performance evaluation of adaptive MMSE rake receiver with MMSE equalizer for (0-4m) NLOS channel (case B)

Fig. 5.9 present the BER performance of the combined 5, 10 fingers MMSE rake and 3 taps MMSE equalizer with 5, 10 fingers and ARAKE MRC rake receiver with perfect channel estimation for the case of CM2 channel.

The result shows performance improvement with increasing number of both rake fingers and equalizer taps. MMSE rake with 5 fingers has almost 1.9 db and 0.2 db gain over MRC SRAKE with 5 fingers and 10 fingers respectively at BER of 0.02 but by appending 3 taps equalizer on MMSE rake with 5 fingers we can get 2.9 db, 1.1 db and 0.2 db gain over MRC SRAKE with 5 fingers and 10 fingers, and 5 fingers MMSE with 3 taps respectively at BER of 0.02. And by appending

3 taps equalizer on 10 fingers MMSE rake we can achieve 0.3 db gain over MRC ARAKE at a BER of 10^{-3}.

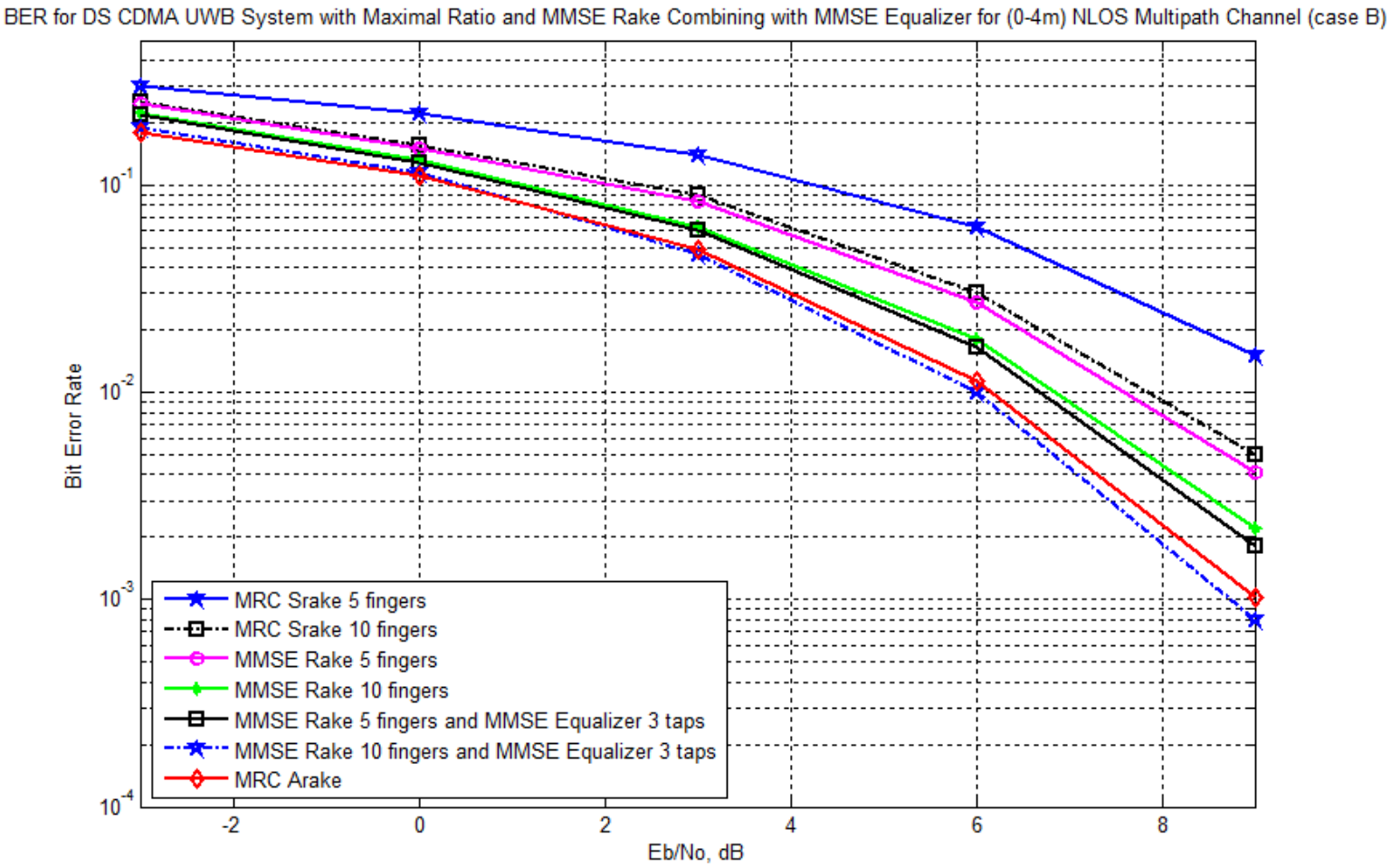

Figure 5.9: BER for DS CDMA UWB System with Maximal Ratio and MMSE Rake Combining with MMSE Equalizer for (0-4m) NLOS Multipath Channel (case B)

5.4.2 Performance evaluation of adaptive MMSE rake receiver with MMSE equalizer for (4-10m) NLOS channel (case C)

Fig. 5.10 present the BER performance of the combined 5, 10 fingers MMSE rake and 3 taps MMSE equalizer with 5, 10 fingers and ARAKE MRC rake receiver with perfect channel estimation for the case of CM3 channel.

The result shows performance improvement with increasing number of both rake fingers and equalizer taps. MMSE rake with 5 fingers has almost 2.6 db and 0.3 db gain over MRC SRAKE with 5 fingers and 10 fingers respectively at BER of

010^{-1} but by appending 3 taps equalizer on MMSE rake with 5 fingers we can achieve 1.3 db gain over 5 fingers MMSE rake and same performance as 10 fingers MMSE rake at a BER of 0.02. And by appending 3 taps equalizer on 10 fingers MMSE rake we achieve 1.5 db and 0.6 db gain and loss over 10 fingers MMSE rake and MRC ARAKE respectively at a BER of 10^{-2}.

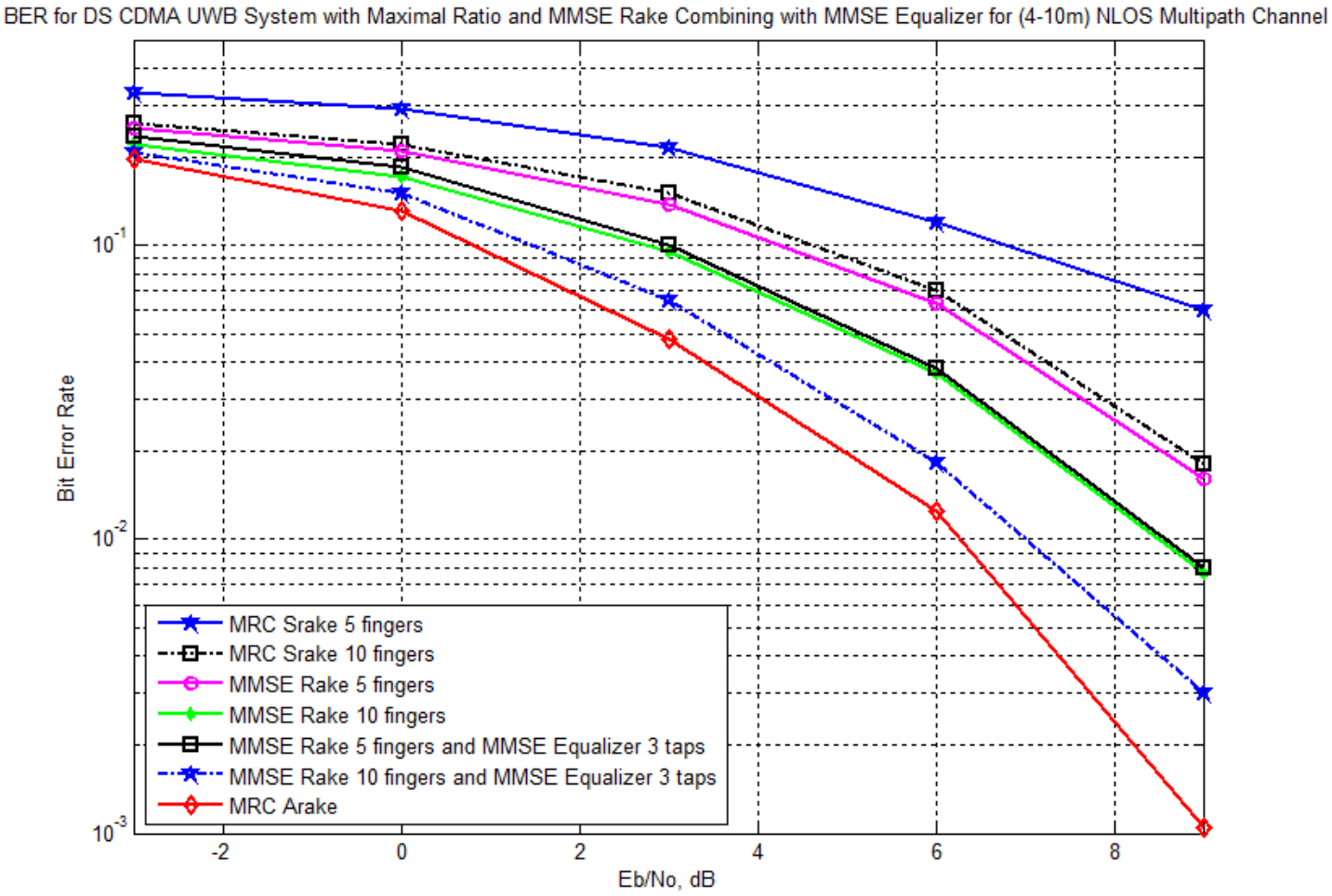

Figure 5.10: BER for DS CDMA UWB System with Maximal Ratio and MMSE Rake Combining with MMSE Equalizer for Extremely NLOS Multipath Channel (case D)

5.4.3 Performance evaluation of adaptive MMSE rake receiver with MMSE equalizer for extremely NLOS channel (case D)

Fig. 5.11 present the BER performance of the combined 5, 10 fingers MMSE rake and 3 taps MMSE equalizer with 5, 10 fingers and ARAKE MRC rake receiver with perfect channel estimation for the case of CM4 channel.

The result shows performance improvement with increasing number of both rake fingers and equalizer taps. MMSE rake with 5 fingers has almost 3 db and 0.4 db gain over MRC SRAKE with 5 fingers and 10 fingers respectively at BER of 010^{-1} but by appending 3 taps equalizer on MMSE rake with 5 fingers we can achieve 1 db and 0.6 db gain and loss over 5 fingers MMSE rake and 10 fingers MMSE rake respectively at a BER of 10^{-1}. And by appending 3 taps equalizer on 10 fingers MMSE rake we achieve 1.2 db and 2.8 db gain and loss over 10 fingers MMSE rake and MRC ARAKE respectively at a BER of 0.02.

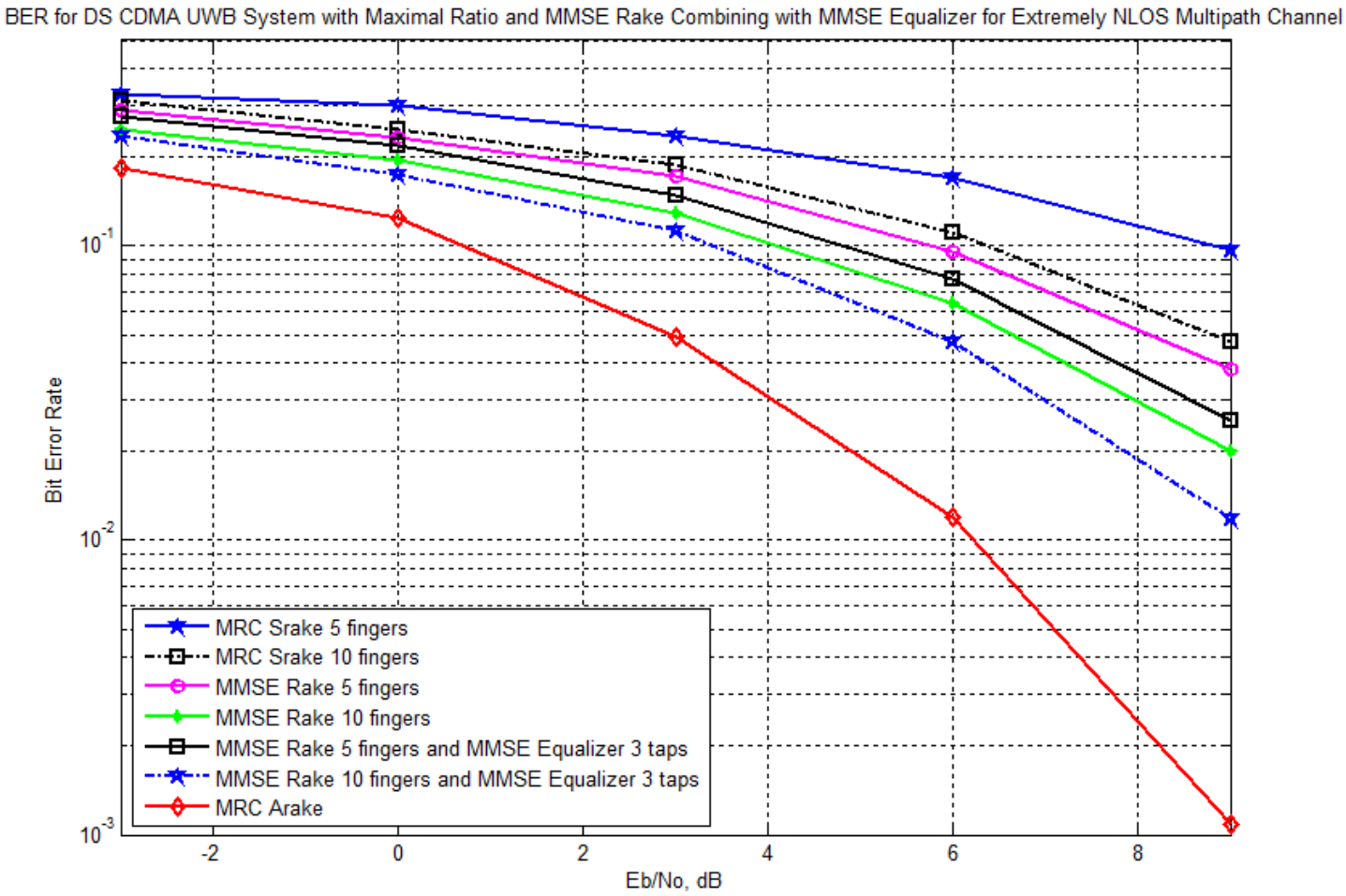

Figure 5.11: BER for DS CDMA UWB System with Maximal Ratio and MMSE Rake Combining with MMSE Equalizer for Extremely NLOS Multipath Channel (case D)

5.5 Performance evaluation of MMSE SC-FDE and MRC rake receiver

In this section, the BER performance analysis and comparison of Single carrier frequency domain equalizer and MRC SRAKE receiver at higher SNR'S is provided. The performance analysis and comparison includes different channel types and number of rake fingers.

5.5.1 Performance evaluation of MMSE SC-FDE and MRC rake receiver for (0-4m) LOS channel (case A)

Fig. 5.12 present the BER performance of the combined 5 fingers MRC SRAKE and 5 taps MMSE equalizer with SC-FDE and with 5 fingers MRC SRAKE receiver with perfect channel estimation for the case of CM1 channel.

The result shows both the 5 MRC SRAKE receiver and the combined 5 MRC SRAKE and 5 MMSE equalizer outperforms the SC-FDE at all SNRs. As we see the trend of the graph the 5 MRC SRAKE receiver and the combined 5 MRC SRAKE and 5 MMSE equalizer don't continue to decrease at higher SNRs as they were decreasing at lower SNRs. This is due to the fact that at higher SNRs MRC rake receiver exhibit an error floor. But, the SC-FDE continues to decrease at all SNRs.

5.5.2 Performance evaluation of MMSE SC-FDE and MRC rake receiver for (0-4m) NLOS channel (case B)

Fig. 5.13 present the BER performance of the combined 5 fingers MRC SRAKE and 5 taps MMSE equalizer with SC-FDE and with 5 fingers MRC SRAKE receiver with perfect channel estimation for the case of CM2 channel.

The result shows both the 5 MRC SRAKE receiver and the combined 5 MRC SRAKE and 5 MMSE equalizer outperforms the SC-FDE at lower SNRs. But, as the SNR increases SC-FDE outperforms the 5 MRC SRAKE receiver. As we see the trend of the graph the 5 MRC SRAKE receiver don't continue to decrease at higher SNRs, specifically beyond SNR=18, as they were decreasing at lower SNRs. But, the appended 5 taps equalizer tries to decrease the BER beyond the error floor. Therefore, by appending a MMSE-LE on MRC SRAKE receiver we can tackle the problem of an error floor over CM2. But, the SC-FDE continues to decrease at all SNRs.

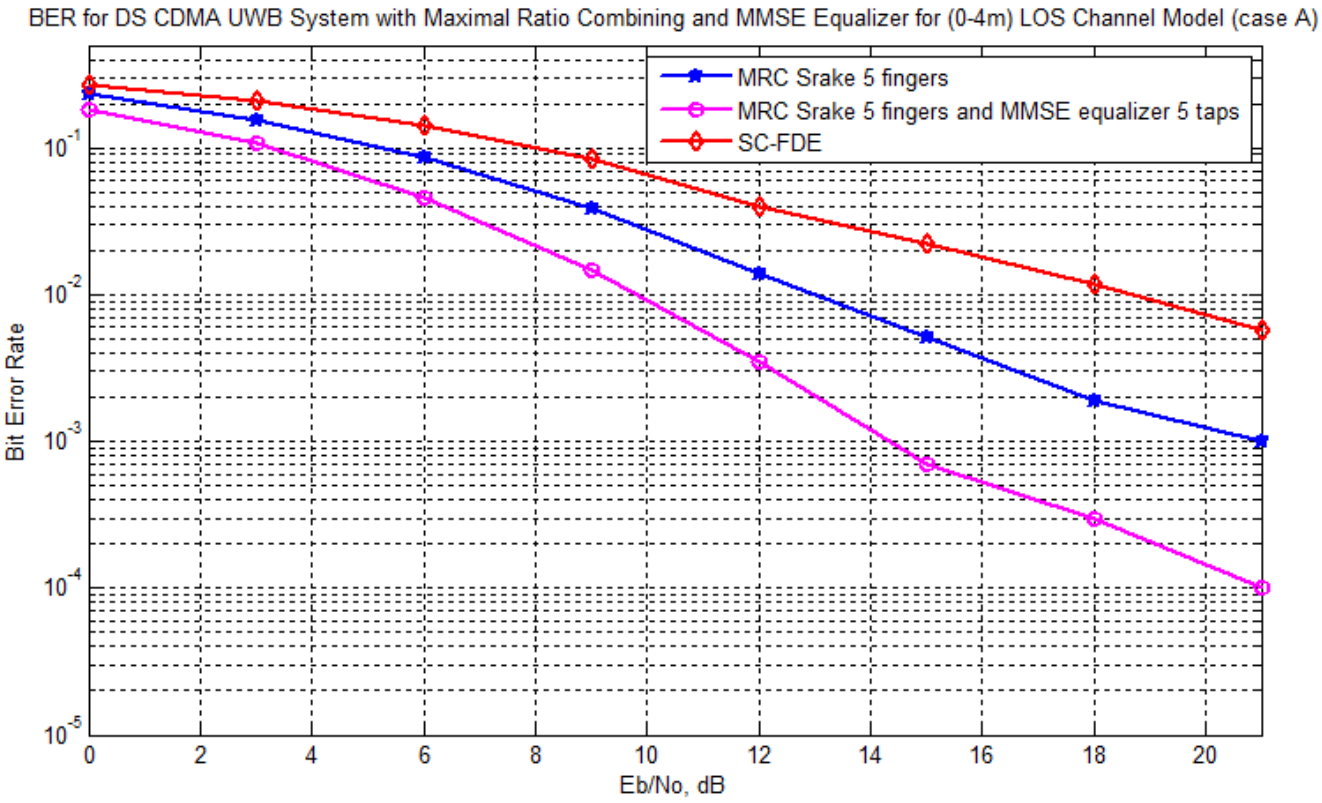

Figure 5.12: BER for DS CDMA UWB System with Maximal Ratio Combining and MMSE SC-FDE for (0-4m) LOS Multipath Channel (Case A)

5.5.3 Performance evaluation of MMSE SC-FDE and MRC rake receiver for (4-10m) NLOS channel (case C)

Fig. 5.14 present the BER performance of the combined 5 fingers MRC SRAKE and 5 taps MMSE equalizer with SC-FDE and with 5 fingers MRC SRAKE receiver with perfect channel estimation for the case of CM3 channel.

The result shows the combined 5 MRC SRAKE and 5 MMSE equalizer outperforms the SC-FDE at lower SNRs. But, as the SNR increases SC-FDE outperforms the combined 5 MRC SRAKE and 5 MMSE equalizer. And SC-FDE outperforms the 5 MRC SRAKE receiver at all SNRs. SC-FDE has almost 4.4 db gain over MRC SRAKE with 5 fingers at BER of 0.02.

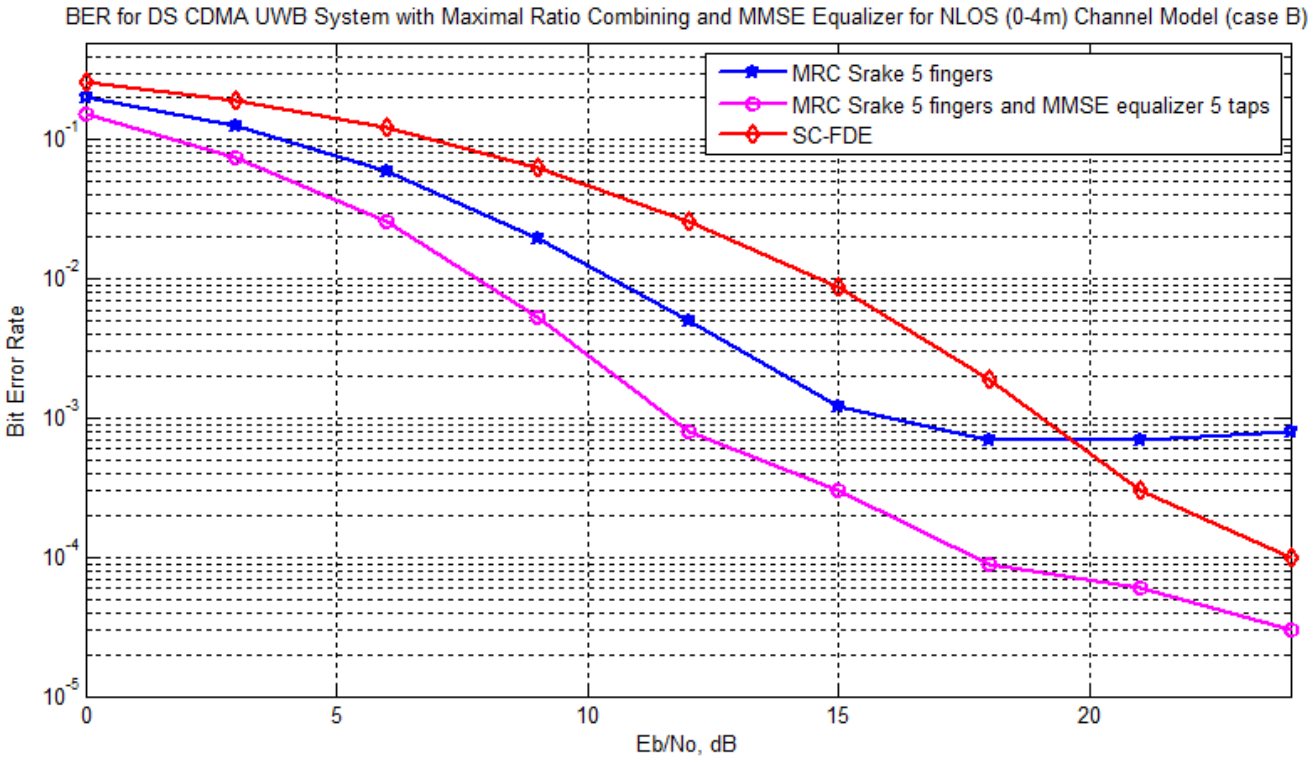

Figure 5.13: BER for DS CDMA UWB System with Maximal Ratio Combining and MMSE SC-FDE for (0-4m) NLOS Multipath Channel (Case B)

5.5.4 Performance evaluation of MMSE SC-FDE and MRC rake receiver for extremely NLOS channel (case D)

Fig. 5.15 present the BER performance of the combined 5 fingers MRC SRAKE and 5 taps MMSE equalizer with SC-FDE and with 5 fingers MRC SRAKE receiver with perfect channel estimation for the case of CM4 channel.

The result shows SC-FDE outperforms the 5 MRC SRAKE, 10 MRC SRAKE and the combined 5 MRC SRAKE and 5 MMSE equalizer at all SNRs. The 15 MRC SRAKE receiver outperforms the SC-FDE at lower SNRs. But, as the SNR increases SC-FDE outperforms the combined 15 MRC SRAKE receiver. SC-FDE has almost 2.4 db, 3.4 db and 10.4 db gain over the combined 5 fingers MRC SRAKE and 5 taps equalizer, 10 fingers MRC SRAKE receiver and 5 fingers MRC SRAKE receiver at BER of 0.06. And also at BER of 0.012, MRC SRAKE receiver with 15 fingers has a SNR loss of about 6.7 db compared to SC-FDE.

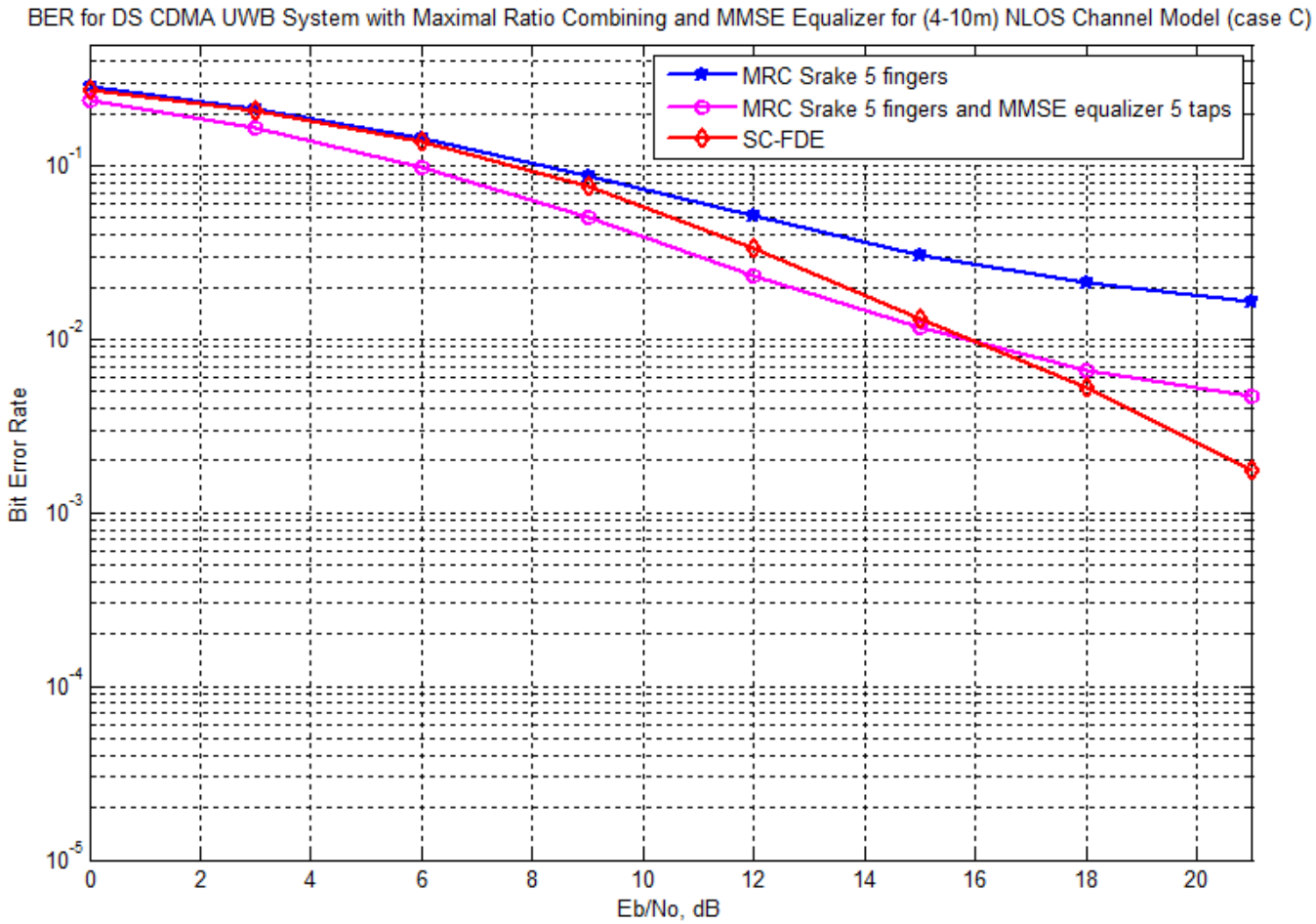

Figure 5.14: BER for DS CDMA UWB System with Maximal Ratio Combining and MMSE SC-FDE for (4-10m) NLOS Multipath Channel (Case C)

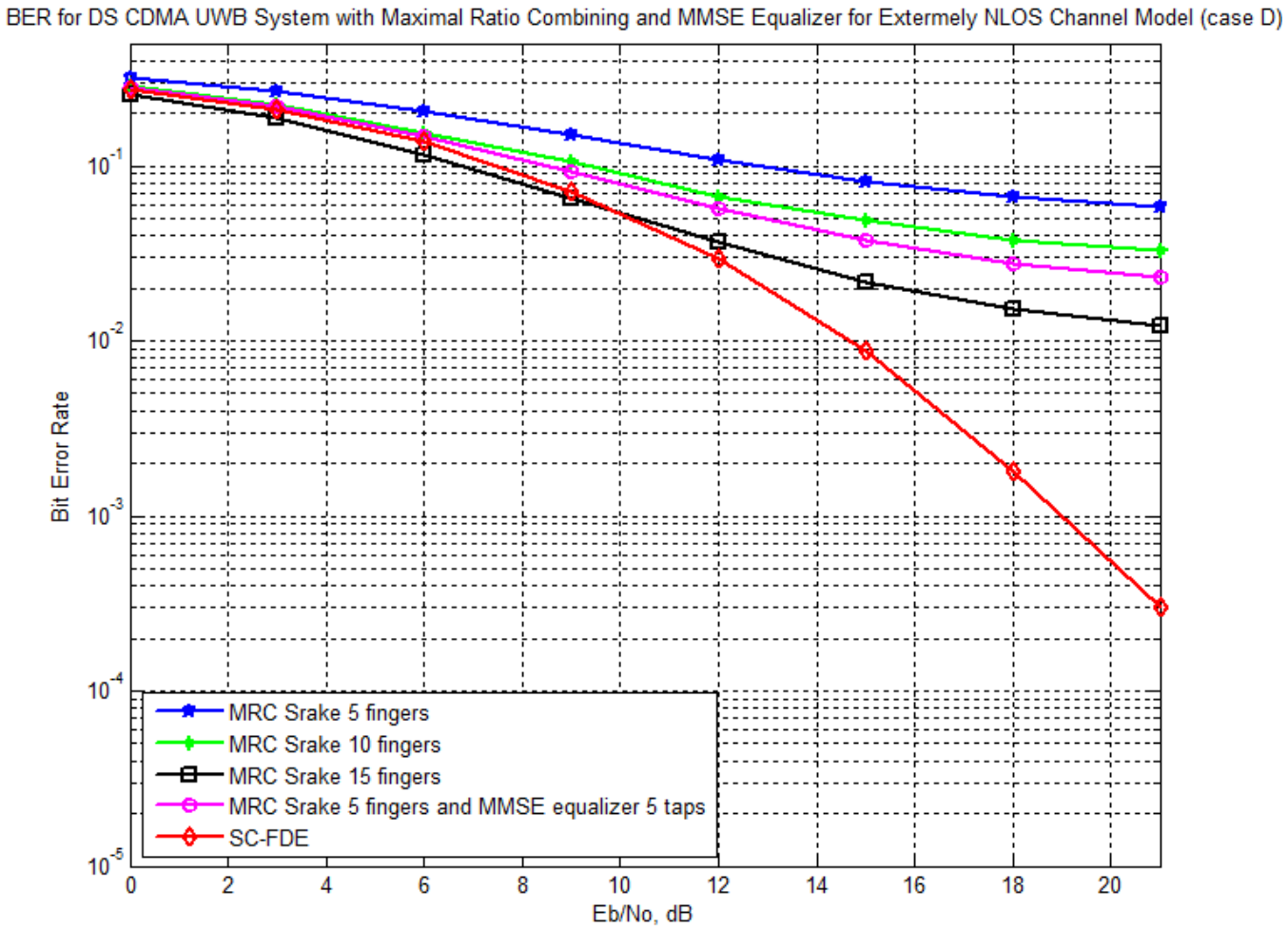

Figure 5.15: BER for DS CDMA UWB System with Maximal Ratio Combining and MMSE Rake with MMSE Equalizer for Extremely NLOS Channel (Case D)

Chapter 6

Conclusion and Recommendation

6.1 Conclusion

In this paper, 2^{nd} order Gaussian pulse were studied for generating the UWB signal. BPSK with pseudo random spreading is selected as the UWB modulation scheme within this project because of its good power efficiency and existence of no spectral lines in it's spectrum.

The UWB receiver structure with different rake types and multiple Rake fingers with different equalizer taps for different channel models was simulated. Its performance was evaluated and compared. We conclude that UWB system can operate perfectly in a low SNR environment due to the properties of UWB signal and combined Rake-equalizer structure.

Using MRC rake receiver the simulation results illustrate that an ideal ARAKE receiver using DS-BPSK-UWB transmitted signal format has the best performance for all type of channel models. The result also shows that at higher SNRs MRC rake receiver exhibit an error floor and appending an equalizer on MRC rake is better than employing additional rake fingers, especially at higher SNRs and relatively large number of fingers.

The proposed Rake-Equalizer outperforms the conventional rake receiver, which maximize the output SNR. The simulation also shows that the cascaded MMSE Rake-Equalizer achieves almost the same BER performance as MRC A-RAKE receiver for CM2 and frequency domain equalizer outperforms time domain MRC rake-equalizer at higher SNRs for CM4.

6.2 Recommendations for Future Work

In this research, many important issues have not been dealt with, or have been considered with simplified assumptions. Hence, there are some areas in which the work of this thesis can be extended. Some topics for future research on cascaded MMSE Rake-Equalizer receivers for UWB wireless communication systems following the direction of this thesis include:

- This work assumes no pulse distortion due to antennas and channel which is not practically applicable. Thus, performance evaluations under the effect of both transmitter and receiver antenna and channel can be further investigated.
- In this thesis, simulations have been carried out assuming that the receiver has perfect channel state information and perfect time synchronization between the transmitter and receiver which is not practical. Therefore, the impact of channel estimation and time synchronization errors on the system performance is another research area that needs further study.
- The computational complexity of the proposed receiver could be another research area.
- FDE needs CP to avoid inter block interference and this CPs should have length equal to or greater than the channel delay spread. But, UWB multipath channel spread over dozens of symbols in the case of ultra high-speed communications of several hundreds Mbps. Therefore, avoiding this large delay spread needs large number of CPs for each block, which affects the throughput of the system. Thus, a method which minimize this large CP or a method which uses this CP to easier channel estimation, synchronization and tracking of time and frequency offset can be further investigated.

Bibliography

[1] *APT AWF report.* [online]. Available: http://www.aptsec.org/Program/AWF/Approved%20Recommendations/(AWF%20Rep1). [cited at p. 10, 14]

[2] *Australias policy.* http://www.acma.gov.au/WEB/STANDARD/pc=PC_2645. [cited at p. 13]

[3] *CEPT resolutions.* http://www.erodocdb.dk/doks/relation.aspx?docid=2188. [cited at p. 11]

[4] *IDA Singapore policy.* http://www.ida.gov.sg/doc/Policies%20and%20Regulation/Policies_and_Re pdf. [cited at p. 15]

[5] *ITU-R TG1/8: Compatibility between ultra-wideband (UWB) devices and radio communications services.* Std. [Online]. Available: http://www.itu.int/ITU-R/study- groups/rsg1/rtg1-8/index.asp. [cited at p. 9]

[6] *ITU recommendations.* http://www.itu.int/rec/R-REC-SM/e. [cited at p. 9]

[7] *Japan UWB Regulation.* Std. [Online]. Available: http://www.soumu.go.jp/s-news/2006/060327 3.html. [cited at p. 14]

[8] *Japans policy.* http://www.rft.jp/UltraWidebandWirelessSystem.html. [cited at p. 14]

[9] B. Allen, M. Dohler, E. E. Okon, W. Q. Malik, A. K. Brown, and D. J. Edwards. *Ultra-Wideband Antennas and Propagation for Communications, Radar and Imaging.* Wiley, London, U.K, 2006. [cited at p. 35]

[10] S.L. Ariyavisitakul, D. Falconer, A. Benyamin-Seeyar, and B. Edison. Frequency domain equalization for single-carrier broadband wireless systems. *IEEE Communication Magazine*, 40(4):58–66, April 2002. [cited at p. 6, 50, 56]

[11] David Barras, Frank Ellinger, and Heinz Jckel. A comparison between ultra-wideband and narrowband transceivers. Technical report, Laboratory for Electronics, Swiss Federal Institute of Technology, Zurich, Switzerland, 2003. [cited at p. 17, 18]

[12] G. S. Biradar, S. N. Merchant, and U. B. Desai. An adaptive mmse-rake receiver for ds-cdma uwb multipath channel. [cited at p. 5]

[13] J. Jeya A Celin and V. Umadevi Chezhian. Adaptive mmse rake receiver for wcdma. *Int. J. Of Advanced Networking and Applications*, 2:621–625, 2010. [cited at p. 3, 5, 39]

[14] J. D. Choi and W. E. Stark. Performance of ultra-wideband communications with suboptimal receivers in multipath channels. *IEEE J. Select. Areas Commun.*, 20:17541766, December 2002. [cited at p. 36, 37]

[15] Conroy, J.L. LoCicero, and D.R. Ucci. Communication techniques using mono pulse waveforms. *IEEE MILCOM*, 2:11911185, 1999. [cited at p. 19]

[16] L. W. Couch. *Digital and Analog Communication Systems*. Prentice Hall, New Jersey, 6^{th} edition, 2001. [cited at p. 23, 24]

[17] Cassioli D., Win M.Z., Vatalaro F., and Molisch A.F. Low complexity rake receivers in ultra-wideband channels. *IEEE Transactions on Wireless Communications*, 6(4), April 2007. [cited at p. 37]

[18] E.H. Dinan and B. Jabbari. Spreading codes for direct sequence cdma and wideband cdma cellular networks. *IEEE*, 36:48–54, September 1998. [cited at p. 31]

[19] T. Eng, N. Kong, and L. B. Milstein. Comparison of diversity combining techniques for rayleigh fading channels. *IEEE Transactions on Communication*, 44(9):1117–1129, September 1996. [cited at p. 38]

[20] M. Eslami and Xiaodai Dong. Performance of rake-mmse-equalizer for uwb communications. *IEEE WCNC*, 2:855–860, March 2005. [cited at p. 50]

[21] Ramirez-Mireles F. and Scholtz R. System performance analysis of impulse radio modulation. In *Radio and Wireless Conference (RAWCON1998)*, CO, USA, 1998. Colorado Springs. [cited at p. 21]

[22] Federal Communications Commission. *Revision of Part 15 of the commission's rules regarding ultra-wide band transmission system*, February 2002. First report and order, ET Docket98 153, FCC 02-48. [cited at p. 2, 8, 11, 12, 15, 16, 17, 18, 35]

[23] Foerster and Jeffrey R. The performance of a direct-sequence spread spectrum ultra-wideband system in the presence of multipath, narrowband, interference, and multiuser interference. In *IEEE Conference on Ultra Wideband Systems and Technologies*, 2002. [cited at p. 27, 28, 29]

[24] J. Foerster. Channel modeling sub-comittee report final. Technical Report 02/490r0-SG3a, IEEE P802.15 WG for WPANs, 2002. [cited at p. 31]

[25] J. Foerster and Q. Li. Uwb channel modeling contribution from intel. Technical report, Intel, September 2002. [cited at p. 39]

[26] Fontana, Robert J., and Steven J. Gunderson. Ultra-wideband precision asset location system. In *IEEE Conference on UWB Systems and Technologies*. Multispectral Solutions, INC. and Naval Facilities Engineering Service Center, May 2002. [cited at p. 2]

[27] S. Gezici, Z. Tian, G. B. Giannakis, H. Kobayashi, A. F. Molisch, H. V. Poor, and Z. Sahinoglu. Localization via ultra-wide band radios: a look at positioning aspects for future sensor networks. 22:70–84, July 2005. [cited at p. 2, 32]

[28] M. Hamalainen, V. Hovinen, R. Tesi, J. H. J. Iinatti, and M. Latva-aho. On the uwb system coexistence with gsm900, umts/wcdma, and gps. *IEEE Journal on Selected Areas of Communication*, 20:1712–1721, December 2002. [cited at p. 44]

[29] R. F. Harrington. Effect of antenna size on gain, bandwidth and efficiency. *Journal of Research of the national bureau of standards - D. Radio Propagation*, 64D(1):1–12, Jan-Feb 1960. [cited at p. 18]

[30] H. Hashemi. The indoor radio propagation channel. In *IEEE*, volume 81, pages 943–968, July 1993. [cited at p. 32, 35, 44]

[31] R. L. Haupt and S. E. Haupt. *Practical Genetic Algorithms*. John Wiley and Sons, New York, 1998. [cited at p. 42]

[32] Monson H. Hayes. *Statistical Digital Signal Processing and Modeling*. John Wiley and Sons, Georgia Institute of Technology, 1996. [cited at p. 40, 41]

[33] Guvenc I. and Arslan H. Performance evaluation of uwb systems in the presence of timing jitter. *IEEE Conference on UWB Systems and Technology*, pages 136–141, November 2003. [cited at p. 18]

[34] J. Ibrahim. Notes on ultra wideband receiver design, April 14 2004. [cited at p. 22, 23, 25]

[35] Y. Ishiyama and T. Ohtsuki. Performance evaluation of uwb-ir and ds-uwb with mmse-frequency domain equalization. *IEEE Conference on Globalcom*, pages 3093–3097, December 2004. [cited at p. 6]

[36] Foerster J., Green E., Somayazulu S., and Leeper D. Ultra wideband technology for short or medium range wireless communications. *Intel Technology Journal*, 2001. [cited at p. 27]

[37] H. Jafarkhani and V. Tarokh. On the computation and reduction of the peak-to-average ratio in multi carrier communications. *IEEE Transaction Communication*, 48(1):37–44, January 2000. [cited at p. 56]

[38] W.C. Jakes. *Microwave Mobile Communications*. John Wiley and Sons, New York, USA, 1974. [cited at p. 32]

[39] J. RALPH JOHLER. Propagation of the low-frequency radio signal. In *Proceedings of the IRE*, pages 404–427, April 1962. [cited at p. 2, 17]

[40] Muhammad Gufran Khan, Jorgen Nordberg, Abbas Mohammed, and Ingvar Claesson. Performance evaluation of rake receiver for uwb systems using measured channels in industrial environments. Technical report, Department of Signal Processing, School of Engineering, Blekinge Institute of Technology, Ronneby, Sweden, 2006. [cited at p. 4]

[41] A.G. Kleini, D.R. Brown IIP, D.L. Goeckels, and C.R. Johnson. Rake reception for uwb communication systems with inter symbol interference. *IEEE Workshop on Signal Processing Advances in Wireless Communications*, 2003. [cited at p. 5, 42]

[42] N. Kong and L. B. Milstein. Combined average snr of a generalized diversity selection combining scheme. In *IEEE International Conference on Communication*, pages 1556–1560, Atlanta, GA, June 1998. [cited at p. 39]

[43] Ning Kong and Laurence B. Milstein. Average snr of a generalized diversity selection combining scheme. *IEEE Communications Letters*, 3(3):57–59, March 1999. [cited at p. 38]

[44] Ladd and et al. Andrew M. On the feasibility of using wireless ethernet for indoor localization. *IEEE Transactions on Robotics and Automation*, pages 555–559, June 2004. [cited at p. 2]

[45] Jr. L.J. Cimini and N.R. Sollenberger. Peak-to-average power ratio reduction of an ofdm signal using partial transmit sequences. *IEEE Communication Letters*, 4(3):86–88, March 2000. [cited at p. 55]

[46] G. Marsh. Uwb-europe is concerned, too. Avionics magazine, 2005. [cited at p. 10]

[47] J.T.E. McDonnell and T.A. Wilkinson. Comparison of computational complexity of adaptive equalization and ofdm for indoor wireless networks. In *PIMRC '96*, pages 1088–1090, Taipei, 1996. [cited at p. 55]

[48] D. R. McKinstry and R. M. Buehrer. Issues in the performance and covertness of uwb communications systems. In *Proceeding of* 45^{th} *Midwest Symposium on Circuits and System*, volume 3, pages 601–604, Tulsa, August 2002. [cited at p. 2, 8, 17]

[49] J. S. McLean. A re-examination of the fundamental limits on the radiation q of electrically small antennas. *IEEE Transactions on Antennas and Propagation*, 44(5):672–676, May 1996. [cited at p. 18, 21]

[50] A. F. Molisch. Ultra-wideband propagation channels theory, measurement, and modeling. *IEEE Transactions on Vehicle Technology*, 54(5):1528–1545, September 2005. [cited at p. 38]

[51] A. F. Molisch, J. R. Foerster, and M. Pendergrass. Channel models for ultra-wideband personal area networks. 10(6):14–21, December 2003. [cited at p. 32, 33, 34]

[52] Andreas F. Molisch. Uwb wireless channels propagation aspects and interplay with system design. Technical report, Mitsubishi Electric Research Labs, Cambridge, USA, December 2004. [cited at p. 32]

[53] Yves-Paul Nakache and Andreas F. Molisch. Spectral shape of uwb signals influence of modulation format, multiple access scheme and pulse shape. Technical report, Mitsubishi Electric Research Laboratory, 201 Broadway,Cambridge,Massachusetts 02139, May 2003. [cited at p. 16]

[54] H. Niu, J. A. Ritcey, and H. Liu. Performance of uwb rake receivers with imperfect tap weights. *IEEE Int. Con. on Acoustic, Speech and Signal Processing*, 4:125–128, April 2003. [cited at p. 3, 42]

[55] John Proakis. *Digital Communications*. McGraw-Hill, New York, 3^{rd} edition, 1995. [cited at p. 52, 53, 54]

[56] Theodore S. Rapport. *Wireless Communication Principles and Practices*. Communications Engineering and Emerging Technologies series. Prentice Hall, 2^{nd} edition, 2001. [cited at p. 51]

[57] G.W. Rice, D. Garcia-Alis, I. G. Stirling, S. Weiss, and R. W. Stewart. An adaptive mmse rake receiver. In *Asilomar Conference on SSC*, volume 1, pages 808–812, October 2000. [cited at p. 3, 39]

[58] Ramachandran I. S. Acquisition of direct-sequence ultra wideband signals. *Wireless Communications and Network Conference*, 2:752–757, March 2005. [cited at p. 17]

[59] Adel A. M. Saleh and Reinaldo A. Valenzuela. A statistical model for indoor multipath propagation. sac-5(2), February 1987. [cited at p. 32, 33]

[60] H. Sari, G. Karam, and I. Jeanclaude. Transmission techniques for digital terrestrial tv broadcasting. *IEEE Communication Magazine*, 33(2):100–109, February 1995. [cited at p. 55]

[61] H. Sato and T. Ohtuski. Frequency domain channel estimation and equalization for direct sequence ultra wideband (ds-uwb) system. *IEEE proceedings communications*, 153:93–98, February 2006. [cited at p. 5]

[62] Scholtz and R. A. Multiple access with time-hopping impulse modulation. *IEEE MILCOM'93*. [cited at p. 19, 28]

[63] R. A. Scholtz, R. Weaver, E. Homier, J. Lee, P. Hilmes, A. Taha, and R. Wilson. Uwb radio deployment challenges. *IEEE PIMRC*, 1:620–625, September 2000. [cited at p. 21]

[64] H. Sheng, A. M. Haimovich, A. F. Molisch, and J. Zhang. Optimum combining for time hopping impulse radio uwb rake receivers. In *IEEE Conference on Ultra Wideband Systems and Technologies*. [cited at p. 3, 38, 39]

[65] H. Sheng, P. Orlik, A.M. Haimovich, L.J. Cimini, Jr., and J. Zhang. On the spectral and power requirements for ultra wideband transmission. In *IEEE International Conference on Communications*, pages 738–742, Alaska, USA, 2003. Anchorage. [cited at p. 20]

[66] Hongsan Sheng, Philip Orlik, Alexander M. Haimovich, Leonard J. Cimini, and Jinyun Zhang. On the spectral and power requirements for ultra-wideband transmission. In *IEEE International Conference on Communications*. Mitsubishi Electric Research Laboratories. TR2003-66. [cited at p. 19, 20]

[67] Marvin K. Simon and Mohamed-Slim Alouini. *Digital Communication over Fading Channels*. John Wiley and Sons, Inc., USA, 2000. [cited at p. 3, 38, 39]

[68] Somayazulu and V. Srinivasa. Multiple access performance in uwb systems using time hopping vs. direct sequence spreading. Technical report, Intel Labs. [cited at p. 28]

[69] B. Spinnler. Equalizer design and complexity for digital coherent receivers. *Journal of Selected Topics in Quantum Electronics*, 16(5):1180–1192, 2010. [cited at p. 55]

[70] G. L. Stber. *Principles of Mobile Communications*. John Wiley and Sons, Norwell, MA, 2^{nd} edition, 2001. [cited at p. 37, 38]

[71] T. Strohmer, M. Emani, J. Hansen, G. Papanicolaou, and A. J. Paulraj. Application of time-reversal with mmse equalizer to uwb communications. In *IEEE Globecom'04*, volume 5, pages 3123–3127, Dec. 2004. [cited at p. 57]

[72] Varghese. Ultra wide band: Standards, technology, oem strategy and markets and application spaces. Technical report, ABI Research, 2004. [cited at p. 2]

[73] S. Verdu. *Multiuser Detection*. Cambridge University Press, Cambridge, UK, 1998. [cited at p. 47]

[74] Matthew L. Welborn. *System considerations for Ultra-Wideband Wireless Networks*. [cited at p. 23, 25]

[75] M. Win and R. Scholtz. Ultra-wide bandwidth time hopping spread spectrum impulse radio for wireless multiple access communications. *IEEE Transaction On Communication*, 48(4):679–691, April 2000. [cited at p. 17, 18, 19]

[76] M. Z. Win and R. A. Scholtz. On the energy capture of ultra-wide bandwidth signals in dense multipath environments. *IEEE Commun. Lett.*, 2:245247, September 1998. [cited at p. 36, 38]

[77] Moe Z. Win and Robert A. Scholtz. Impulse radio: How it works. *IEEE Communications Letters*, 2(2), February 1998. [cited at p. 17, 19]

[78] Ning Xie and Yuanping Zhou. An adaptive nonlinear rake receiver in uwb wireless communications. In *IEEE International Conference on Networking, Sensing and Control*. [cited at p. 39]

[79] L. Yang and G. B. Giannakis. Ultra-wide band communications: an idea whose time has come. *IEEE Signal Processing Magazine*, 21(6):26–54, November 2004. [cited at p. 2, 8]

[80] Dongsong Zeng. *Pulse Shaping Filter Design and Interference Analysis in UWB Communication Systems*. PhD thesis, Virginia Polytechnic Institute and State University, 2005. [cited at p. 29]

[81] J. Zhang, T. D. Abhayapala, and R. A. Kennedy. Performance of ultra wideband correlator receiver using gaussian monocycles. In *ICC*, pages 2192–2196, 2003. [cited at p. 19]

Appendices

Appendix A

Appendix title